

A HUMAN DRIVER MODEL FOR AUTONOMOUS LANE CHANGING IN  
HIGHWAYS: PREDICTIVE FUZZY MARKOV GAME DRIVING STRATEGY

A Dissertation  
by  
SERDAR COSKUN

Submitted to the Office of Graduate and Professional Studies of  
Texas A&M University  
in partial fulfillment of the requirements for the degree of  
DOCTOR OF PHILOSOPHY

Chair of Committee, Reza Langari  
Committee Members, Pilwon Hur  
Swaroop Darbha  
Shankar P. Bhattacharyya  
Head of Department, Andreas A. Polycarpou

December 2018

Major Subject: Mechanical Engineering

Copyright 2018 Serdar Coskun

## ABSTRACT

This study presents an integrated hybrid solution to mandatory lane changing problem to deal with accident avoidance by choosing a safe gap in highway driving. To manage this, a comprehensive treatment to a lane change active safety design is proposed from dynamics, control, and decision making aspects.

My effort first goes on driver behaviors and relating human reasoning of threat in driving for modeling a decision making strategy. It consists of two main parts; threat assessment in traffic participants, ( $TVs$ ) states, and decision making. The first part utilizes an complementary threat assessment of  $TVs$ , relative to the subject vehicle,  $SV$ , by evaluating the traffic quantities. Then I propose a decision strategy, which is based on Markov decision processes (MDPs) that abstract the traffic environment with a set of actions, transition probabilities, and corresponding utility rewards. Further, the interactions of the  $TVs$  are employed to set up a real traffic condition by using game theoretic approach. The question to be addressed here is that how an autonomous vehicle optimally interacts with the surrounding vehicles for a gap selection so that more effective performance of the overall traffic flow can be captured. Finding a safe gap is performed via maximizing an objective function among several candidates. A future prediction engine thus is embedded in the design, which simulates and seeks for a solution such that the objective function is maximized at each time step over a horizon. The combined system therefore forms a predictive fuzzy Markov game (FMG) since it is to perform a predictive *interactive* driving strategy to avoid accidents for a given traffic environment. I show the effect of interactions in decision making process by proposing both cooperative and non-cooperative Markov game strategies for enhanced traffic safety and mobility. This level is called the *higher level controller*. I further focus on generating a driver controller to complement the automated

car's safe driving. To compute this, model predictive controller (MPC) is utilized. The success of the combined decision process and trajectory generation is evaluated with a set of different traffic scenarios in dSPACE virtual driving environment.

Next, I consider designing an active front steering (AFS) and direct yaw moment control (DYC) as the *lower level controller* that performs a lane change task with enhanced handling performance in the presence of varying front and rear cornering stiffnesses. I propose a new control scheme that integrates active front steering and the direct yaw moment control to enhance the vehicle handling and stability. I obtain the nonlinear tire forces with Pacejka model, and convert the nonlinear tire stiffnesses to parameter space to design a linear parameter varying controller (LPV) for combined AFS and DYC to perform a commanded lane change task. Further, the nonlinear vehicle lateral dynamics is modeled with Takagi-Sugeno (T-S) framework. A state-feedback fuzzy  $\mathcal{H}_\infty$  controller is designed for both stability and tracking reference. Simulation study confirms that the performance of the proposed methods is quite satisfactory.

## ACKNOWLEDGMENTS

Last four years of my Ph.D. study at the Texas A&M University has been a great experience and success that I would have never thought to become true. First of all, I would like to thank my advisor, Dr. Langari, for his support and always driving me to the right direction in research. I have developed discipline and skills to overcome any of the challenges I have encountered along the way. This work would not have been possible without the guidance of him.

I would like to thank the committee members for their suggestions and criticisms that eventually better increased the quality of this work. I would also like to thank to my colleagues for useful discussions and always encouraging me to create something better in research.

Special thank goes to the Turkish Ministry of National Education for their continuous financial support throughout my graduate studies in the United States of America.

Most importantly, I would like to express my sincere feelings to my family. They have been always supportive since I made the decision of pursuing my graduate degrees abroad. Without them, I would never have been able to become the person I am today.

## CONTRIBUTORS AND FUNDING SOURCES

### **Contributors**

This work was supervised by a dissertation committee consisting of Professor Reza Langari, Pilwon Hur, and Swaroop Darbha of the Department of Mechanical Engineering and Professor Shankar Bhattacharyya of the Department of Electrical and Computer Engineering.

All work for the dissertation was completed by the student, under the advisement of Reza Langari of the Department of Mechanical Engineering.

### **Funding Sources**

This graduate study was supported by the Turkish Ministry of National Education with the Law number 1416, under the grant name Graduate Studies Scholarship in the United States of America.

## NOMENCLATURE

Driver model	Overall model of autonomous driving
Hybrid system	Combination of discrete and continuous system dynamics
FMDP	Fuzzy Markov decision process
FMG	Fuzzy Markov game
SV	Subject car
Lead car	The followed car by the subject car
TVs	Traffic vehicles
Kinematic model	Point-mass vehicle model
Gap	Longitudinal space between two traveling vehicles
IDM	Intelligent driver model
QP	Quadratic programming
Convex set	A set wherein any two points connect without leaving the set
Reach	Reachable states of a dynamic system
Trajectory	A line connects a vehicle's initial and final states in a planar plane
<i>RP</i>	Relative position
<i>RV</i>	Relative velocity
<i>CV</i>	Cruising velocity
MPC	Model predictive control
AFS	Active front steering

DYC	Direct yaw moment control
LMIs	Linear matrix inequalities
Reference Model	Linearized model of nonlinear vehicle model
BRL	Bounded real lemma
LPV	Linear parameter varying
T-S	Takagi-Sugeno

## Symbols

$k$	Discrete Time Index
$\Delta(k), t_s$	Sampling Time
$x$	Longitudinal Driving Direction on a Road Frame
$y$	Lateral Driving Direction on Road Frame
$q$	Threat Between SV and a TV
$a$	Action of SV and TVs
$u_x$	Acceleration of SV and TVs in Longitudinal Direction
$u_y$	Acceleration of SV and TVs in Lateral Direction
$lc$	Veering
$N$	Prediction Horizon
$\mathcal{L}$	Transition Probabilities
$\varrho_1$	Weight Term on Gap
$\varrho_2$	Weight Term on Distance to Lead Vehicle
$\Psi$	Gap Length Between TVs
$\tau$	Time to Reach to a Selected Gap
$\pi$	Remaining Gap Length from the Lead Vehicle
$m$	Mass of Car

$W_c$	Width of Car
$v_x$	Longitudinal Velocity
$v_y$	Lateral Velocity
$y_{ref}$	Reference Lane Target
$T$	Headway Time
$\mathcal{K}$	Gain of Heuristic IDM
$d_{dc}$	Decision Evaluation Distance
$W_L$	Lane Width
$Q_{v_x}$	Running Cost Weight on Reference Longitudinal Velocity
$Q_y$	Running Cost Weight on Lateral Lateral
$Q_{v_y}$	Running Cost Weight on Lateral Velocity
$R_{u_x}$	Weight on Longitudinal Acceleration
$R_{u_y}$	Weight on Lateral Acceleration
$\dot{\psi}$	Yaw Rate
$\beta$	Vehicle Side Slip Angle
$F_{yf}, F_{cf}$	Lateral Front Tire Force
$F_{yr}, F_{cr}$	Lateral Rear Tire Force
$F_{lf}$	Longitudinal Front Tire Force
$F_{lr}$	Longitudinal Rear Tire Force
$C_f$	Front Tire Cornering Stiffness
$C_r$	Rear Tire Cornering Stiffness
$\alpha_f$	Front Tire Slip Angle
$\alpha_r$	Rear Tire Slip Angle

$\delta_f$	Front Steering Angle
$\delta^*$	Corrective Steering Angle
$M$	Yaw Moment
$l_f$	Front Tire Distance from Center of Gravity
$l_r$	Rear Tire Distance from Center of Gravity
$t_f$	Front Axle Length
$t_r$	Rear Axle Length
$J$	Moment of Inertia
$Y_w$	Lateral Wind Gust Disturbance
$L$	Look Ahead Distance
$s$	Side Slip Ratio
$\mu$	Tire-Road Friction Coefficient
$F_z$	Tire Vertical Force
$\mathcal{J}$	Multi-Objective Quadratic Cost Function
$\mathcal{H}_\infty$	$\mathcal{H}_\infty$ Optimal Control
$\mathcal{L}_2$	$\mathcal{H}_\infty$ Norm for Nonlinear Systems
$\ y\ _2$	$\mathcal{L}_2$ Norm of a Signal $y$
$\gamma$	$\mathcal{H}_\infty$ Performance Index

## TABLE OF CONTENTS

	Page
ABSTRACT . . . . .	ii
ACKNOWLEDGMENTS . . . . .	iv
CONTRIBUTORS AND FUNDING SOURCES . . . . .	v
NOMENCLATURE . . . . .	vi
TABLE OF CONTENTS . . . . .	x
LIST OF FIGURES . . . . .	xiii
LIST OF TABLES . . . . .	xvii
1. INTRODUCTION AND LITERATURE REVIEW . . . . .	1
1.1 Background . . . . .	1
1.2 Objectives . . . . .	3
1.3 Background and Literature Review . . . . .	5
1.3.1 Driver Decision Models (Higher Level Controller) . . . . .	5
1.3.2 Markov Decision Process (MDPs) . . . . .	17
1.3.2.1 MDPs in autonomous driving . . . . .	18
1.3.3 Game Theory . . . . .	20
1.3.3.1 Game Theory in autonomous driving . . . . .	20
1.3.4 Trajectory Planning for Autonomous Vehicles . . . . .	22
1.3.5 Longitudinal Vehicle Control . . . . .	24
1.3.6 Lateral Vehicle Control . . . . .	26
1.3.7 $\mathcal{H}_\infty$ Based Linear Parameter Varying (LPV) Control . . . . .	27
1.3.8 LPV Control in Automative Research . . . . .	28
1.3.9 Takagi-Sugeno $\mathcal{H}_\infty$ Control Strategy . . . . .	33
1.3.10 Driving Safety . . . . .	34
1.3.11 Contribution of the Dissertation . . . . .	36
2. DECISION MODEL . . . . .	39
2.1 Instantaneous Threat Estimation of TVs Using Fuzzy Logic . . . . .	40
2.1.1 Fuzzy Sets and Membership Functions . . . . .	42

2.1.2	Fuzzy Inference . . . . .	46
2.1.3	Simulation . . . . .	48
2.1.3.1	Car following model . . . . .	48
2.1.3.2	Simulation set-up . . . . .	49
2.2	Prediction . . . . .	52
2.3	Markov Decision Process . . . . .	55
2.3.1	Markov Chain . . . . .	55
2.3.2	MDP Modeling in Autonomous Driving . . . . .	57
2.3.3	MDP for Gap Selection . . . . .	58
2.3.4	Bellman's Equation and System Algorithm . . . . .	64
2.4	Markov Game . . . . .	66
2.4.1	Nash Equilibrium for Bimatrix Games [110] . . . . .	68
2.4.2	Markov Game for Gap Selection . . . . .	69
2.4.3	Bellman Equation for Markov Game . . . . .	77
2.5	Optimal Control Problem . . . . .	80
2.5.1	Model Predictive Control . . . . .	82
2.6	Trajectory Generation . . . . .	83
2.7	dSPACE Simulation Results . . . . .	86
2.8	Conclusion . . . . .	91
3.	VEHICLE LATERAL DYNAMICS AND CONTROL . . . . .	94
3.1	Linear Bicycle Model . . . . .	95
3.1.1	$\mathcal{H}_\infty$ Steering Control Design . . . . .	99
3.1.1.1	Performance weight selection . . . . .	100
3.1.1.2	Human driver model control for lane change maneuver .	104
3.1.2	Simulation Results . . . . .	105
3.2	Nonlinear Vehicle Model . . . . .	109
3.2.1	Simplified Model . . . . .	111
3.2.2	Tire Model . . . . .	112
3.2.3	Control Design Procedure . . . . .	113
3.2.3.1	Performance weight selection . . . . .	115
3.2.3.2	LPV/ $\mathcal{H}_\infty$ controller design . . . . .	115
3.2.4	Simulation Results . . . . .	120
3.3	Takagi-Sugeno Modeling for Vehicle Lateral Dynamics . . . . .	126
3.3.1	T-S Fuzzy modeling . . . . .	128
3.3.2	Controller Design . . . . .	132
3.3.3	Fuzzy $\mathcal{H}_\infty$ Controller Synthesis . . . . .	134
3.3.4	Simulation Results . . . . .	136
3.4	Conclusion . . . . .	140
4.	CONCLUSION . . . . .	143

REFERENCES . . . . .	145
----------------------	-----

## LIST OF FIGURES

FIGURE	Page
1.1 Driver model of an autonomous vehicle . . . . .	4
1.2 Schematic diagram of the proposed driver model . . . . .	5
1.3 Kondo's driver model . . . . .	8
1.4 Transfer function of driver model . . . . .	9
1.5 A schematic process of a human like decision making. Human brain collects the information from environment and processes based on a subjective reasoning process and executes an output according to the current state of cognition. . . . .	15
1.6 Illustration of an MDP with two states and two actions. The transition probabilities and rewards are given by tuples $(p, R)$ . . . . .	18
1.7 An example of a path . . . . .	23
1.8 A car following model in highway driving. The subject car is in the middle, and the front vehicle is the lead car. The subject vehicle reacts to the change in the speed of the lead car. The rear car also reacts to the speed change of the subject car. . . . .	25
1.9 Type of suspension systems . . . . .	30
1.10 An emergency situation in traffic. The driver is not able to respond to the situation sufficiently. The proposed system take over the control of the vehicle and executes a <i>human</i> like decision to avoid the object as well as not crashing the other cars. . . . .	35
2.1 System model with related traffic quantites of each $TVs$ . Notice that the relative distance values are defined from each $TVs$ and velocities are also shown for each $TV$ . . . . .	41
2.2 Gaussian membership function for relative position. Notice that the centering of each linguistic label is defined en terms of $SV$ speed. . . . .	43

2.3	Gaussian membership function for relative velocity. Notice that the centering of each linguistic label is defined en terms of <i>SV</i> speed. . . . .	44
2.4	Gaussian membership function for cruising velocity. Notice that the centering of each linguistic label is defined en terms of <i>SV</i> speed. . . . .	44
2.5	Gaussian membership function for threat . . . . .	45
2.6	A cartesian coordinate is assigned for each vehicle. . . . .	50
2.7	This graph is intended to show the visual set-up with two camera orientations. Green vehicles denote the <i>TVs</i> in the left lane, light blue vehicles are the <i>TVs</i> in the right lane. Animation is seen at 2 seconds . . . . .	50
2.8	Animation snapshot at 12 seconds . . . . .	51
2.9	Animation snapshot at 33 seconds . . . . .	51
2.10	Accelerations of vehicles . . . . .	52
2.11	Positions of vehicles . . . . .	53
2.12	Velocities of vehicles . . . . .	53
2.13	Threat of vehicles in left lane . . . . .	54
2.14	Threat of vehicles in right lane . . . . .	54
2.15	Markov chain with 16 states . . . . .	56
2.16	An MDP with 16 states . . . . .	57
2.17	Scenario description . . . . .	58
2.18	Lane changing model . . . . .	59
2.19	Solution of MDP . . . . .	62
2.20	A Markov game with multiple agents . . . . .	67
2.21	Example of equilibrium . . . . .	69
2.22	General non-zero-sum Markov game set-up with multiple agents . . . . .	70
2.23	Markov game matrix . . . . .	72
2.24	Solution of game with candidate generation by prediction . . . . .	75

2.25	A cartesian coordinate system is assigned to all the vehicles. The quantities such as length and width of cars are same for all vehicles, which is only depicted on <i>SV</i> . . . . .	88
2.26	This graph is intended to show the visual set-up, with two different camera orientations of the simulated traffic. First, the <i>SV</i> starts with an initial speed of 22 m/s and it encounters an obstruction in its drive lane and searches for a gap. . . . .	90
2.27	<i>SV</i> turns on the turning signal and adjusts its speed in order to merge the gap ahead of <i>TV2</i> . Even though <i>TV2</i> 's objective is to prevent <i>SV</i> from lane changing, <i>SV</i> seeks to maximize the lower bound of <i>TV2</i> 's action . . . . .	91
2.28	This is a cooperative case where <i>SV</i> turns on the turning signal to the right gap in of <i>TV4</i> and <i>TV</i> yields to <i>SV</i> for lane changing. . . . .	92
2.29	As <i>SV</i> merges, <i>TV4</i> decelerate to open a larger gap to merge in, consequently, eases the lane change process. . . . .	92
3.1	Schematic view of vehicle lateral dynamics . . . . .	96
3.2	Control structure of a lane change maneuvering . . . . .	99
3.3	Weighting control structure . . . . .	101
3.4	Input shaping filter . . . . .	104
3.5	Disturbance profile . . . . .	106
3.6	Control inputs . . . . .	107
3.7	Reference tracking . . . . .	107
3.8	Yaw angles . . . . .	108
3.9	Vehicle dynamical model . . . . .	110
3.10	Cornering force for $\mu=[0.1, 0.3, 0.5, 0.7, 0.9]$ . . . . .	113
3.11	Cornering stiffness for $\mu=[0.1, 0.3, 0.5, 0.7, 0.9]$ . . . . .	114
3.12	The control system structure . . . . .	116
3.13	Weighting control structure . . . . .	117
3.14	Tire cornering stiffness change in road profile . . . . .	122

3.15 Wind disturbance . . . . .	123
3.16 Commanded steering . . . . .	123
3.17 Yaw rate outputs . . . . .	125
3.18 Slip side angle outputs . . . . .	126
3.19 Yaw moments . . . . .	126
3.20 Yaw rate vs steering . . . . .	127
3.21 Triangular membership functions . . . . .	129
3.22 State-feedback tracking controller . . . . .	133
3.23 Commanded steering for double lane changing . . . . .	137
3.24 Yaw rate outputs . . . . .	139
3.25 Slip angle outputs . . . . .	139
3.26 Yaw moment . . . . .	140
3.27 Steering-yaw rate outputs . . . . .	141

## LIST OF TABLES

TABLE	Page
2.1 Fuzzy inference rule table . . . . .	48
2.2 Design parameters used in simulation . . . . .	55
2.3 Design Parameters Used in Optimization . . . . .	87
2.4 Initial conditions of vehicles for scenario1 . . . . .	89
2.5 Initial conditions of vehicles of scenario 2 . . . . .	89
3.1 Vehicle parameters . . . . .	108
3.2 Vehicle parameters . . . . .	124
3.3 Fuzzy Rule Table . . . . .	131
3.4 Vehicle parameters . . . . .	138

## 1. INTRODUCTION AND LITERATURE REVIEW

### 1.1 Background

Even with the enhanced safety measures integrated in modern vehicles, the increasing number of vehicles on roads continues to produce a large number of traffic accidents on a yearly basis. In the last decades, autonomous driving has been a popular research area both in industry and academia. One of main objectives of autonomous vehicle research is to prevent the accidents caused by human errors. Because the traffic collisions are still one of the leading causes of deaths in entire world. In 2016, there were 40,200 people killed and 2 million more were injured in motor vehicle crashes in the United States [1]. The financial effects of the road crashes to the USA is a total cost of \$432.5 billion per year, an increase of 12 % from 2015 [1]. In this regard, the car manufacturers have offered a variety of safety systems in their cars that range from the adaptive cruise control to lane departure warning system and anti-lock braking systems. Some other examples include braking assistance systems [2, 3], traction control systems [4], collision warning systems [5], lane-keeping systems, and lane change support [6, 7]. Research studies in active safety system design does not only involve automation of individual vehicle subsystems, but also includes improved functionality of sensing and decision-making. The introduction of sensor technology in vehicles has enabled new possibilities of providing information concerning vehicle surroundings. This information is used to identify obstacles on the road that can be further analyzed by a decision-maker to execute the best possible actions such as a lane change or braking to avoid an accident. In the case of references on a roadway, the sensing systems are classified into two categories [8]: look-down and look ahead systems. Look-down sensing systems (either electrified wires or permanent magnets) have the advantages of being reliable, yielding accurate results and good performance under different weather

conditions. Richard Bishop addresses the above considerations in his paper [9]. The paper mentions about the main components in autonomous driving technology, including the vehicles vision systems, radar systems as well as the applications in adaptive cruise control and collision warning systems.

Intelligent transportation systems (ITS) is a premier forum that covers a variety of applications. I primarily focus on human-vehicle interaction in automotive systems. Therefore understanding human behavior is the main pillar of above autonomous driving technologies. The topic of human drivers has been studied in the literature [10]. It is important to point out that there is no comprehensive method that captures of all human behaviors. However, several contributions have been made to the field in the recent decades. Hancock et al. [11] explains the human factor in Intelligent Vehicle and Highway Systems design. The main focus on sense of safety in driving. Second issue addressed is drivers workload such as navigation of traffic, vehicle controls and collision avoidance. Several tasks combined makes a reliable and safe design challenging task. Parker *et al.* [12] investigate driver errors and violations. Tendency to a make error is divided in two parts; drivers misjudgment and experience and deliberate driving violations. Salvucci [13] explores human driver cognitive architecture for control and decision making. The model discovers the limitations of general human abilities in driving domains. Trulls Vaa [14] explains perception of risks, the consciousness in driving, as well as cognitive human driver models. [15] examines human drivers in dynamics and control point of views. Human belief state determines the responses to a given traffic situation [16]. The decisions are simply made based on the perception of a driver, which mostly rely on subjective reasoning process [17]. A decision is made by a driver at each instant of time. As soon as a decision is made, an action of accelerating, decelerating or keeping the current state of the vehicle is performed by the driver. Human driving factor, therefore, has significant influence on driving. For example, the gender and age have important differences on driving style as well. One can

claim that the safety is directly related to the age of the driver since the young drivers pose more aggressive style than that of old drivers.

With this regard, It is quite essential to approximate a driver's intention to a real time driving with a set of logical decision methods. This is to say, I develop a stochastic decision reasoning method based on a set of established logical driver perceptions for an emergency lane change problem. The model relies on a Fuzzy Markov Decision process based discrete dynamics and a Quadratic programming based MPC control for appropriate maneuvers to avoid accidents. The trajectory is then followed by a controller wherein a nonlinear vehicle model and a Linear Parameter Varying controller are employed. Overall system forms a hybrid system structure to approximate the human reasoning process to the actual mechanical output of the vehicle.

## 1.2 Objectives

In this work, we focus on designing an active safety system with a two level structure with a driver decision model algorithm that addresses the problem of avoiding obstacles in a lane in a three lane highway driving environment, and a driver driving model that performs a lane change task to a desired lane by combining several theories in the field of study. The driver decision model executes a decision based on stochastic reasoning of human with the fuzzy Markov game (FMG). This step determines an action with the most beneficial to the driver (*highest safety*), also the target lane as well as the target velocity of the subject vehicle by taking into account the interactions with surrounding vehicles. The target outcomes are fed to a trajectory generator where the subject vehicle's motion is planned. The combined assessment of the designing is performed in several driving simulations.

The next objective is to be able to follow this trajectory with the highest accuracy in a real driving scenario. With this regard, I consider a real vehicle dynamics model

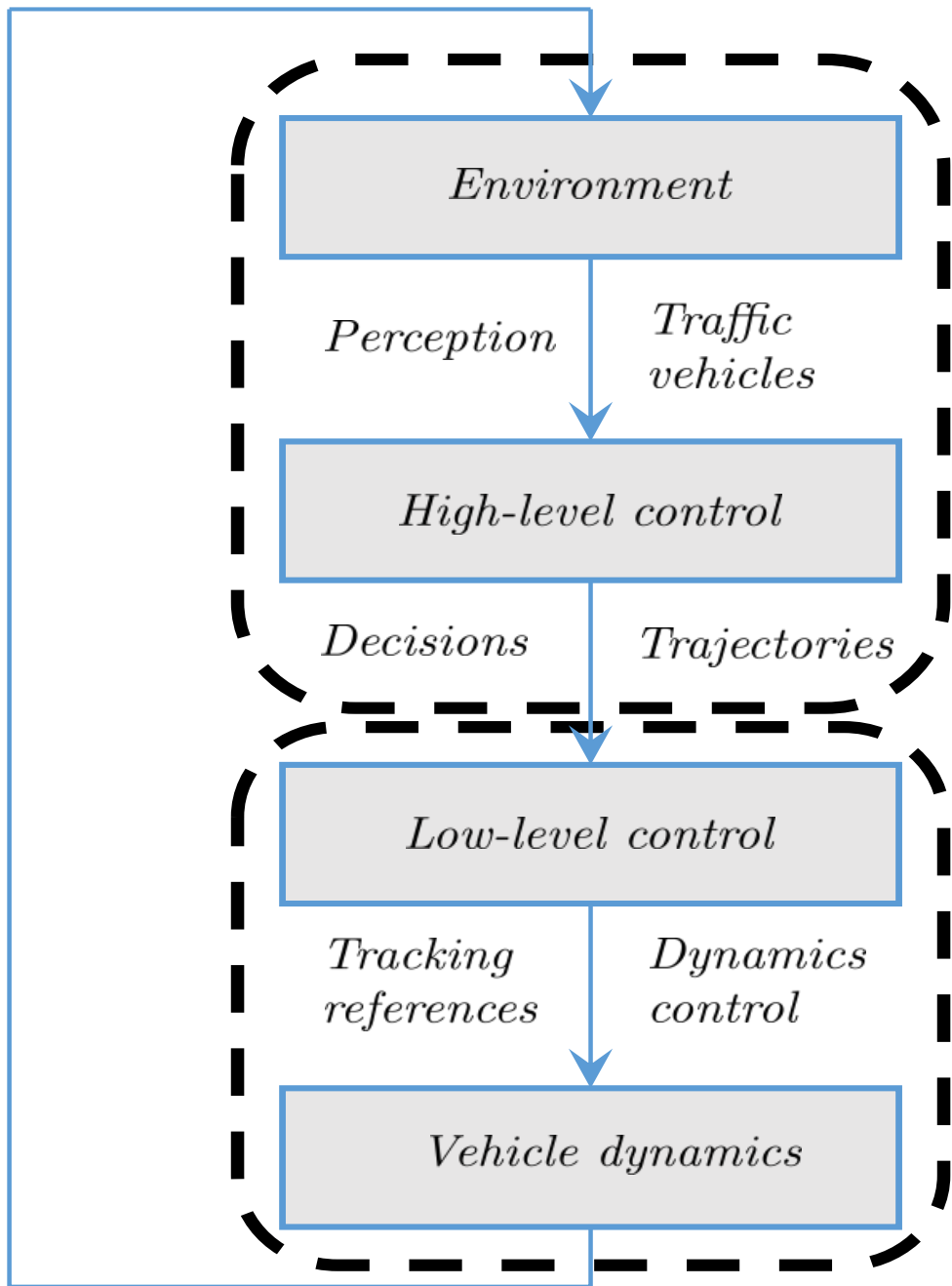


Figure 1.1: Driver model of an autonomous vehicle

and controller design to follow the online generated path in a simulation model. The driver driving model has the actual dynamics of a vehicle and a mechanical controller to follow the reference trajectory with the highest accuracy. The overall design includes the techniques of the artificial intelligence, the convex optimization and the robust control concepts to create an emergency lane change active safety system in highway driving.

### 1.3 Background and Literature Review

#### 1.3.1 Driver Decision Models (Higher Level Controller)

Understanding of a human driver behavior has been an attractive topic to many researchers. With the high demand of the mathematical models in accordance with different kinds of applications, there has been a variety of driver models proposed. Some of the demands to be mapped in driver models are listed as;

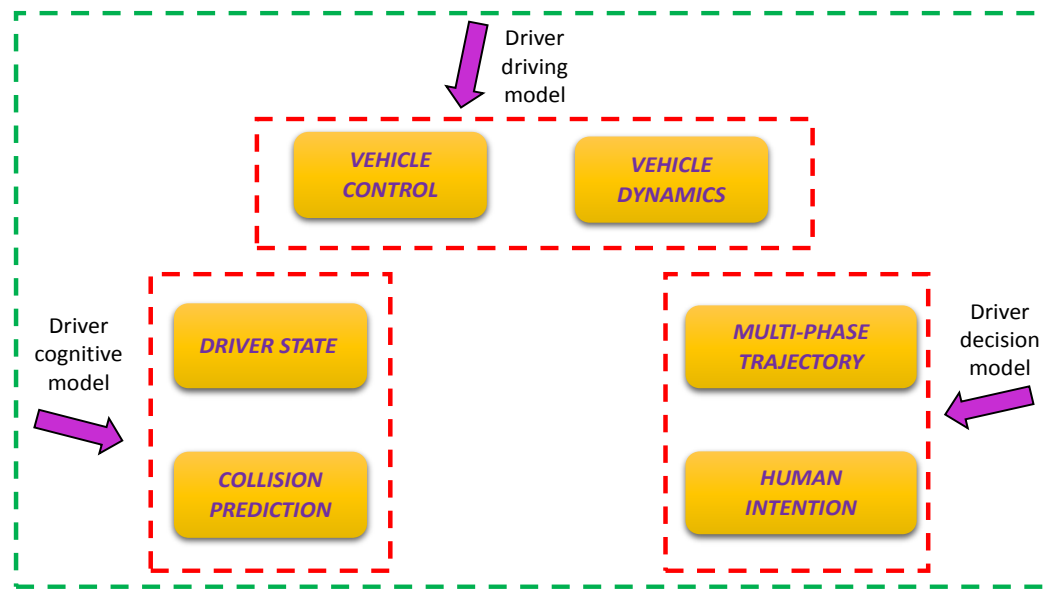


Figure 1.2: Schematic diagram of the proposed driver model

- General driver skills, information perception and processing, time delays, preview, adaptation,
- Learning and planning ability (path and speed adjustments),
- Types of drivers such as experience, age, and aggressiveness,
- Features like emotions, concentrations and driver's psychological state etc.

Depending on the application discussed above, several ideas have been proposed. One major aspects of the proposed models lies down on mathematical modeling such as using control theory (transfer functions, optimal and adaptive control), fuzzy logic, and neutral networks -hybrid approaches, which generally lead to differential equations. We will start the discussion of the problem of driver modeling from classical transfer function models to fuzzy logic and game theoretical based modeling as well as stochastic models such as Markov models.

Considering a design of an advanced driver assistance system, it the main aim of investigation to form the overall design as automobile-driver coupled system. After defining driving task and environment where it is indeed necessary to introduce the traffic dynamics into the design. We can write down the main concerns of analysis with the following headlines

■ The vehicle:

design and control of vehicle components; including vehicle dynamics and material design of subcomponents.

■ The driver:

understanding individual driver as well as interaction of the drivers in a traffic situation; path and velocity planners; subjective driver behaviors for decision making.

■ The environment:

traffic flow; influence of other traffic participants; modeling of the traffic system.

■ The combined system:

accident possibilities; accident prevention; driver support and learning tasks.

The extensive driver models built based upon individual driver behavior (i.e., missing driver interaction dynamics) are available in the literature. Most of developed models have considered to control lateral vehicle dynamics while longitudinal dynamics is often thought to follow a given speed profile (i.e., car following models are shown in the upcoming subsections), independent of steering task of the driver. Plöchl *et al.*[18] explain several driver models in their paper. This dissertation introduces some of the models as background information in the field. Kondo *et al.* introduce one of the fundamental driver modelings in the literature [19]. They considered a 2-wheel vehicle model on a straight way with constant velocity and wind disturbances, Kondo's model adjust the vehicle's position by steering to a point with which the vehicle centre line coincides. A preview distance  $L$  is defined in the reference. The main idea is to reduce the deviation  $\Delta_{y_{vehicle}}$  in a distance  $L$  ahead of the vehicle i.e., looking-ahead distance. The relation of the figure is defined with the following equation

$$\Delta_{y_{vehicle}} \approx y(t) + L\psi(t) = y(t) + T_{vehicle}v\psi(t) \approx y(t + T_{vehicle}) \quad (1.1)$$

where preview time  $T_{vehicle} = L/v$ , vehicle speed  $v$ , yaw angle  $\psi(t)$  and deviation is defined  $y(t)$ . The changes on the lateral deviation i.e.,  $\Delta_{y_{vehicle}}$  is interpreted as the change on the lateral direction with respect to the preview time i.e.,  $y(t + T_{vehicle})$  From a control theory point of view, a proportional steering control strategy,  $C(s) = K$  leads to the steady-state error to zero i.e.,  $\Delta_{y_{vehicle}} = 0$ . In [20] another human tracking based model is given.

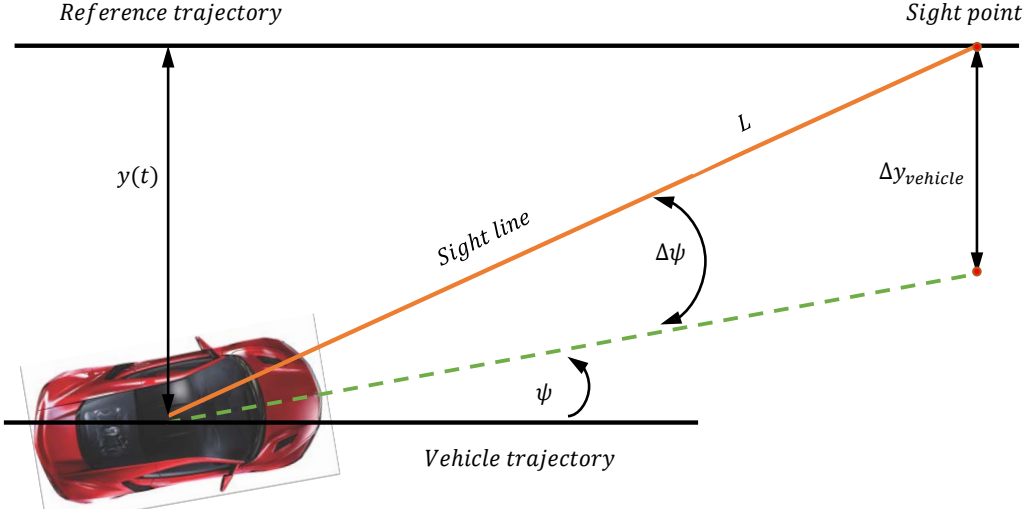


Figure 1.3: Kondo's driver model

$$C(s) = \frac{K(T_L s + 1)}{(T_I s + 1)(T_N s + 1)} e^{-\tau_r s} \quad (1.2)$$

In this model, human reaction time is given  $\tau_r$  and the neuromuscular delay time is  $T_N$  are human properties, perform independently from the task. The other parameters  $K, T_L, T_I$  are associated with system. Kondo later introduced a second driver model that presents a linear deviation of the yaw angle and lateral position. This is an inspiring model, which have been modified and used in the literature. Another driver model is proposed in [21, 22]. The main idea is to compensate the deviation of the lateral position of the vehicle  $\Delta y_{vehicle}$ , with respect to a reference target position and the yaw angle error.

There are approaches in driver modeling that take into account when the road is straight and curved  $\rho_r$ . One of the works [23] Reid et al. define the steering control law as follows

$$\delta_c = K_c \rho_r^* + K_\psi \Delta\psi_e + K_y \Delta y_e \quad (1.3)$$

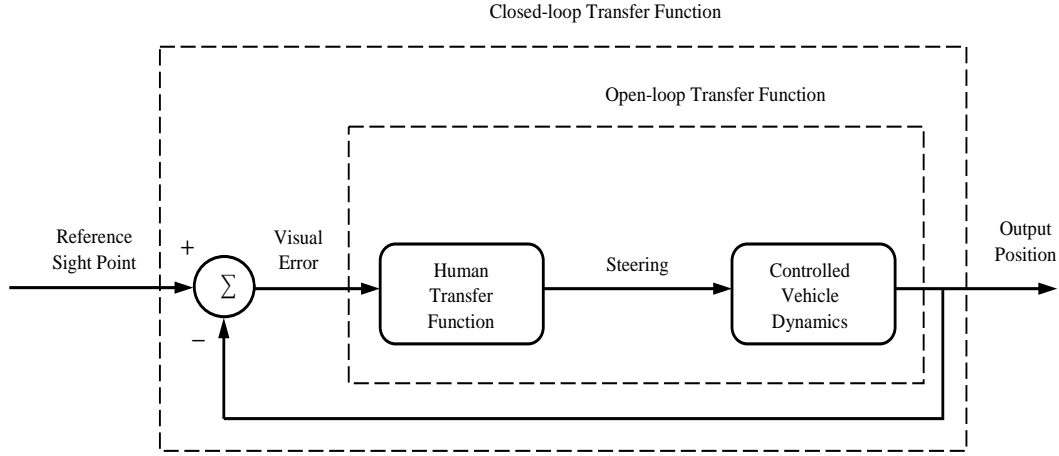


Figure 1.4: Transfer function of driver model

where  $\rho_r^*$  is the road curvature point ahead, which will be previewed by the car after the preview time  $T_P$ , the difference between the vehicle heading angle and the heading angle of the roadway at a point is  $\Delta\psi_e$ , and  $\Delta y_e$  is the distance from vehicle's center line to the lane center-line at a point.

Based on the driver models, the human regulation control tasks are studied in frequency domain [24]. The open-loop transfer function i.e.,  $C(s)G(s)$ , which the combined form of driver  $C(s)$  and vehicle dynamics  $G(s)$ , is described the crossover model with

$$C(s)G(s) = \frac{\omega_c}{s} e^{-\tau_r s}, \quad (1.4)$$

that imposes a behavior amount of  $-20\text{dB/decade}$  in the magnitude due to the integral, and a phase shift  $-90^\circ$  around the crossover frequency  $\omega_c$ . Even though human driver is capable of compensating tracking errors regardless of vehicle characteristics, the input excitation signal restricts the crossover model behavior, especially in high gain at different driving maneuvers.

The idea of combined driver models, which has two-level structure is not a new idea proposed in the literature. Donge in [25] proposed a two level model where the road characteristics and a driver model form a layer, separated from the vehicle dynamics. He defines an anticipatory open-loop and a compensatory closed-loop control. The open-loop control determines the anticipatory steering response to be able to run of the path curvature. The parameters of interests in this layer are estimated by measuring the desired path curvature and the steering angle of the driver. Donge also suggest that human driver anticipate the change in road curvature and initiate front steering before the curve begins. A differential equation to model of the required anticipatory steering angle is proposed in [26]

$$T_2^2 \ddot{\delta}_a(t) + T_1 \dot{\delta}_a(t) + \delta_a(t) = V_a \kappa(t + T_a) \quad (1.5)$$

where  $T_a$  is the anticipation time and  $\kappa$  is the desired path curvature. In order to determine the open-loop steering angle to follow a given trajectory with high accuracy for a 2-wheel vehicle model, the parameters  $T_2$ ,  $T_1$  and  $V_a$  are set as the functions of vehicle parameters and speed. In the compensatory closed-loop control level is responsible of stabilization of the driver steering wherein actual and desired path curvature is compared, i.e.,  $\Delta\kappa$ , along with the observation of the heading angle error of the vehicle  $\Delta\psi$  and lateral deviation of the vehicle  $\Delta y$ . The mathematical formula of the compensatory steering angle is

$$\delta_c(t) = -[h_k \Delta\kappa(t - \tau_r) + h_\psi \Delta\psi(t - \tau_r) + h_y \Delta y(t - \tau_r)]. \quad (1.6)$$

where  $\tau_r$  is the lag of human driver, and the gains  $h_\kappa, h_\psi, h_y$  are computed based on the measurement difference, open-loop control contribution, and minimizing a quadratic function.

Taking into account the vehicle's nonlinear dynamics, several nonlinear control meth-

ods have been proposed to present a driver model in [27]. With a multi-level structure, in which a guidance level sets the reference trajectory and velocity profile of the vehicle to a target point. In the stabilization level, a position controller to force the current state of the vehicle i.e., current target point to a desired target point with a suitable steering wheel angle and brake/acceleration. In this level, the vehicle position on  $x, y$  axis is controlled by nonlinear front lateral tyre forces and longitudinal tyre forces, which allows one to simultaneous control of lateral and longitudinal dynamics.

Another type of modeling of a human driver is fuzzy logic control (FLC). The fuzzy logic control relies on analyzing input values in terms of logics that is resemble of human thinking process, and a useful tool process of decision making when the system structure is very complicated. In terms of application, there are fewer works in the literature. One of the leading works have been proposed in [28]. The overall structure of the control loop is drawn below. Assuming a complete preview information regarding upcoming road curvature on the reference, the controller is formed in feedforward, feedback, and gain scheduling rules. The inputs to the feedback rules are defined as the combination of state errors of the system, i.e.,  $[y, \dot{y}, \dot{\psi} - \dot{\psi}_d]$  the vehicle's lateral error with respect to the road center, the lateral velocity error, and the yaw rate errors respectively. The inference rules consist of linguistic variables  $LE$  (associated with  $y$ ),  $CLE$  (associated with  $\dot{y}$ ),  $YWR$  (associated with  $\dot{\psi} - \dot{\psi}_d$ ), and  $\Delta FB$  (associated with  $\delta_{fb}$ ). A feedback rule is given with the following form:

$$\text{IF } LE \text{ is } A_{LE} \text{ AND } CLE \text{ is } A_{CLE} \text{ AND } YWR \text{ is } A_{YWR} \text{ THEN } \Delta FB \text{ is } A_{\Delta FB} \quad (1.7)$$

where linguistic values of  $A_i$ ,

$$A_{LE} \in \{NB, NS, NIL, PS, PB\},$$

$$A_{CLE} \in \{NB, NS, NIL, PS, PB\},$$

$$A_{YWR} \in \{NB, NS, NIL, PS, PB\},$$

$$A_{\Delta FB} \in \{NH, NB, NM, NS, NIL, PS, PM, PB, PH\},$$

with the 5 different subsets for  $A_{LE}$ ,  $A_{CLE}$ ,  $A_{YWR}$  are given ( $NB \Rightarrow$  negative big,  $NS \Rightarrow$  negative small,  $NIL \Rightarrow$  nil  $PS \Rightarrow$  positive small,  $PB \Rightarrow$  positive big) with triangular membership functions. Therefore,  $5^3 = 125$  rules in feedback rule base. For defuzzification, 9 subsets with 4 new different subsets given (( $NH \Rightarrow$  negative huge,  $NM \Rightarrow$  negative medium,  $PH \Rightarrow$  positive huge,  $PM \Rightarrow$  positive medium) that results in a crisp steering angle  $\delta_{fb}$ .

A wheel steering preview angle term  $\delta_{pr}$  is generated with respect to preview weight  $p$  divided by the future curvature  $\rho$ , over preview time window [28]. Consequently, the  $\delta_{pr}$  takes the form

$$\delta_{pr} = \frac{p_c}{\rho_c} + \frac{p_n}{\rho_n} \quad (1.8)$$

where  $p_c$  and  $p_n$  are the current and next radii of curvature preview parameters, respectively. The detailed information on selection of the parameters is given in [28].

The final steering wheel angle based on the feedback rule base and the preview rule base is determined in the gain scheduling rule base by taking into account the vehicle speed  $v$ . There velocities  $v_1 = 5m/s$ ,  $v_2 = 12,5m/s$ , and  $v_3 = 20m/s$  are introduced in the feedback and preview rule bases and the gain scheduling rule is therefore defined

$$\mathcal{IF} V \text{ is } A_V \text{ THEN } \delta_c = \delta_{fb}^i + \delta_{pr}^i, \quad (1.9)$$

where  $A_V \in \{\text{small, medium, big}\}$  at  $v_i (i = 1, 2, 3)$ . More details can be found [28].

Moreover, the artificial neural networks (NN) is a powerful tool to present a human driving behavior. A longitudinal model, based on NN, is studied in [29] where the goal is to follow a reference velocity in different driving cycles. A block diagram is shown below. Two NN controllers are responsible for different goals. The fixed NN is to model a driver for reference velocity following  $r(t)$ . The NN is trained with input/output data. The inputs are the error  $e(t) = r(t) - v(t)$ , where  $v(t)$  is the velocity of the vehicle,  $r(t)$ , preview velocity  $r(t + k_1)$   $k_1 = 1.1\text{sec}$ , and the time delayed error  $e(t - k_2)$   $k_2 = 0.4\text{sec}$ . The adaptive NN controller functions with the driver model, as the name refers it compensates the  $e(t)$  with respect to the changes in road conditions.

*Most of the models introduced above only considers modeling a human driver model are useful when the implementation only requires individual car behavior without taking into account other cars actions. Current trend in autonomous driving involves not an action of the vehicle determined for individual benefit but an action executed after the other cars behaviors have been assessed.* This also opens a door to implement a control system structure for autonomous vehicles includes a two level structure where a higher level controller (driver model) assesses the uncertain driving environment, creates reference trajectories for the lower lever controller to follow, and provides safe driving along with fuel economy and comfort, while a lower level controller performs the commanded actions. The autonomous vehicle has several features that are associated with drivers behavior when they encounter varying traffic situations. A higher level controller or so called driver models offer an approximation of a driver behavior. This module is also called planning route. As the name denotes, route planning (i.e., the state in which the vehicle be in the next time step), and behavior decision-making (i.e., discrete values of the states wherein a continuous decision is produced at each time step) are main elements of this module. Route planning generates safe driving areas for autonomous vehicle. The

behavior decision-making provides reasonable driving actions such as turning left, turning right as well as accelerating and decelerating turning in different directions based on how the driving environment is defined. Yoo and Langari in [30] presented a game-theoretic risk estimation of the other cars behavior and corresponding time evolution of the collision areas. A predictive driving controller successfully avoids the collision area based on the subject car's safety assurance level. They first define the relative dynamics of two interacting vehicles, attached relative to the vehicle of interest. A hybrid model is formed such that lane change decision leads to two modes, i.e., approaching the adjacent lane and stabilization in the adjacent lane.

$$\begin{aligned} f_{approach} &= \frac{K}{T}(x + a), \\ f_{stabilization} &= -\frac{K}{T}(x - b) \end{aligned} \tag{1.10}$$

where  $T$  denotes the period of lane changing,  $K, a, b$  are related to model parameters. Incorporating the driver's aggressiveness, an aggressive driver is assumed to complete a lane change task in shorter time. A discrete forward reachable set analysis forms an unsafe region for the subject vehicle. A non-cooperative Nash game along with an utility function in driver's decision model is employed to estimate the player's driving strategy according to the subject vehicle's strategy and the hybrid mode of the system. Model predictive control adjust the longitudinal control of the subject vehicle to stay outside of the collision region. The optimization is given

$$\underset{u}{\text{minimize}} \quad J = \int_{t_0}^{t_f} (x^T Q x + u^T R u) dt$$

$$\text{subject to } \dot{x} = f(x, u), x_1(t_0),$$

$$x_1 \geq C_{v,upper} \vee x_1 \leq C_{v,lower},$$

$$x_2(t_f) = 0,$$

$$a_{min} \leq \dot{u} \leq a_{max}.$$

where  $J$  is the quadratic cost function with weights  $Q, R$ , the period for the cost function to be minimized  $[t_0, t_f]$ ,  $f(x, u)$  denotes the system dynamics with  $x$  is velocity and  $u$  is control input,  $C_v$  is the collision cross section area in  $\mathbb{R}^2$ . Simulations are performed for timid and aggressive drivers. The subjective collision perception for different types of drivers affects the recognition of risk and driver's driving controller allows the subject vehicle to stay outside of the region.

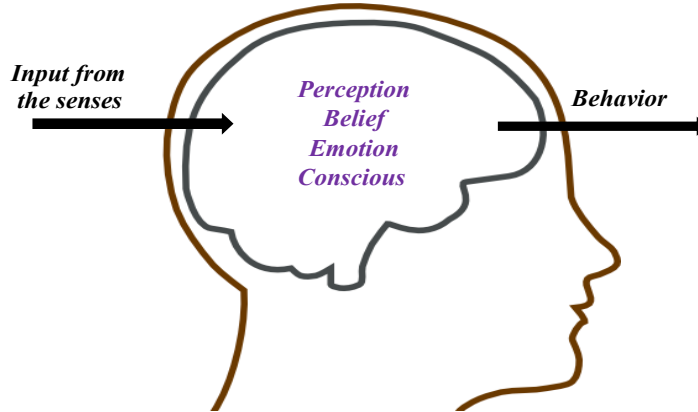


Figure 1.5: A schematic process of a human like decision making. Human brain collects the information from environment and processes based on a subjective reasoning process and executes an output according to the current state of cognition.

Neutral networks is another approach used in autonomous driving. The neutral networks is often called as black box. It can function as controller after a sufficient training process. Shai Shalev-Shwartz *et al.* [31] proposes a neutral network based driving strategy where the system is trained with real time data. Then the future behavior of the cars can be easily predicted. Kim and Langari use a higher level decision strategy where the analytic hierarchy process (AHP) is used to by evaluating driving safety, traffic flow, and the fuel economy simultaneously in [32]. The proposed adaptive AHP is able to handle the decision making process under different traffic situations and driving modes.

The driving is an uncertain dynamical process. It is quite hard to create a deterministic driver model due to uncertainty of the driver behavior under different environments. Markov Chains is a promising tool to predict driver behavior in such cases. A discrete Markov process is a stochastic process that satisfies the Markov properties. The discrete Markov process produces transitional probabilities of a finite number of future events without any knowledge of the past events. The fact that the next event only depends on the present event is one of the key properties of a Markov process. The term one-step transition probability is used to define the conditional probability of visiting a particular state in the next transition given the current state [33]. We first define the state of the system at time  $t$  as  $S(t)$ . A set of finite number of states is indexed by integers from 0 to  $n$ . Let us denote  $P(S(t) = i)$  be the probability of being in state  $i$  at  $t$  time. And  $P_{ij}$  denotes the transition probability of state  $j$  given that the current state is in state  $i$  at time  $t$ .

$$P(t) = \begin{bmatrix} P_{00}(t) & P_{01}(t) & \dots & P_{0n}(t) \\ P_{10}(t) & P_{11}(t) & \dots & P_{1n}(t) \\ \vdots & \vdots & \ddots & \vdots \\ P_{n0}(t) & P_{n1}(t) & \dots & P_{nn}(t) \end{bmatrix}$$

In [34], the authors proposed a stochastic driver model based on Markov Chains. Ex-

perimentally collected data is used to estimate the transition probabilities that lie in a convex uncertainty set. The model predicts a set of trajectories in the subsequent time interval for different environments and states of the vehicle.

### 1.3.2 Markov Decision Process (MDPs)

We can divide the decision making into two categories; the deterministic and the stochastic decision outcomes. For the stochastic outcomes, the different outcomes have different utilities. A good decision making weights the all these outcomes utilities to the probabilistic numbers. Human reasoning relies on a decision making with several outcomes. The quality of an outcome is subjective i.e., It depends on the human perception. With this regard, modeling of the human decision model with a set of outcomes is a good approach in a decision process. Since the quality of a decision is determined by a particular driving conditions i.e., a rational decision might result in a good outcome in normal driving condition while a rational decision might lead to an accident in an abnormal driving condition, a decision made by human drivers associated with stochastic outcomes will be the ground of our research activity. *For lane changing maneuver, the driver is influenced by surrounding vehicles behaviors.* This means that the likelihood for specific outcomes is determined by the vehicles in neighboring lanes.

The main decision considerations for a lane change maneuver in an obstacle avoidance are the followings:

1. Which gap to choose for merging in neighboring lanes.
2. When to initiate the actual maneuver into the gap.
3. If the maneuver is able to performed.
4. If the maneuver is safe for avoiding the obstacle.

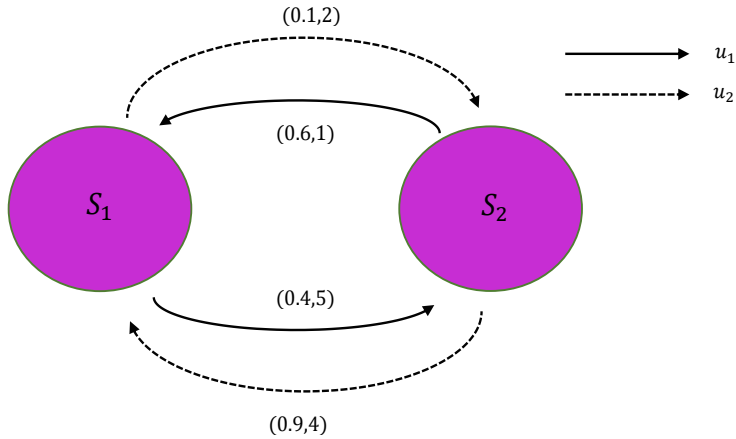


Figure 1.6: Illustration of an MDP with two states and two actions. The transition probabilities and rewards are given by tuples  $(p, R)$

The outcomes of the decision is based on the probabilities and the utilities (*rewards*), so that the estimation of these set of numbers is crucial. In this work, It is assumed the sensor system has a perfect measurement. This means that the detection of the vehicles as well as the objects is unlimited. The sensor system also has the complete information of the velocities and relative positions of the vehicles to the subject vehicle. The objective of the proposed model and algorithm is to capture a human like reasoning of a decision to be made. In the solution process, some simplified assumptions are carried out. There is an assumed available gap as well as the detection of an object is drive lane is fully known.

### 1.3.2.1 MDPs in autonomous driving

Markov decision process has been used as a decision-making model in autonomous vehicle research. It has several features such as modeling the uncertainty with a set of probabilistic numbers, executing several possible actions in a given traffic condition, and being able to capture human reasoning that makes a logical selection among all possible alternatives in a decision making process. In order to enhance the understanding the

MDPs, the basic concepts are demonstrated in this section.

Markov Decision processes (MDPs) are powerful tools for sequential decision in stochastic environments where an agent has to execute an action to achieve an objective. Executing an action  $u \in \mathcal{U}$ , given the system is in a state  $s \in \mathcal{S}$  is defined as a policy  $\varphi : s \rightarrow u$ . In order to find such an optimal policy i.e.,  $\varphi^*$ , a linear programming or a dynamic programming equation is iteratively solved.

Brechtel *et al.* [35] consider a discretized MDP model derived from a continuous state-space model is proposed. They extend the discussion by including the uncertainties in the driving with the Partially Observable Markov Decision Processes (POMDP) in [36]. Their solution of the problem based on the position and velocity states of cars. Ulbrich *et al.* [37] consider the Partially Observable Markov Decision Processes (POMDP) to model the uncertain and dynamic driving environment for a single lane driving. They use a small set of 8 to describe the highway driving situations. The high computational burden observed in [35, 36] is solved with signal processing networks to simplify their POMDP solution. Even though their POMDP set-up can be practical, computation time remains a challenge and It is not suitable for online application in an emergency lane change decision making. Moreover, their work only considers a lane change into one gap and the selection between the gaps is not addressed. Wei *et al.* [38] presents a point-based Markov Decision Process algorithm is proposed as an approximate solution to the POMDP for a single lane autonomous driving behavior. The uncertain behaviors of traffic participants are considered to implement in a specific traffic situation. They introduce a set of cost functions to model the driving environment for decision making. Only a longitudinal control of the subject vehicle is considered in their work. These and similar higher level controller designs are increasingly being considered to both avoid and minimize accidents and as a prelude to fully autonomous driving systems of the future.

### 1.3.3 Game Theory

Game theory has been used widely as a decision maker in social sciences and in engineering field because of its advantage to model the interactions between players. There are mainly two types of games; cooperative and non-cooperative games. The first case where the players benefit from individual coalitions, the joint action sum of collective objectives of the players. In this case, the players receive information about their actions, subsequently exchange information of their payoff's. The second case the objectives are conflicted where the players seek to achieve their own strategies regardless of what the other player gains. Moreover, a non-cooperative game is also characterized as the players do not exchange information about their individual actions, rather the decision are made independently.

#### 1.3.3.1 Game Theory in autonomous driving

Game theory is a promising decision making for autonomous vehicles where It does not only predict the subject car's behavior but also evaluates and sets up a game according to the surrounding vehicle's behavior i.e., the lateral and longitudinal movement, or more complicated movement can be considered simultaneously. A cooperative multi-agent system is modeled by combining the individual cost function into a team cost function in [39]. Nash-bargaining solution is proposed for minimum individual cost by maximizing the difference between cooperative and non-cooperative cases. Kita in [40] developed a game theoretic interactions model of cars in a merging-giveaway scenario. A pair of merging and through cars interaction is explicitly considered, which they take the best actions from their perspectives, thus the game forms a two-person non-zero-sum non-cooperative game. In [41], the authors considered a lane-changing model in a connected environment where the notion of incomplete information is utilized in a two-person non-zero-sum non-cooperative game solution. Wang et. al in [42] proposed a differential game where the

controlled vehicles execute decisions according to the expected behaviors of other vehicles. In this work, two game solutions are proposed; non-cooperative game where the vehicles optimize their own costs and cooperative game where the collective cost function is optimized with coalitions. Yu *et al.* in [43] consider a human-like game theoretic model of lane changing involving interaction with surrounding drivers using the turn signal and lateral moves and their aggressiveness. In [44], dynamic lane change decision making is performed by utilizing the idea of Receding Horizon control. The decisions are updated as new information is available to the autonomous vehicle. Some other examples of the design of the higher level controller using the Game theory for autonomous lane changing in [45, 46] where a subject vehicle and the other traffic participants determine their actions within an optimization framework. In [46], the authors set up a scenario where the cars are driven on a 3-lane highway environment. They establish an action space as follows;

1. Maintain current speed
2. Accelerate to a speed up to  $110 \text{ km/h}$
3. Decelerate to a speed up to  $50 \text{ km/h}$
4. Move to the left lane
5. Move to the right lane

It is important to note that the actions provided by a higher-level controller in which the action commands are fed to a lower level controller to be performed by vehicle level dynamics and controller. A reward function is defined as summation of driver interests.

$$R = w_1c + w_2h + w_3e, \quad (1.11)$$

where  $w_i, i = 1, 2, 3$  are the defined weights for the terms  $c$  collision,  $h$  headway,  $e$  effort. For more details how these terms are defined, please see [46]. In this work, the driver's policies are stochastic and two approaches are employed for mapping. Level- $k$  approach and Jaakkola reinforcement algorithm. Main idea behind this, to obtain a driver policy that relies on the observation and interaction of the other drivers in traffic. Simulation results assess the effects of driver aggressiveness on the number of collisions and lane changes.

### 1.3.4 Trajectory Planning for Autonomous Vehicles

The problem of trajectory/path planning has been extensively researched in the literature. Path and speed planner can be seen as an internal driver task, which can be incorporated in the driver model. Many driver models require a desired path to follow, which is either assumed to be given or generated by a separate tool. A *path* is defined as a continuous sequence of configurations that connects an initial configuration to a terminating configuration [47]. In other words, a path is a geometric line on which the vehicle follows in order to reach a final point without colliding an obstacle. A *path-planning* algorithm then computes a feasible trace of a geometric configuration for an autonomous vehicle such that the design constraints i.e., road limits, vehicle dynamical limits, and traffic rules etc..are satisfied. A *maneuver* characterizes the motion of the vehicle in a road geometry. Some examples of maneuvers include 'turning right', 'turning left', or going straight'. On the other hand, the *trajectory planning* concerns a vehicle's motion in real-time from one possible state (velocities and positions) to another by satisfying the vehicle's dynamics constraints, safety constraints, design constraints as well as the rules of traffic [48]. In this regard, trajectory planning (or trajectory generation) is divided into sub-levels;

1. Finding the best path according to the vehicle dynamics limits to follow.
2. Finding the best maneuver to perform under constraints.

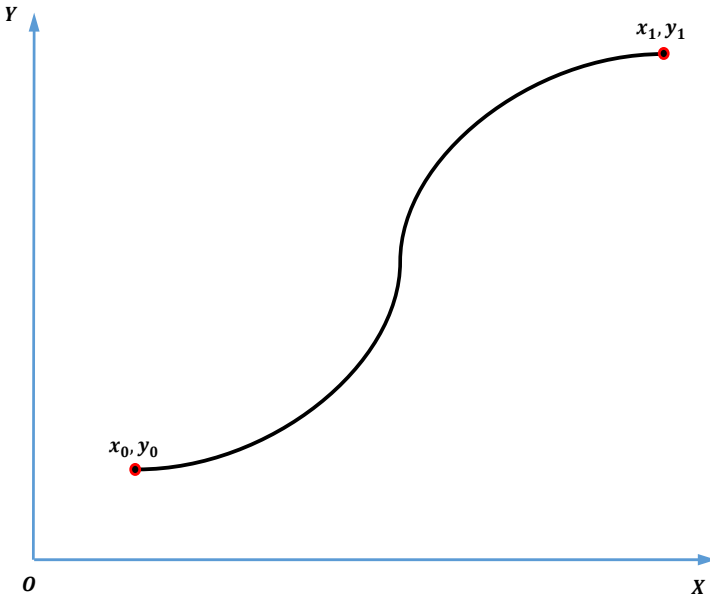


Figure 1.7: An example of a path

3. To be able to avoid an object in traffic.
4. Adapting the planning of a path according to the sudden change in traffic.

Vehicle kinematics and road entities have been considered in all existing studies. This is a founding element of path planning - trajectory generation problem in autonomous driving. A high amount of research has been made in trajectory generation for longitudinal and lateral movement for vehicle following as well as avoiding obstacles. Most of the works in the fields consider a lane change decision has been made by a higher lever controller or a driver decision model, then a feasible trajectory is computed satisfying the design objectives [49, 50]. Nilsson *et al.* [51, 52] consider utilizing a point-mass vehicle model to compute a maneuver in vehicle's longitudinal and lateral direction as well as a longitudinal velocity profile by using Model Predictive Control (MPC). Then the planned path is followed by a lower level controller wherein the vehicle dynamical model and a

Nonlinear Model Predictive Controller are employed. The trajectory generation is formulated within quadratic programming where the longitudinal and lateral control objectives are satisfied simultaneously. They introduce the Forward Collision Constraint (FCC) and the Rear Collision Constraint (RCC) as linear inequality constraints to avoid a crash with a car in the drive lane. Rosolia at al. [53] consider a point mass model and an MPC in outer loop to generate a collision free track and Proportional Integral (PI) control and bicycle model are used to track the trajectory in inner loop. Hosseini *et al.* [54] proposes an adaptive collision warning algorithm that supports the driver for collision avoidance. Their solution relies on two main functions; the first function is to generate a feasible trajectory based on the vehicle and road limits, a steering is performed for a safe lane change, the second function is to trigger an alarm signal to the driver when required. In their optimization solution, a bicycle model of a vehicle is employed. The steering control input is minimized by simultaneously satisfying the systems dynamics as well as design constraints.

### 1.3.5 Longitudinal Vehicle Control

An autonomous vehicle is required to perform two main tasks, i.e. to maintain a safe longitudinal spacing relative relative to the leading vehicle and to control the lateral motions of the subject vehicle [55]. The technical discussion to identify the longitudinal control behavior of drivers are sparse as compared to the works about lateral control behaviors in the literature. Longitudinal spacing of vehicles are particularly important from the safety point of view. The spacing is measured by the physical dimensions of the vehicles as well as the gaps between them. To this end, two microscopic measures the distance headway and distance gaps are widely used. These quantities are used to characterize an important concept in transportation community, so called car following models. Car following models produce an acceleration of the vehicle, which subsequently establishes

an effective traffic simulations, based on relative position, relative velocity, the velocity of the autonomous vehicle as well as lag in perception. One of the commonly used car following models is the General Motor's model, which is proposed by Gazis *et al.* [56]. In this model, the motion of the subject car is governed by an equation, the acceleration is the response of the model. Another model is the Gipp's car following model, proposed by Peter G. Gipps [57]. This model ensures a safe distance between the subject car and the car in front of it. The GM's model fails to consider in this regard. Optimal velocity model [58, 59] is defined that each driver tries to obtain an optimal velocity based on the relative distance and velocity. This is a dynamic model that the car's acceleration is proportional to its optimal speed and actual speed. The intelligent driver model (IDM) is also a well-known car following model, proposed by Treiber *et al.* in [60, 61], produces an acceleration as a continuous function of the velocity  $v_\alpha$ , the velocity difference  $\Delta v_\alpha$ , the net distance gap  $s^*$ .



Figure 1.8: A car following model in highway driving. The subject car is in the middle, and the front vehicle is the lead car. The subject vehicle reacts to the change in the speed of the lead car. The rear car also reacts to the speed change of the subject car.

$$\dot{v}_\alpha = a \left[ 1 - \left( \frac{v_\alpha}{v_0} \right)^\delta - \left( \frac{s^*(v_\alpha, \Delta v_\alpha)}{s_\alpha} \right)^2 \right] \quad (1.12)$$

where  $\delta$  and the maximum acceleration  $a$  are the model parameters.

There are several studies proposed to apply the above methods in advanced driver assistance systems. For example, Adaptive cruise control (ACC) is an extensively studied problem in the literature [62, 63, 64, 65]. Similarly to the car following models, a desired space and a velocity profile are obtained by continuously adjusting the vehicle's acceleration profile.

### 1.3.6 Lateral Vehicle Control

Vehicle's lateral behavior can be characterized in terms of lane change and merge operations [66, 67, 68]. For this purpose, researchers sometimes consider the lane change process as a decision making. Because a lane change depends on multiple objectives, such as speed profile, relative distance objectives before and after lane change as well as avoiding an obstacle in drive lane and a good reference trajectory to follow with high accuracy. Thus a lane change model should take into account several decision parameters. For example, Gipp's has proposed a set of factors that leads the driver to change a lane. Ahmed *et al.* [69] has proposed a gap acceptance model to assess whether the drivers have minimum acceptable gaps between the host vehicle and following vehicles. These methods have been well used in transportation research community.

For lane change control, the lateral dynamics of the vehicle is considered. A reference trajectory following is maintained by steering control [70]. Good set-point tracking of the trajectory during lane change does not only achieve safety but also improves driving comfort and fuel efficiency. In [71] authors model the nonlinear vehicle dynamics by an approximate hybrid affine model. They employ a time-optimal robust control algorithm to control the yaw rate and lateral velocity. In [72] authors implement frequency shaped linear quadratic (LQ) control. Kim and Langari proposed [73] a neuromorphic strategy, and robustness of the design is investigated by altering the uncertain cornering stiffness. Hatioglu *et al.* [74] a virtual yaw reference controller is considered and a robust switching

controller is utilized to generate steering commands for the vehicle to track the given reference trajectory. Abe in [75] a human-driver model (HDM) based controller is proposed. A look ahead distance consistent with vehicle speed is considered.

### 1.3.7 $\mathcal{H}_\infty$ Based Linear Parameter Varying (LPV) Control

The  $\mathcal{H}_\infty$  control design finds a controller that provides both closed-loop stability and a satisfied level of performance index for reference tracking and disturbance rejection. Since  $\mathcal{H}_\infty$  is a disturbance rejection technique, the main purpose is minimizing the effect of input disturbance on the output of the system. The  $\mathcal{H}_\infty$  norm of a stable transfer function  $G(s)$  is the largest input/output root mean square (RMS) gain i.e.,

$$\|G\|_\infty = \sup_{u \in L_2, u \neq 0} \frac{\|z\|_{L_2}}{\|u\|_{L_2}} = \sup_\omega \sigma_{max}(G(jw)). \quad (1.13)$$

The 2-norm, denoted by  $\|y\|_2$ , is defined as

$$\|y\|_2 \triangleq \sqrt{\int_0^\infty y^T(t)y(t)dt}.$$

Linear Parameter Varying (LPV) systems are described as the systems whose matrices are assumed to be affine with the variations.

$$G : \begin{cases} \dot{x}(t) = A(\rho(t))x(t) + B(\rho(t))w(t) \\ z(t) = C_1(\rho(t))x(t) + D(\rho(t))w(t) \end{cases} \quad (1.14)$$

Basically, LPV systems are expressed in terms of Linear Matrix Inequalities (LMI) , then the system matrices that are depend on the scheduling parameters are solved with currently available optimization methods [76]. The benefit of that technique is the information for all variations and the rates of variation in system are expressed in affine forms global optimization methods are used to solve them. These type of the systems are con-

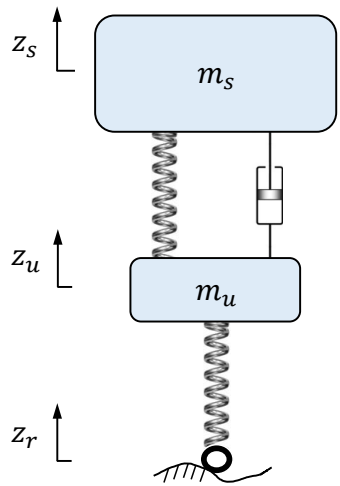
trolled with the LPV controllers. LPV control is capable of measuring the the variations and schedule the system parameters accordingly. Lyapunov functions are the essential element in order to establish stability and performance of the LPV gain scheduled systems. There are fixed Lyapunov functions, [77] or parameter-dependent [78, 79]. The latter condition simply means a parameter-dependent LPV controller used to control parametrically depended plant, whose parameter variation and rates are known. The second controller capture the whole variation during the process, therefore it provides less conservative approach. A single Lyapunov functions may be used for a parameter varying plant. However, stability and performance specification may not be met in the closed loop system due to the arbitrary fast variation in the scheduling parameters. As a result, the system may not be internally stable for all variations. When the internal stability of LPV system is guaranteed, the Bounded Real Lemma(BRL) condition is satisfied. A continuous differentiable matrix is sought such that the derivative of the matrix is decaying the zero exponentially. This simply gives the notion of the stability of the system.

### 1.3.8 LPV Control in Automative Research

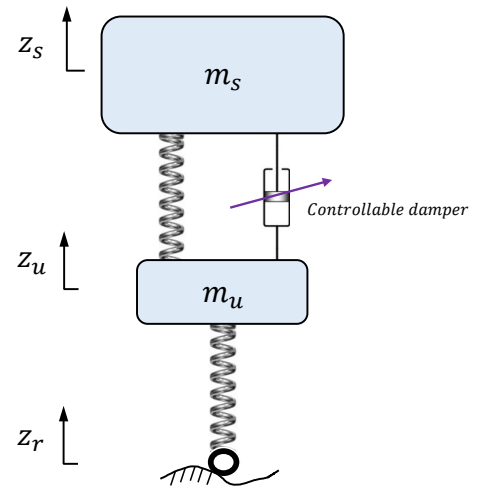
There are three main control developments to achieve performance requirements in passenger cars. First is the ride comfort that is associated with acceleration sensed by passengers, second is the road handling that is related to alternations in tyre forces due to road surface changes, and the last one is suspension deflection that is associated with the body displacement of the car with respect to the road. The control of the these subsystems is always conflicting. I first review some of the relation works in suspension control domain. The suspension control part can be categorized into passive suspensions, semi-active suspensions, and active suspensions controls. While active suspensions offer good ride, handling, vehicle posture, and stability than that of the counter parts semi-active suspensions, the energy consumption, cost, and complexity requirements are important negative

factors in implementation. Semi-active dampers fall into between passive and active suspension. The cost and installation are more beneficial as well as the feature of continuously controlled damping. The suspension system includes a damper or a shock observer that does not require much energy to operate. Within the limited context, I present some of the related literature works in control design perspective i.e., increasing ride comfort and road holding in view of road disturbances.

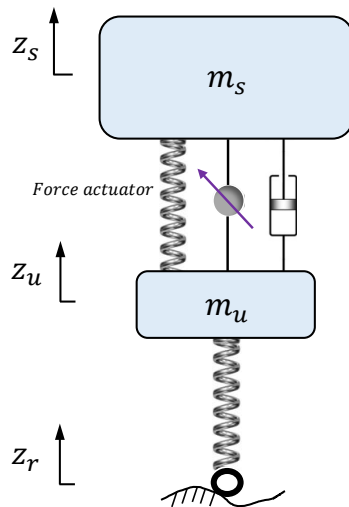
C. Poussot-Vassal *et al.* [80] proposed a semi-active suspension control. They first introduce a nonlinear quarter car model and experimentally obtained semi-active suspension system. Then the authors develop the internal stability and performance criteria within the LPV theory. The main contributions follow to fulfill the dissipative actuator constraint such that a type of robust norms (i.e.,  $\mathcal{H}_\infty$  and  $\mathcal{H}_2$ ) is established. The design is robust against model uncertainties. The design is computationally effective since it involves a simple scheduling strategy based on a static actuator model. Simulations and experimental results are perform to fulfill theoretical findings. Anh-Lam Do *et al.* [81] give a quarter vehicle model with a semi-active damper in the LPV framework with nonlinear static semi-active damper model. The nonlinear static semi-active damper model presents the bi-viscous and hysteric behavior of the design. The dissipativity constraint is turned into input saturation that is scheduled in polytopic way. The input saturation problem is integrated with the initial model to synthesize the LPV controllers. Convex optimization based the  $\mathcal{H}_\infty$  control design method is applied. The frequency and time domain results showed that the performance objectives as well as dissipativity constraint of the damper are simultaneous achieved. M.Q.Nguyen *et al.* [82] consider the design of a semi-active suspension control problem based on Finsler's lemma in the LPV state feedback framework. The design first employs an LPV form of the suspension system and dissipativity constraints as generalized sector condition. Two different Lyapunov functions are used; one of the stability and the other one for the disturbance rejection. Obtained polytopic system allows to



(a) Passive suspension



(b) Semi-active suspension



(c) Active suspension.

Figure 1.9: Type of suspension systems

compute LPV controllers by using LMIs. Input saturation conditions and a performance comfort level are demonstrated as satisfying design objectives. The work [83] considers to mitigate the conflict between ride comfort and road-holding by allowing the continuous control of the damper force in the semi-active suspension systems. As the actuator saturation limits are enforced in the performance limits, their work is unique in terms of incorporating the actuator limits in form of saturation indicator parameters that is included in the LPV plant model. The LPV controller is synthesized using a full-vehicle model. As expected, the model leads to complexity of the controller compared to quarter vehicle suspension model. To solve this, the authors employ a disturbance-feedforward output-feedback controller to exploit the separation principle. This performance of the controller is compared with various types of existing methods in simulation study. Michael Fleps-Dezasse *et al.* [84] introduce a new scheduling parameter, called saturation transformer into the LPV plant. The saturation indicator and the saturation transformer capture the force constraint of the semi-active damper. The LPV controller is synthesized by gridding of the parameter space using a parameter dependent Lyapunov function. Different road profile excitations are used to show the benefits of the controller experimentally.

The LPV control design opens a door to tackle with parameter uncertainty and/or non-linearity of the system by converting it into parameter space. Inspired by this, A. Zin *et al.* [85] proposed an LPV/ $\mathcal{H}_\infty$  controller design with respect to suspension spring coefficient for active suspension systems. Their proposed control strategy compromises safety/comfort performances adapted online according to the driving situation. The control design is in the view of global chassis control (GCC) framework wherein a switching control signal for ride comfort/road holding is produced with respect to the suspension subsystem. In [86] the design of an active suspension system in the LPV framework is also presented. The relative displacement between the chassis and wheel assembly is used to stiffen as the suspension limits are reached. The  $\mathcal{H}_\infty$  controllers ensure either passenger

comfort or suspension travel as the primary objective of the design. The  $\mathcal{H}_\infty$  controllers are blended into the LPV controller, subsequently forms a nonlinear controller for the design of nonlinear active suspension.

Since the emergency lane changes involve severe driving maneuvers at high speed, the consideration of vehicle lateral stability generated by yaw moment is a must to create an overaly stable control system structure for an emergency lane changing intelligent system. The steering control methods are quite effective when the lateral tire forces are constant. The methods collapse when the vehicle tire forces reach saturation limit; resulting the loss of steer-ability leads to a high level accident possibility. Uncertainties in cornering stiffness as a result of tire-road friction efficient and vehicle load distribution affect the stability of the entire system. To solve this, researchers have proposed vehicle stability control systems that mainly use direct yaw moment to keep the vehicle stable. Consequently, active front steering (AFS) system is combined with the direct yaw moment controller (DYC). In [87], coordinated control of AFS and DYC for stability and better vehicle handling is proposed. They employ an 8-DOF nonlinear vehicle model and tyre model. The authors develop a procedure based on an optimal guaranteed cost (LQR), and the effect of uncertainty on the cornering stiffnesses is discussed. The control objective to reduce the negative influence of the norm-bounded time-varying cornering stiffness uncertainty on the vehicle dynamics control with respect to the change in driving conditions. Hui Zhang *et al.* [88] considered the vehicle lateral dynamics stabilization problem with time-varying longitudinal velocity. The longitudinal velocity is presented by a polytope with finite vertices and cornering stiffness is represented with norm-bounded uncertainty. An LPV model of the vehicle is introduced based on the varying longitudinal velocity and cornering stiffness. The control objective is to minimize the sideslip angle with a prescribed level of yaw rates. In the control design, a set of objectives i.e., the sideslip angle, yaw rate, and the control efforts, they propose a multi-objective energy-to-peak control with  $\mathcal{D}$  stability. The same

problem of the vehicle lateral control and increased stability by combined AFS/DYC is addressed in [89]. Here, the authors consider a varying range of longitudinal velocity and the nonlinear tire model in vehicle modeling same and the nonlinear tire model is reformulated into a linear model with norm-bounded uncertainties. Then, an augmented linear parameter varying (LPV) model is combined with robust-gain scheduling state-feedback control, based on a proportional- integral (PI) control law. Some of the differences are to use one more actuator and vehicle tracking control is considered such that the vehicle yaw rate follow the desired value. Moustapha Doumiati *et al.* [90] considered a coordinated control of active front steering and rear breaking. It main idea is when the vehicle reaches handling limits, the braking and steering cooperate to ensure the vehicle stability. The control goal is to adjust the yaw rate of the vehicle to the desired value by the driver, and limiting the braking actuator when the vehicle goes towards instability. Actuator coordination task is achieved by a LPV controller. By monitoring the sideslip angle dynamics, a single exogenous parameter is scheduled in LPV controller. The polytypic solution for the LPV is synthesized within the  $\mathcal{H}_\infty$  framework. Simulation results are performed both in time and frequency domain. Poussot-Vassal *et al.* [91] present a methodology that integrates and coordinates braking and front steering to enhance vehicle handling and stability within the  $\mathcal{H}_\infty$  control framework. The coordination task is achieved by using braking control switch, activated only the vehicle losses handling limit. The activation parameter is used as scheduling parameter in the control design.

### 1.3.9 Takagi-Sugeno $\mathcal{H}_\infty$ Control Strategy

Takagi-Sugeno (T-S) proposed a method of designing and analysis of nonlinear systems by presenting a set of local linear systems. The structure of the local linear models has the same size state vectors for each element. The local dynamics in different regions is presented with the same size state-space equations and fuzzy blending of the sub-linear

models forms the overall nonlinear dynamics. Thus, the main advantages of the (T-S) fuzzy modeling is that the controller is designed in a particular operation zone, and fuzzy interpolation mechanism is employed to take into account the contribution of the each sub-model with a set of weighting functions. The control design method is carried out based on the fuzzy model with the so-called parallel distributed compensation (PDC) scheme [92, 93, 94]. The overall controller is expressed as a smooth blending of the individual controllers together with the membership functions. Linear  $\mathcal{H}_\infty$  type of control methods have been implemented for each linear subsystem in the literature. In [95], state-feedback  $\mathcal{H}_\infty$  control is implemented to solve the problem of robust regulation of a nonlinear magnetic bearing system. Robust static output-feedback controller design against sensor failure for vehicle dynamics within T-S fuzzy framework is addressed in [96]. In [97], T-S fuzzy control is used to model the nonlinear Electric Steering System (EPS) for both saturated and constrained input cases through LMIs stabilization conditions for state-feedback controllers. In [98], the authors consider T-S modeling of nonlinear Brush tire model and longitudinal velocity by 16 sub-models of dynamics and state feedback control is applied with electric motor torques.

### 1.3.10 Driving Safety

Driving is always performed in lateral and longitudinal direction on a road frame. The longitudinal safety of driving considers a safe distance from the following cars [99]. The lateral safety of driving takes into account lane change maneuvers provided that there exist an Minimum Safety Spacing for Lane Changing is by Karanis and Ioannou in [100]. Most of the driver assistance systems take over the control of the vehicle when an accident is inevitable. In order to assess the safety of decision and subsequently planned trajectory, collision possibility index has been proposed.

There are two approaches assess the safety of a planned trajectory for autonomous cars.

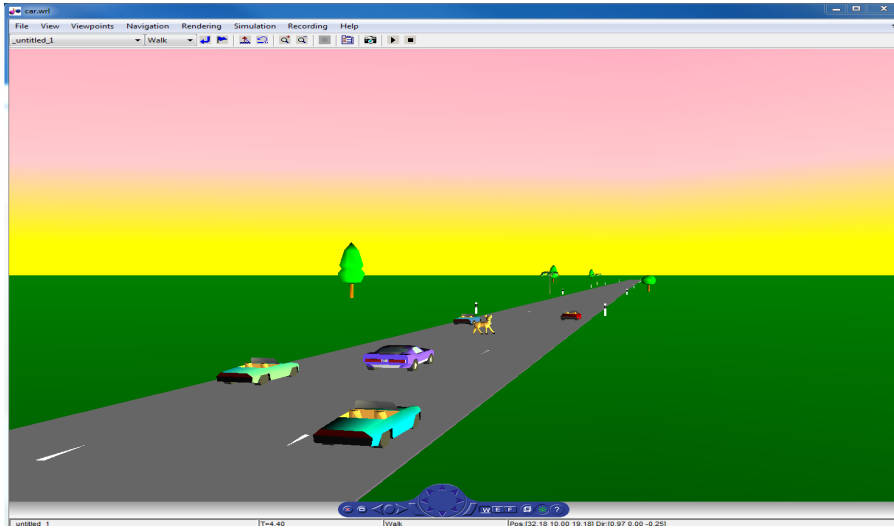


Figure 1.10: An emergency situation in traffic. The driver is not able to respond to the situation sufficiently. The proposed system take over the control of the vehicle and executes a *human* like decision to avoid the object as well as not crashing the other cars.

The first is the Monte Carlo simulation for assessing the future behavior of traffic participants [101]. Broadhurst *et al.* [102] use a probabilistic distribution of vehicle motions on a planning path to assess their danger. They consider the all possible control inputs for all vehicles in a road scene. The control inputs that lead to a collision are eliminated. A probability distribution over all control inputs gives the likelihood of a collision of any two objects. Althoff and Mergel [103] compare the Markov chain abstraction and the Monte Carlo simulation for the probability prediction of traffic situations. The uncertainly in the obstacle detection is incorporated for future probabilistic occupancy of obstacles in road. This analysis is useful to optimize the planned paths such that the autonomous car comes not get close to the object as well as the other cars. Then a crash probability is introduced to identify a trajectory with the least crash probability among all the planned.

The second analysis tool to evaluate the safety of a planned trajectory is computed via reachability analysis. Reachable set is defined as the all possible trajectory of a dynamic

system with respect to the all possible control inputs from all the possible states. This verifies one to evaluate all the behaviors of the closed loop system such that the system stays in desired range of operation and do not get into a forbidden region in state space [104]. This analysis is quite useful for *hybrid* systems (discrete-continuous) where the analytic solution tools are limited. Althoff *et al.* [105, 106] proposed a reachability analysis for the planned trajectory of autonomous car. They evaluate the crash probability of the subject car and the traffic participants along the planned trajectory. They compute stochastic reachable sets based on initial probability distribution of traffic participants. Then a safe planned trajectory can be executed for the subject car. The driving safety for autonomous cars requires to find a final *safe* set. This allows one to confirm a safe transition of a vehicle's state during autonomous driving.

### 1.3.11 Contribution of the Dissertation

As the name denotes, the main purpose of this research work is to design an autonomous driving strategy to fulfill the need in an advanced driver assistance system so called emergency lane change assistance system in passenger cars. I consider the assistance system as cooperative copilot to real drivers. Therefore understanding the human factors is an essential element of this work. Because the autonomous car should be able to function as good as a human driver so that approximation and/or complementing human driver driving behaviors are the key results in this research. Thus the proposed work fulfills the increasing need in the real world human like application of design and control in the development of intelligent transportation systems (ITS). It is the main goal of the proposed architecture to integrate a quantitative and comprehensive driver model of a human with multi-level automation scheme. This way enables us to carefully capture some of the considerations in analytical way such as environmental conditions of traffic i.e., threat assessment of traffic participants, human like decision making with maximum

benefit or rewards i.e., Markov decision processes to compute the best action, visual information from eyes to draw a safe trajectory planning for the autonomous car i.e., safe path generation for obstacle avoidance, and steering and braking control like human actions to move the vehicle to a safe lane according to the generated path. Further, game theoretic approach is utilized to take advantage of the interactions between the vehicles. This opens a door for new directions of research to formulate the problem as connected vehicles. Main contributions of this dissertation proposal is, a) I develop an threat calculation in  $TVs$  states, i.e., position and velocity values, in an elegant way by fuzzy logic; b) I develop a more realistic Markov decision model to an intelligent selection of a gap even in tight traffic conditions with maximum benefit to the autonomous vehicle as well as vehicles in surrounding; c) I present a game theoretical modeling of traffic and embedded into the MDP modeling to form a multi-agent environment decision making model, Markov game; d) real-time simulations are performed in a driving simulator, dSPACE.

The second part of the dissertation finds a solution to lateral dynamics and control of the real nonlinear vehicle model. Since the emergency lane changes involve severe driving maneuvers at high speed, the consideration of vehicle lateral stability generated by yaw moment is a must to create an overaly stable control system structure for an emergency lane changing intelligent system. Thus we focus on designing a AFS/DYC as lower level controller that performs a lane change task with enhanced handling performance in the presence of varying front and rear cornering stiffnesses. The main contributions of this part are as follows: a) I propose a new control scheme that integrates active front steering and the direct yaw moment control to enhance the vehicle handling and stability; b) I obtain the nonlinear tire forces with Pacejka model and convert the nonlinear tire stiffnesses to parameter space to design a linear parameter varying controller (LPV) for combined AFS and DYC to perform a commanded lane change task; c) in terms of following desired references with high accuracy, our control approach does not only follow

the controlled variables of interest i.e., the desired yaw rate but also follows uncontrolled variables i.e., side slip angle with respect to varying cornering stiffnesses; d) modeling the nonlinear tire forces by fuzzy blending operation, which explicitly represents the nonlinearity; e) I propose novel linear fuzzy blended  $\mathcal{H}_\infty$  state-feedback control strategy with an augmented control law successfully compensates the error deviations for tracking the references along with a computationally fast solution; f) as the main objective of our research, the proposed vehicle control structure contributes to the overall robustness of the autonomous lane changing intelligent system.

## 2. DECISION MODEL

This chapter aims at presenting state of the art hierarchical driver model for a human driver model. The main goal of the proposed architecture is to integrate a quantitative and comprehensive driver model of a human with multi-level automation scheme. The first effort focuses on driver behaviors and relating human reasoning for modeling a decision making strategy. I evaluate the instantaneous threat of traffic participants ( $TVs$ ) by using the fuzzy estimated traffic quantities. Then the obtained threat values are converted to transition probabilities with a logistic function, eventually form final *transition* function for each of the  $TVs$  relative to the subject vehicle ( $SV$ ). I then use Markov decision processes (MDPs) for the  $SV$  to output sequential decisions for lane changing problem. In this model, the  $SV$  is the only adaptive agent in the world where the  $TVs$  are considered as part of the environment. One of the major questions to be addressed in autonomous driving is that how to determine a strategy profile with respect to  $TV's$  schemes. To finish this, the interactions are captured through game theoretic approach, which enables the autonomous vehicles to characterize their behaviors. To sum up, I construct a multi-agent Markov game for the traffic problem. Moreover, since the driving is a dynamically evolving process, a decision made at current time is obsolete for the next time steps. Consequently, it is important repeatedly make decisions and adjust it as the time proceeds. Prediction is therefore an important tool to determine the autonomous vehicles decision strategies over a  $N$  step prediction horizon. Thus, the decision making strategy is named as a predictive fuzzy Markov game ( $FMDPs$ ) to model the traffic environment where predicted reactions of multiple agents/players is used to establish more effective driving decision method. This level is called the *higher level controller* for intelligent vehicle design framework. I further focus on generating a trajectory for the  $SV$  to complement the safe drive in different

traffic situations. The traffic environment is formulated within a quadratic programming ( $QP$ ) optimization and solved for collision avoidance within convex optimization framework. The ability of generating traffic dependent decision making and trajectory planning is demonstrated through simulations in multiple vehicles driving simulations.

## 2.1 Instantaneous Threat Estimation of $TVs$ Using Fuzzy Logic

One of the main advantages of fuzzy logic is to define linguistic variables and a set of rules to emulate human driver's behavior. This scheme provides a tolerance of uncertainty and imprecision. Indeed human driver perception of traffic that relies on linguistic variables such as dangerous or safe driving, represented with fuzzy rules is a quite powerful methodology to model a traffic environment instead of using crispy values.

We are interested in modeling drivers driving style through a complementary threat estimation using fuzzy sets. The design and test of threat estimation algorithm adapts to drivers driving style, based on information available through sensors. Complete state information of the vehicles is assumed to be known where the design is able to closely interact with change of vehicle states online in terms of velocities and positions. This online adaptation of traffic may have an appropriate role in reducing traffic accidents for possible applications in autonomous driven as well as human driven vehicles.

The problem under consideration is depicted in Figure 2.1. We model threat assessment of  $TVs$  relative to  $SV$  in most common highway scenario with 3-lanes and it can easily be extended to more lanes highway scenarios. The  $SV$  is equipped with an estimator, which monitors and collects the state information of the vehicles in the environment. Then the goal of the estimator is to calculate the relative threat of the  $TVs$  with respect to the change in their driving styles. More clearly, the relative change in  $TVs$  states, i.e., velocities and positions, which will subsequently determine how the  $SV$  observes threat quantity. The following notation will be used throughout the paper to denote the vari-

ables related to the positions and velocities of *TVs*:  $i = (r, l)$  denotes the right and left lanes and  $j = (r, f)$  denotes rear and front i.e., the longitudinal positions and velocities of *TVs* relative to the *SV* in road frame. For example,  $d_{rr} = \text{abs}|x_{rightrear} - x_{subject}|$ , relative longitudinal distance between the subject car and the car in the right rear lane,  $v_{lf} = v_{leftfront} - v_{subject}$  is the relative velocity difference between the subject car and the car in the left front lane, and  $v_{lr_{cv}}$  denotes the cruising velocity of the car in the left rear lane.

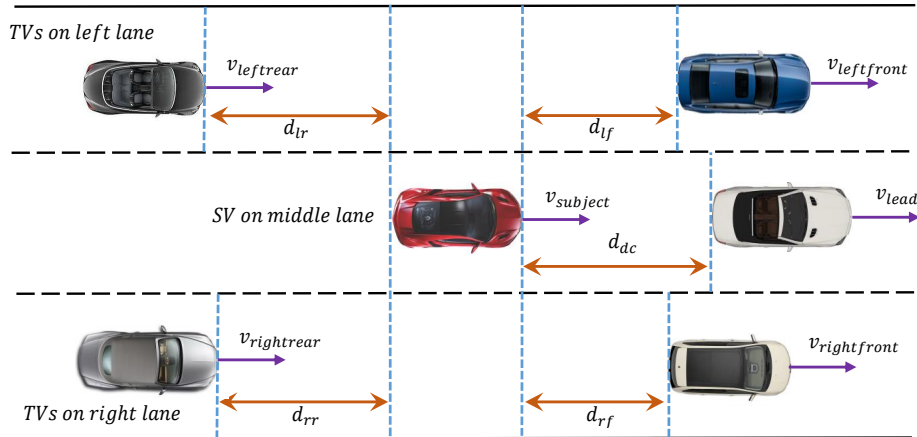


Figure 2.1: System model with related traffic quantites of each *TVs*. Notice that the relative distance values are defined from each *TVs* and velocities are also shown for each *TV*.

A simplified discretized vehicle's point mass vehicle model is utilized for the vehicles to estimate their relative threats.

$$\begin{pmatrix} x(k+1) \\ v_x(k+1) \end{pmatrix} = \begin{pmatrix} 1 & t_s \\ 0 & 1 \end{pmatrix} \begin{pmatrix} x(k) \\ v_x(k) \end{pmatrix} + \begin{pmatrix} 0 \\ 1 \end{pmatrix} (u_x(k)) \quad (2.1)$$

where  $k$  is the discretized time notation the state vector  $\xi(k+1) = [x(k) \ v_x(k)]^T$  denotes the longitudinal position, the longitudinal velocity, respectively. The control input  $u(k) =$

$u_x(k)$  denotes the acceleration values in longitudinal direction.

### 2.1.1 Fuzzy Sets and Membership Functions

Input variables are defined by several fuzzy sets that are modeled with membership functions where the linguistic labels are assigned. The inference process maps these linguistic variables to a fuzzy output by applying fuzzy rules [107]. Finally, defuzzification process gives a crispy output to implement in a given system. We define 3 inputs,  $\{RP, RV, CV\}$ , the relative positions and relative velocities between  $TVs$  and  $SV$  and cruising velocities of  $TVs$ , and 1 output  $\{q\}$ . In this work, traffic measurements of positions and velocities of  $TVs$  are modeled with fuzzy logic, and an instantaneous threat quantities are defined with the notation  $q$  of  $TVs$  relative to the  $SV$ . The  $TVs$  state variables, i.e., velocities and positions, are taken into account using fuzzy blending of the membership functions to produce a subjective threat output for the  $SV$ . In a compact way, we can write the following;

$$q_{ij}(k) = (RP_{ij}(k), RV_{ij}(k), CV_{ij}(k)) \quad (2.2)$$

where the threat value  $q_{ij}(k)$  at time instant  $k$  depends on relative position between the  $SV$  and a  $TV$ , i.e.,  $RP_{ij}(k)$ , relative velocity between the  $SV$  and a  $TV$ , i.e.,  $RV_{ij}(k)$ , and cruising velocity of a  $TV$ , i.e.,  $CV_{ij}(k)$ . The relative threat values of the  $TVs$  is modeled such that  $SV$  mimics their driving habits. This is an important classification to extract information about the traffic condition where the driver type is not known in advance but can be estimated through the states of driven vehicle.

Gaussian membership functions are defined for the linguistic variables for each input and outputs. The assigned labels to the input  $RP$ ; small (SM), medium (ME), and high (HG), to the input  $RV$ ; negative (NE), zero (ZE), and positive (PO)<sup>1</sup>, to the input  $CV$ ;

---

<sup>1</sup>Negative velocity means that a  $TV$  is going away from  $SV$  and positive velocity implies an approaching

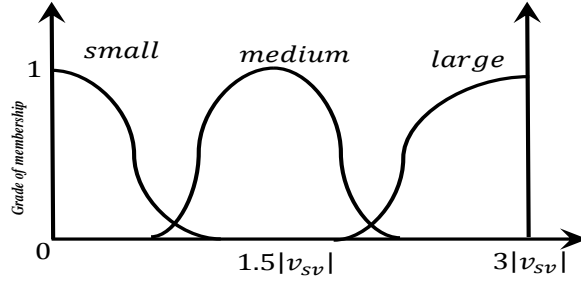


Figure 2.2: Gaussian membership function for relative position. Notice that the centering of each linguistic label is defined en terms of *SV* speed.

slow (SL), normal (NR), and high (HG). The linguistic labels for the  $q$ ; low (LW), normal (NR), and high (HG). Note that threat is a subjective quantity and depends on driver's perception of traffic environment. Therefore we propose a solution which quantitatively fulfills a realistic human observation of threat assessment.

Next we define the Gaussian membership functions with parameters. Note that the notation  $(i, j)$  is omitted for convenience.

The *RP* membership parameters are given as

$$Gauss(RP; c_{RP}, \sigma_{RP}) = e^{-1/2} \left( \frac{RP - c_{RP}}{\sigma_{RP}} \right)^2 \quad (2.3)$$

$$c_{RP} = \begin{cases} 0, & \text{small} \\ 1.5|v_{sv}|, & \text{medium} \\ 3|v_{sv}|, & \text{large} \end{cases} \quad \sigma_{RP} = 0.3 * v_{sv} \quad (2.4)$$

---

*TV to the SV.*

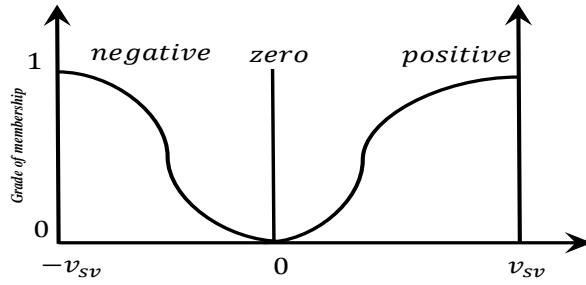


Figure 2.3: Gaussian membership function for relative velocity. Notice that the centering of each linguistic label is defined en terms of *SV* speed.

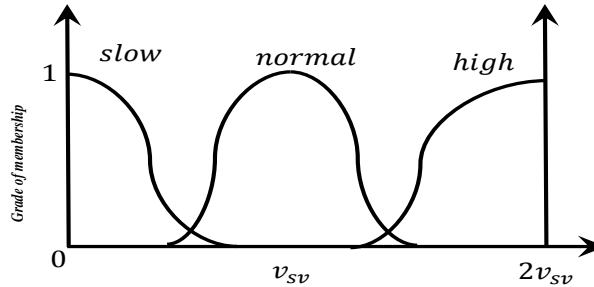


Figure 2.4: Gaussian membership function for cruising velocity. Notice that the centering of each linguistic label is defined en terms of *SV* speed.

The *RV* membership parameters are given as

$$Gauss(RV; c, \sigma_{RV}) = e^{-1/2} \left( \frac{RV - c_{RV}}{\sigma_{RV}} \right)^2 \quad (2.5)$$

$$c_{RV} = \begin{cases} -v_{sv}, & \text{negative} \\ 0, & \text{0} \\ v_{sv}, & \text{positive} \end{cases} \quad \sigma_{RV} = \begin{cases} 0.3 * v_{sv}, & \text{neg or pos.} \\ 0.01, & \text{zero} \end{cases} \quad (2.6)$$

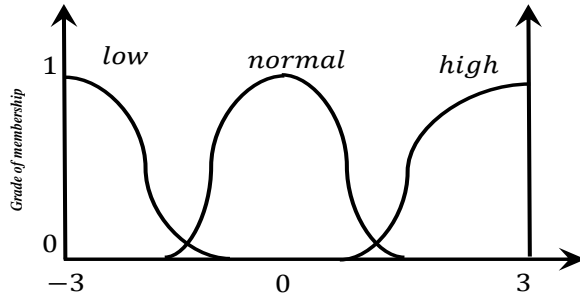


Figure 2.5: Gaussian membership function for threat

The  $CV$  membership parameters are given as

$$Gauss(CV; c_{CV}, \sigma_{CV}) = e^{-1/2} \left( \frac{CV - c_{CV}}{\sigma_{CV}} \right)^2 \quad (2.7)$$

$$c_{CV} = \begin{cases} 0, & \text{slow} \\ v_{sv}, & \text{normal} \\ 2v_{sv}, & \text{high} \end{cases} \quad \sigma_{CV} = 0.3 * v_{sv} \quad (2.8)$$

The  $q$  membership parameters are given as

$$Gauss(\text{threat}; c_{\text{threat}}, \sigma_{\text{threat}}) = e^{-1/2} \left( \frac{\text{threat} - c_{\text{threat}}}{\sigma} \right)^2 \quad (2.9)$$

$$c_{\text{threat}} = \begin{cases} -3, & \text{low} \\ 0, & \text{normal} \\ 3, & \text{high} \end{cases} \quad \sigma_{\text{threat}} = 0.4 \quad (2.10)$$

Generally, there are several considerations to choose a membership function type over

the other types. For example, representation, adaptation, optimization, and continuity are some of the considerations. The advantageous of Gaussian membership functions are simple in design, they have few parameters in presentation, and continuous functions.

**Remark 1:** Notice that the Gaussian membership function elements, i.e., center and standard deviation values depend on the *SV* speed seen in Figures 2.2, 2.3, 2.4. This make sense since the *SV* observes the threats of *TVs* based on how the states of its own driving. Notice also that the threat is varied between -3 and 3. These bounds are heuristically defined. It is *assumed* that most for the drivers threat value obeys a normal distribution shown in Figure 2.5.

### 2.1.2 Fuzzy Inference

It is important to ensure that the proposed method is real time applicable; fast evaluation of fuzzy rules is vital. However, in order to capture a more realistic estimation, the rules may be enumerated. The number of fuzzy rules is  $3^3 = 27$ .

Model rule 1: IF  $RP$  is SM,  $RV$  is NE, and  $CV$  is SL THEN

$q$  is NR

Model rule 2: IF  $RP$  is SM,  $RV$  is NE, and  $CV$  is NR THEN

$q$  is NR

Model rule 3: IF  $RP$  is SM,  $RV$  is NE, and  $CV$  is HG THEN

$q$  is HG

:

Model rule 25: IF  $RP$  is LG,  $RV$  is PO, and  $CV$  is SL THEN

$q$  is LW

Model rule 26: IF  $RP$  is LG,  $RV$  is PO, and  $CV$  is NR THEN

$q$  is NR

Model rule 27: IF  $RP$  is LG,  $RV$  is PO, and  $CV$  is HG THEN

$q$  is NR

Fuzzy rule inference determines the outputs threat value with a set of designed rules. It is interpreted that the proposed framework exhibits a freedom such that the designer can obtain several modes based on the set of defined rules. The rule table is shown in Table

2.1.

Table 2.1: Fuzzy inference rule table

Inputs		Linguistic description														
RP	SM	SM	SM	SM	SM	SM	SM	SM	SM	SM	ME	ME	ME	ME	ME	ME
RV	NE	NE	NE	ZE	ZE	ZE	PO	PO	PO	NE	NE	NE	ZE	ZE	ZE	ZE
CV	SL	NR	HG	SL	NR	HG	SL	NR	HG	SL	NR	HG	SL	NR	NR	NR
Output $q$	NR	NR	HG	NR	NR	HG	NR	HG	HG	LW	NR	NR	LW	NR		

### 2.1.3 Simulation

#### 2.1.3.1 Car following model

In order to ensure a smooth traffic flow of  $TVs$ , the following car following formula is proposed, which is a modified version of the Intelligent Car Following Model (IDM) [60].

$$\dot{v}_{TV} = \mathcal{K} \left[ 1 - \left( \frac{x^*(x_0, v_{TV}, T)}{x_{current}} \right)^2 \right] \quad (2.11)$$

where  $x^* = x_0 + v_{TV}T$ .  $x_0$  is the minimum gap of a  $TV$  vehicle that follows a lead  $TV$  with a certain headway time  $T$  and its speed  $v_{TV}$ . Follower  $TV$  vehicle reacts to the change in speed of the lead  $TV$  and maintains a headway value, which proportional to the desired headway time. This model is characterized as follow-the-leader model same as

Inputs		Linguistic description														
RP	ME	ME	ME	ME	LG											
RV	ZE	PO	PO	PO	NE	NE	NE	ZE	ZE	ZE	PO	PO	PO	PO	PO	PO
CV	HG	SL	NO	HG	SL	NR	HG									
Output $q$	NR	NR	NR	HG	LW	LW	LW	LW	LW	NR	LW	NR	NR	NR	NR	NR

optimal velocity model Bando *et al.* [58] with the additional objective of achieving a safe headway distance between cars.

### 2.1.3.2 *Simulation set-up*

For the simulation model, each car is assigned a coordinate system and has certain length and width in a three lane highway set-up, seen in Figure 2.6. All cars travel in the middle of lanes unless a lane changing is taking place. The *TVs* speeds are independent of the *SV*'s speed. For simplicity, we assume the center of gravity of each car is exactly at the middle.  $l_f$  and  $l_r$  are defined as the distances for the center of gravity for all cars.  $W_c$  is the total width of a vehicle and  $W_L$  is the lane width. *SV* only travels in one direction i.e., backwards traveling is not considered and can be initially positioned on different lanes. The flow of *TVs* is maintained by an heuristic car following model in equation 2.11. The simulations are performed on a computer equipped with an Intel *Xeon E5 2.6 GHz* CPU. A virtual world of traffic is visually demonstrated by VR Sink 3D animation environment that is run on a Simulink® model where the fuzzy threat algorithms are packed. The main objective of this work is to consider a general scenario where the *SV* travels in the middle lane of 3-lanes highway and the *TVs* are traveling in the neighboring lanes. We seek to find the vehicles threat values, which also provides drivers of *TVs* driving style, relative to the *SV*. The reason why such a scenario of driving is considered is that the proposed method may later be used decision making and control applications. Since the *SV* can be equipped with autonomous control driving algorithm where continuously assessment of traffic follow in the vicinity is required for future driving strategy.

The Figure 2.6 shows 5 cars where the red car is the *SV* and *TVs* are in the neighboring lanes. The objective is to asses the *TVs* relative threat to the *SV* since the *SV* will search for a gap to merge in the later sections, information about following *TVs* are important. We can see a 3D animation environment, depicted in Figure 2.7, which ease

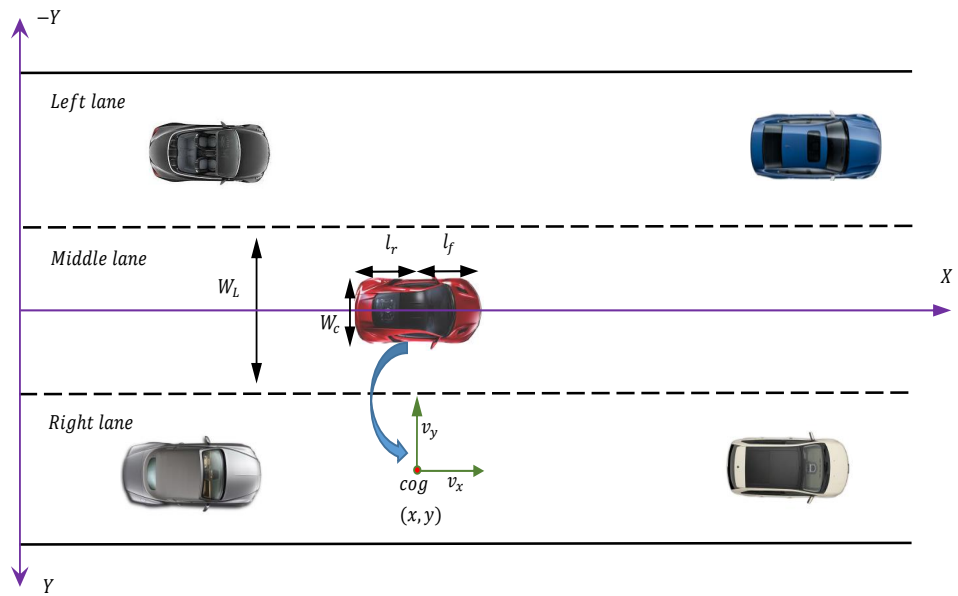


Figure 2.6: A cartesian coordinate is assigned for each vehicle.

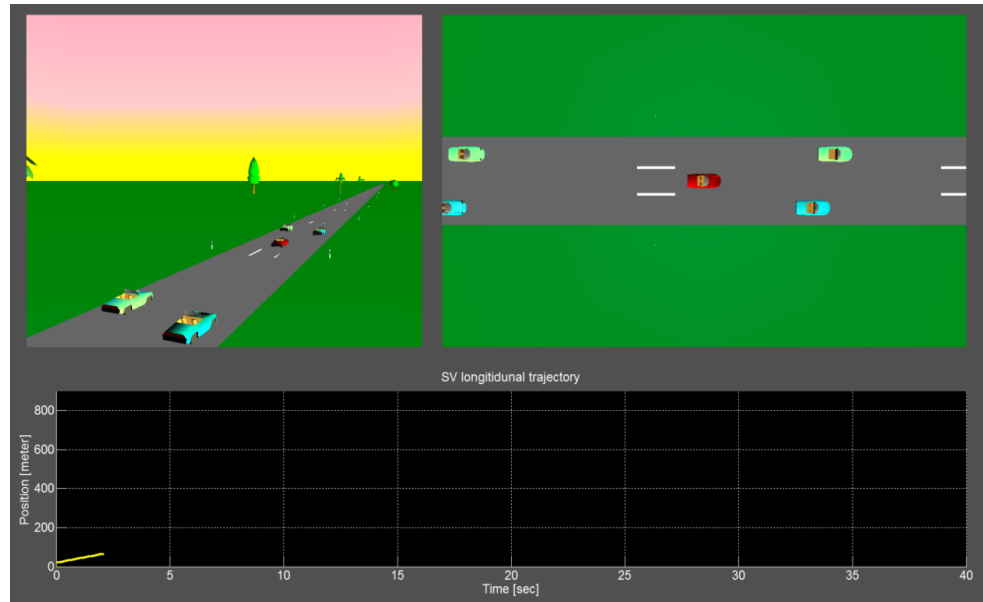


Figure 2.7: This graph is intended to show the visual set-up with two camera orientations. Green vehicles denote the *TVs* in the left lane, light blue vehicles are the *TVs* in the right lane. Animation is seen at 2 seconds

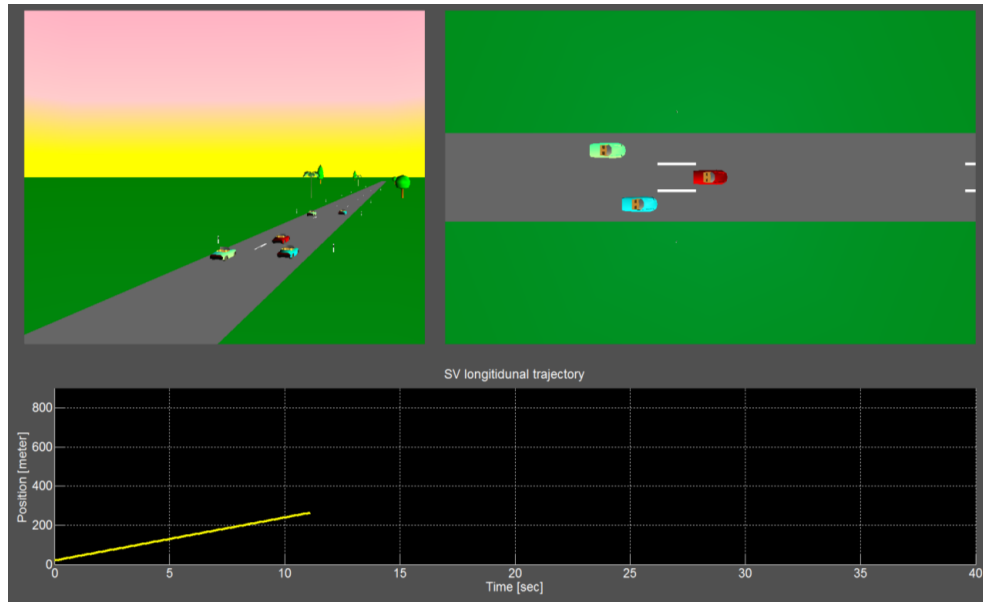


Figure 2.8: Animation snapshot at 12 seconds

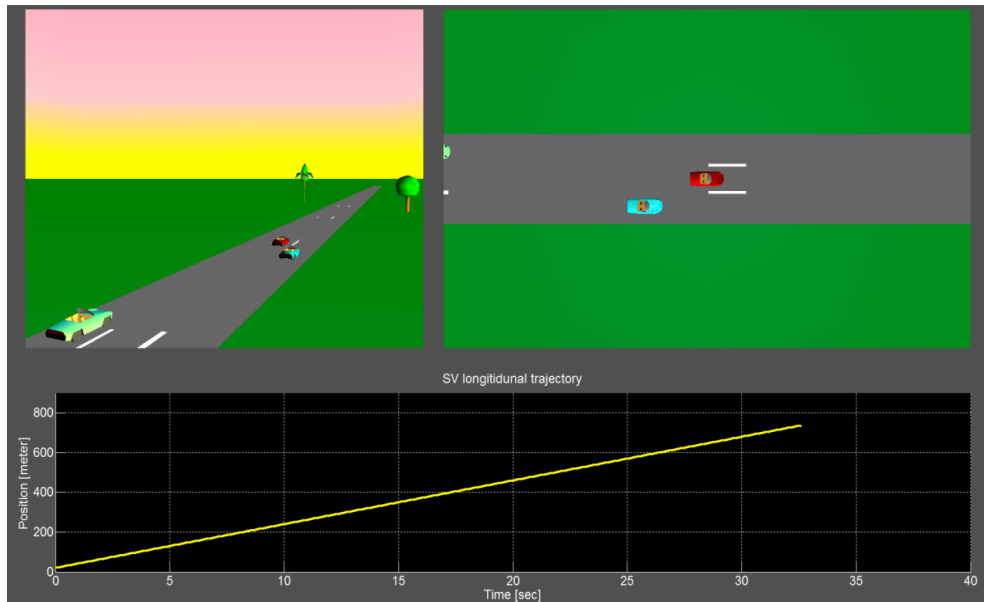


Figure 2.9: Animation snapshot at 33 seconds

to interpret the traffic situation. Different acceleration profiles are given to  $TVs$  in Figure 2.10 such that the  $SV$  estimates the current values at each time step. Corresponding velocity and position figures are also made available to readers in Figure 2.11 and 2.12. As seen in animation at time 12 seconds in Figure 2.8 where two following  $TVs$  are fast approaching to the  $SV$ . The corresponding relative threats are observed in Figure 2.13 and 2.14. One can notice that when the  $SV$  gets further away in Figure 2.9, the relative threat values go low.

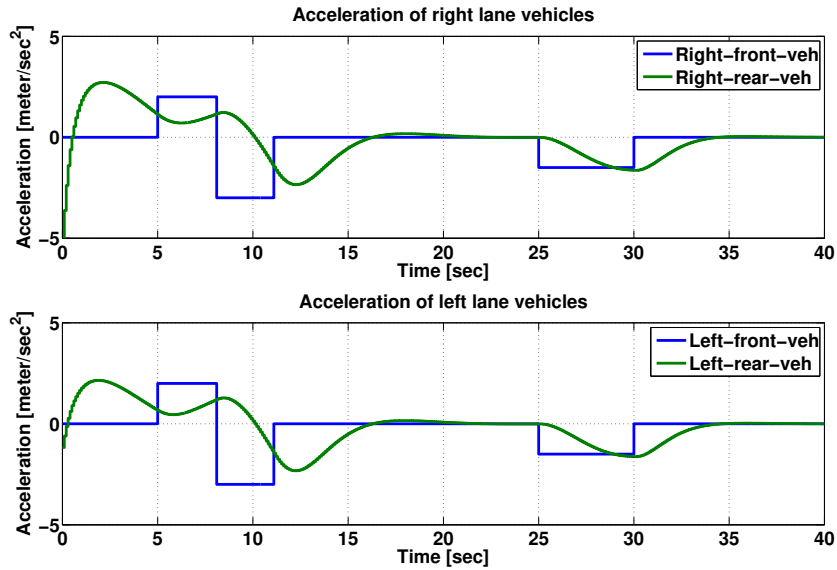


Figure 2.10: Accelerations of vehicles

## 2.2 Prediction

Prediction is an important method to predict a possible future behavior of a system. In autonomous driving, its essential to incorporate an prediction module in the decision process. Its known that one can only make a prediction based on the information at the

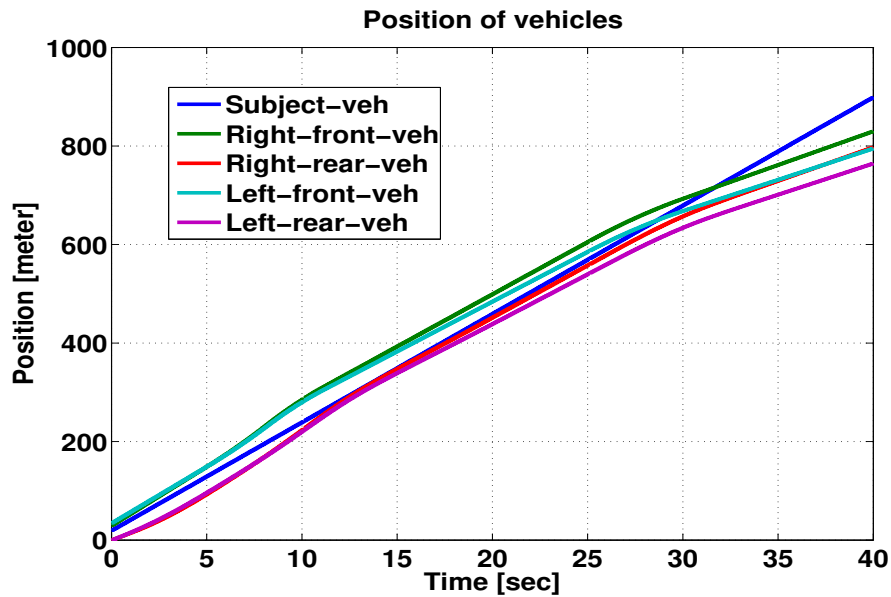


Figure 2.11: Positions of vehicles

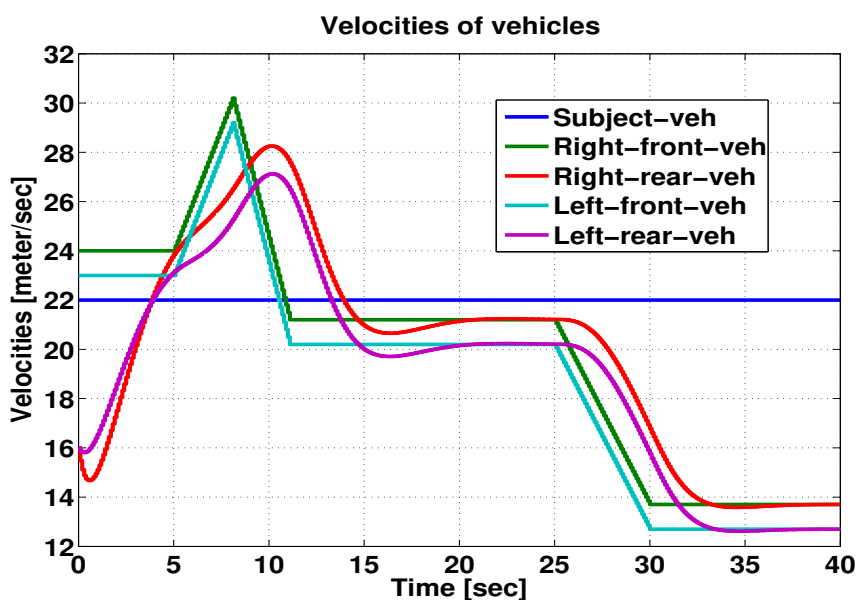


Figure 2.12: Velocities of vehicles

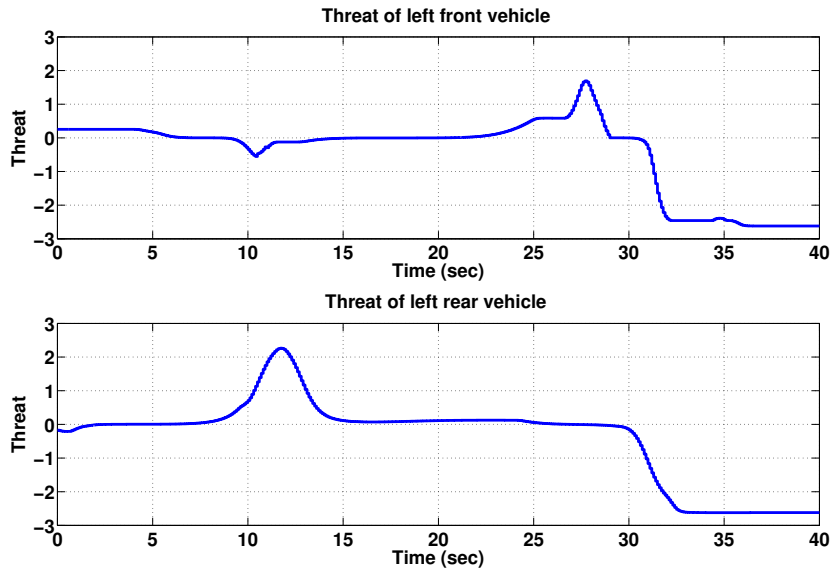


Figure 2.13: Threat of vehicles in left lane

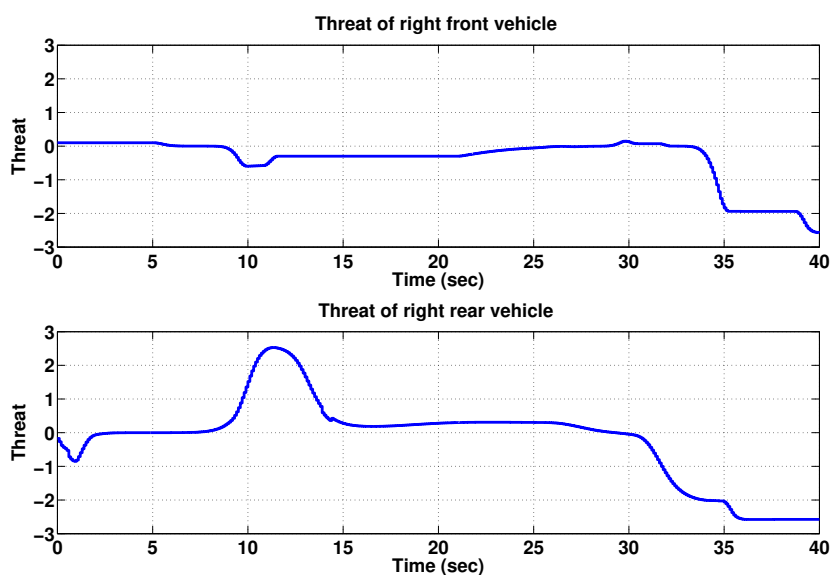


Figure 2.14: Threat of vehicles in right lane

Table 2.2: Design parameters used in simulation

$t_s$	0.1	$l_f$	2	$l_r$	2	$Q_{v_y}$	10
$\varrho_2$	2	$l_r$	2	$u_y$	[-3,3]	$Q_y$	20
$t_s$	0.1	$W_c$	2	$y_{ref}$	[-3.3,3.3]	$\mathcal{K}$	5
$t_{lc}$	2	$N$	2	$R_{u_x}$	10	$T$	1.3
$\Psi$	3	$v_x$	[0,30]	$R_{u_y}$	10		
$W_L$	3.3	$v_y$	[-5,5]	$Q_{v_x}$	20		

current time step, which implies the future behavior of a dynamic object is only guessed at the time of prediction. This makes sense since if the behavior of the object changes in the interval of prediction horizon, the final position at the end of that prediction horizon does not match with the performed evaluation at the initial time step. There might be unpredictable change in the acceleration value such that the prediction at the end of time horizon at  $k + N$ , the position value changes. But it still provides a perfect *guess* to determine the final states with bounded input cases. This is the main motivation to include a prediction in the decision method to terminate if the final position of  $SV$  poses an unsafe situation at the end of the lane change.

## 2.3 Markov Decision Process

We first provide the definition of Markov chain

### 2.3.1 Markov Chain

A Markov process consists of a finite set of states  $S$ , a set of initial states  $S_0$ , a finite set of transition probability distribution matrix,  $\mathcal{T}$ , that affects which transition can occur at which state and the resulting state. An MP is presented by 2 main components  $\langle S, \mathcal{T} \rangle$  where

- $S$  is the set of all possible states (finite) of  $s(k)$  at time  $k$

- $\mathcal{T}$  is the  $\mathcal{S} \times \mathcal{S} \rightarrow [0, 1]$  is the transition function where  $\mathcal{T}(s(k+1), s(k))$  gives the probability of ending in state  $s(k)$

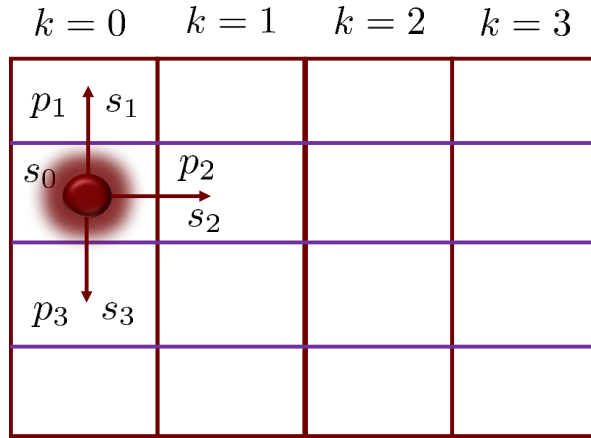


Figure 2.15: Markov chain with 16 states

In Figure 2.15, an agent is at state  $s_0$  at time  $k$  and possible probabilistic transitions are shown to next states.

An MDP is presented by the tuple  $\langle \mathcal{S}, \mathcal{A}, \mathcal{T}, \mathcal{R}, \gamma \rangle$  where

- $\mathcal{S}$  is the set of all possible states of  $s(k)$  at time  $k$
- $\mathcal{A}$  is the set of all possible actions of  $a(k)$  at time  $k$
- $\mathcal{T}$  is the  $\mathcal{S} \times \mathcal{A} \times \mathcal{S} \rightarrow [0, 1]$  is the transition function where  $\mathcal{T}(s(k+1)|a(k), s(k))$  gives the probability of ending in state  $s(k+1)$ , if the agent performs the action  $a(k)$  in state  $s(k)$
- $\mathcal{R}$  is the  $\mathcal{S} \times \mathcal{A} \times \mathcal{S} \rightarrow \mathbb{R}$  is the reward function where  $\mathcal{R}(s(k+1)|s(k), a(k))$  gives the reward in state  $s(k+1)$  by executing the action  $a(k)$  in state  $s(k)$

- $\gamma$  is the discount factor,  $0 < \gamma < 1$

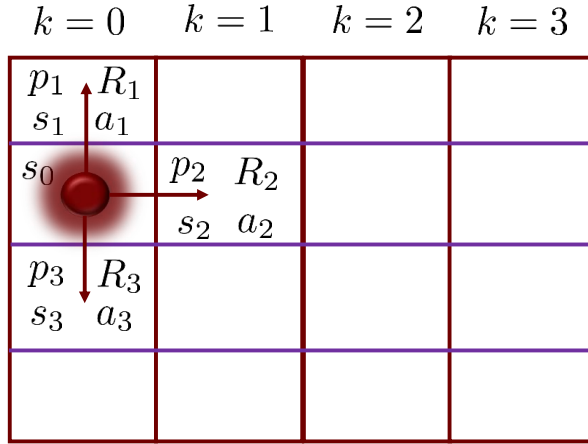


Figure 2.16: An MDP with 16 states

In Figure 2.16, we define 3 actions for the same agent and rewards at each state that the objective is to collect the maximum reward with chosen actions.

### 2.3.2 MDP Modeling in Autonomous Driving

Markov decision process is a useful tool to model traffic environments for an autonomous vehicle navigation. The main idea here is to define a world that is composed of small rectangular objects. These objects are called states, which are connected by the actions of the autonomous vehicle. We can assign values, i.e., negative and positive rewards in the states such that the behavior of the autonomous vehicle is manipulated in a desired way. Motivated by this useful knowledge, the road is modeled as a grid-world over a horizon. Each rectangular object represents the travel time in the direction of driving. Basically, the size of the rectangles depends on the vehicle speed and sampling time of data collection, which is received by sensors. Then states are the number of rectangu-

lar objects in the world and actions are the longitudinal accelerations that connect them. Transition probabilities are calculated by threat assessment. The motivation behind is that for each target gap, the threat of vehicle's can be blended in the decision making process. MDP is employed to respond to rewards in the world thus the choices of rewards force the vehicle to behave in a desired way. Cumulative rewards are then maximized through a path in the grid world from a starting state to an end state. Then the term policy is defined as the overall behavior of MDP.

### 2.3.3 MDP for Gap Selection

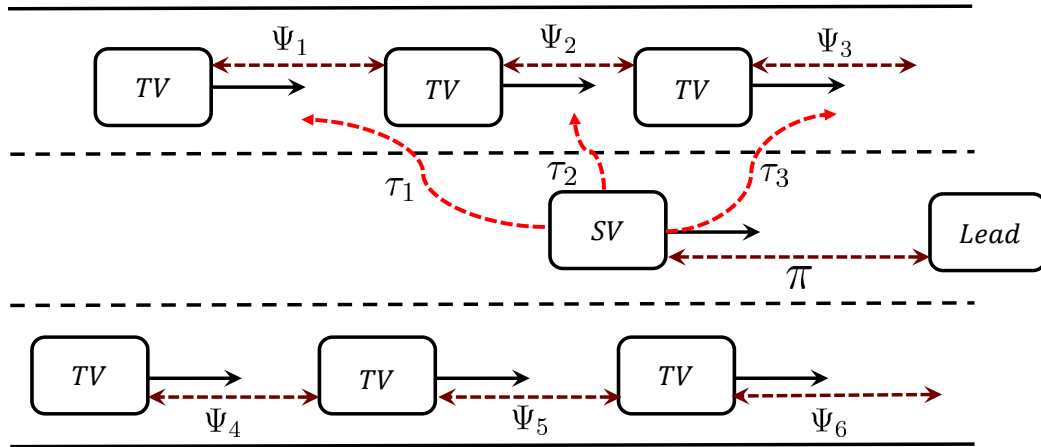


Figure 2.17: Scenario description

In Figure 2.17, the *SV* encounter an obstruction in current drive lane with a vehicle ahead and seeks to merge to possible gap by adjusting its speed and then merging. Therefore we can treat this mandatory lane changing problem in two major stages; adjustment stage and merging stage. In Figure 2.18, the *SV* targets the gap between the *TVs*. By using acceleration in longitudinal direction, the position is adjusted and merging completes

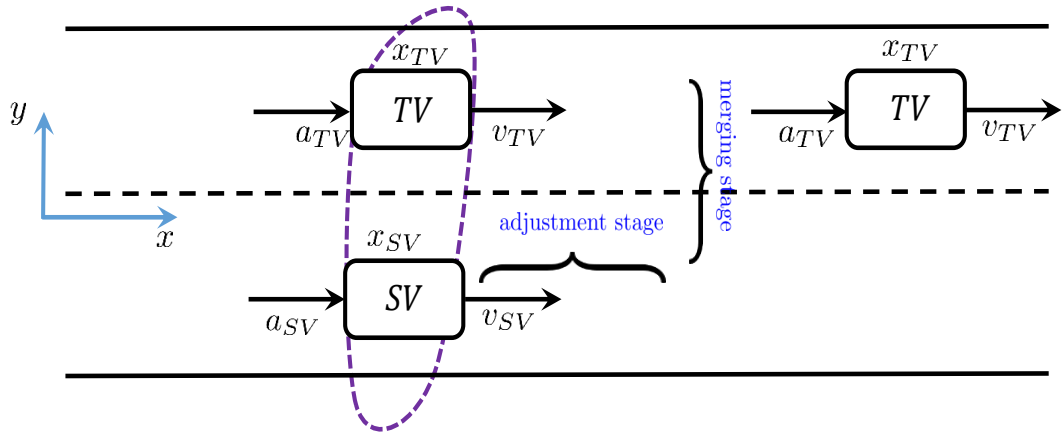


Figure 2.18: Lane changing model

the lane changing. A reward function is defined for  $SV$  to assess the benefits of gaps to lane changing. Equation 2.12 defines 3 variables in the reward function.

- Longitudinal distance between vehicles, i.e.,  $\Psi_i$
- Time to reach to that gap, i.e.,  $\tau_i$
- Remaining longitudinal space to the lead vehicle, i.e.,  $\pi$

$$\mathcal{R}(s(k+1), a(k), s(k)) = \varrho_1 \frac{\Psi_i(k)}{\tau_i(k)} + \varrho_2 \pi(k). \quad (2.12)$$

$$\mathcal{T}(s(k+1), a^{SV}(k), s(k)) = 1 - \mathcal{L}_i \quad (2.13)$$

where  $i = 1, 2, \dots, n_{gap}$  and  $\varrho_1, \varrho_2$  are the user defined weight terms. The benefit or a gap depends on the adjustment stage, i.e.,  $\tau$ . For example, even when the gap length  $\Psi$  is large,  $\tau$  makes it less valuable in the reward function since it divides the value. And remaining longitudinal space to the lead vehicle, i.e.,  $\pi$  is also an important element because its value is not good if a large acceleration is needed for a gap, consequently the  $SV$  gets closer to the lead car, which is not a good strategy in mandatory lane changing. Equation 2.13 gives

the transition probabilities, which is a function of threat assessment.

Algorithm that defines the behavior of  $SV$  in terms of an objective function, variables, and constraints is given as

$$a^{SV*}(k) = \arg \max_{a^{SV}}(k) \sum_{k=1}^N \left[ \mathcal{R}(s(k+1)|s(k), a^{SV}(k)) + \gamma \sum_{s(k)} \mathcal{T}(s(k+1)|s(k), a^{SV}(k)) \times \mathcal{V}(s(k)) \right], \quad (2.14)$$

**where**

$$a^{SV*}(k) = (u_x^{SV*}(k), lc^{SV*}(k)) \quad \text{and} \quad a^{SV}(k) = (u_x^{SV}(k), lc^{SV}(k)), \quad (2.15)$$

**with**

$$\mathcal{V}(s(k+1)|u_x^{SV*}(k), lc^{SV*}(k)) \geq \mathcal{V}(s(k+1)|u_x^{SV*}(k), lc^{SV}(k)), \quad \forall lc^{SV}(k), \quad (2.16)$$

$$\mathcal{V}(s(k+1)|u_x^{SV*}(k), lc^{SV*}(k)) \geq \mathcal{V}(s(k+1)|u_x^{SV}(k), lc^{SV*}(k)), \quad \forall u_x^{SV}(k), \quad (2.17)$$

**subject to**

$$\begin{pmatrix} x(k+1) \\ v_x(k+1) \end{pmatrix} = \begin{pmatrix} 1 & \Delta(k) \\ 0 & 1 \end{pmatrix} \begin{pmatrix} x(k) \\ v_x(k) \end{pmatrix} + \begin{pmatrix} 0 \\ \Delta(k) \end{pmatrix} u_x(k), \quad (2.18)$$

$$u_{x_{min}} \leq u_x(k) \leq u_{x_{max}}, \quad (2.19)$$

$$sgn(\Delta u(k+1)) = sgn(\Delta u(k)), \quad (2.20)$$

$$v_{x_{min}} \leq v_x(k) \leq v_{x_{max}}, \quad (2.21)$$

$$\tau_i(k) \leq N, \quad i = 1, 2, \dots, n_{gap}, \quad (2.22)$$

$$\min(\mathcal{G}_i(k)) \leq \Psi_i(k), \quad i = 1, 2, \dots, n_{gap}, \quad (2.23)$$

$$\pi(k) \geq \min(\pi(k)). \quad (2.24)$$

Recall that  $N$  is the prediction horizon in which we maximize the cumulative rewards and its value 4 *seconds* in equation 2.14. It is seen that the optimal action points, i.e., the optimal policy is sought  $a^{SV^*}(k)$  at each time instants among all the existing ones of  $a^{SV}(k)$ . Immediate rewards and discounted value of successor states are maximized with  $a^{SV^*}(k)$  in equation 2.14 over the prediction horizon  $N$ . Equation 2.15 shows the elements of optimal action candidates, the longitudinal acceleration and lane change target values, i.e.,  $a^{SV^*}(k) = (u_x^{SV^*}(k), lc^{SV^*}(k))$ . The optimal points are the best possible selections such that the conditions in 2.16 and 2.17 hold. Equation 2.18 shows the system dynamics along with the longitudinal acceleration bounds in equation 2.19 and sign change constraints in equation 2.20, which guarantees the direction of control input does not change in the optimal policy. Equation 2.21 is for bounding the speed and the condition  $\tau_i(k) \leq N$  restricts the solution of adjustment stage is inside the horizon  $N$  in equation 2.22. Minimum gap condition to check as well as safe remaining gap before lane changing are also included in the design by the equations 2.23 and 2.24, respectively. Optimal policy is solved through prediction. How the solution propagates is seen in 2.19 where a set of possible candidates at time  $k$  is produced and above algorithm searches the best one, i.e., the maximized reward objectives in order to implement in proceeding time. This module is called as higher-level decision making module, which has enough detailed information

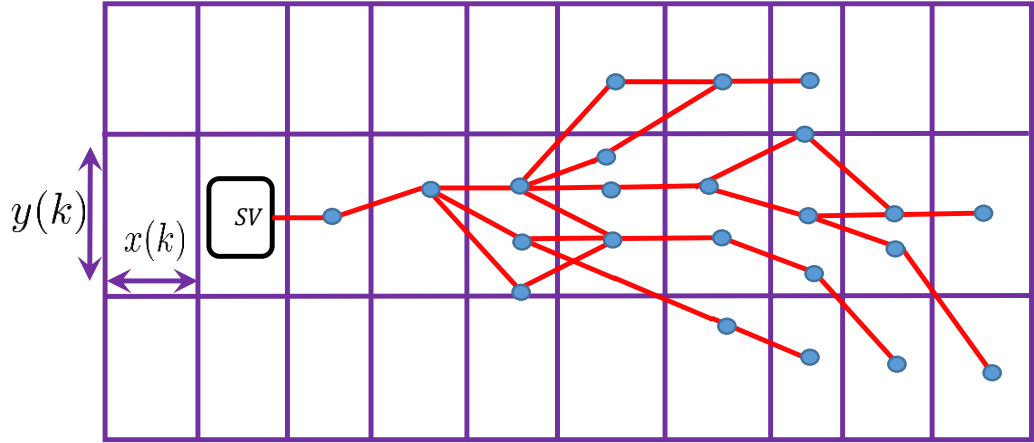


Figure 2.19: Solution of MDP

to re-evaluate the decision. For instance, when *SV* does not find an optimal lane changing policy from equation 2.14, it can abort the lane changing in current time and seeks for another optimal solution. In this level, all the possible consideration for a lane change is taken into account, the lower-level control can smoothly achieve the commanded tasks in the hierarchical framework. It is assumed that the road geometry is known by the agent. We define the state space as containing the *SV* and *TVs* state quantities on a moving state information grid, which is centered around the *SV*. And it is constructed over a prediction horizon at each time step.

$$states = \begin{cases} s(k) = (x(k), y(k)), & \text{2D position,} \\ \#gap, & \text{number of gaps,} \end{cases}$$

$$transitions = \begin{cases} 1 - \mathcal{L}_i(k), & \text{transiting} \\ \mathcal{L}_i, & \text{staying} \end{cases}$$

where  $i$  is the number of gap. Recall that I model the road ahead by a grid-world and positions  $(x(k), y(k))$  correspond to the next time step that  $SV$  travels on. Terminal states are the gaps where the  $SV$  evaluates to merge in. Starting from the terminal state, backwards propagation assigns values for every states and the  $SV$ 's objective at each time step of travel is to drive in the direction of accumulating the maximum reward starting from the initial state towards the terminal state. Also, the transitions to a particular gap is determined with threat estimation. Meaning that a probabilistic value is calculated at each time instant and input to our grid world where there are 40 time steps ( $N = 4$ , time horizon and  $\Delta(k) = 0.1 \text{ secs}$  sampling time) exist. Therefore, a set of predicted threat values is used in the solution of MDP at current time.

**Remark 1:** I propose a dynamic model to enumerate different lane-changing strategies. In real life driving, drivers look for several gaps and adjust the vehicle speed during the lane changes according to the surrounding vehicles. This occurs in response to the subjective reasoning process of human drivers. In this regard, I develop a framework in which *most* of the driving habits of human can be captured. To conclude this, drivers feeling of safely to avoid a traffic conflict can be modeled through a set of decision logics, which rely on perceptions of human drivers.

**Remark 2:** Above decisions are high level decisions. This level determines the target gap to merge and the amount of speed changes required during the lane changing. The MPC trajectory planner uses the information to generate a maneuver as a result of decision process with the objective of

1. keeping the subject vehicle at its reference velocity,  $v_{ref}$ ,
2. maintaining the center line of the selected lane,  $y_{ref}$ ,

It is pointed out that the decisions are made by MDP, which takes into account avoiding collisions in the neighboring lanes with an environment abstraction. When the lane change

is completed, the flow of the traffic is maintained by a microscopic traffic model.

### 2.3.4 Bellman's Equation and System Algorithm

The defined model matrices above guides the behavior of the autonomous car. To execute a decision for MDP problems requires evaluating the Bellman's dynamic programming equation until it converges to a defined infinitesimal small error bound. The first method is to iterate the value function  $\mathcal{V}(s(k+1))$  that specifies how the state  $s$  is valuable under the policy  $\varphi(k)$  for the set of actions  $a(k)$ . The autonomous car finds the optimal action, which results in maximum expected reward. This action is called optimal policy. The second method is to iterate the policy function by starting with an optimal policy, which maximizes the expected reward. This policy leads to a set of optimal actions. The Bellman's equation for the value iteration is given by

$$\mathcal{V}(s(k+1)) = \max_{a(k)} \sum_{k=1}^N \left[ \mathcal{R}(s(k+1)|s(k), a(k)) + \gamma \sum_{s(k)} \mathcal{T}(s(k+1)|s(k), a(k)) \times \mathcal{V}(s(k)) \right], \quad (2.25)$$

The value function iterates until it converges to the prescribed error bound. The optimal policy by considering all possible actions from each state is given as

$$\varphi^*(s(k)) = \arg \max_{a(k)} \sum_{k=1}^N \left[ \mathcal{R}(s(k+1)|s(k), a(k)) + \gamma \sum_{s(k)} \mathcal{T}(s(k+1)|s(k), a(k)) \times \mathcal{V}(s(k)) \right], \quad (2.26)$$

which is used by our autonomous car to achieve the safest transition to a lane. The algorithm is given as

$$\mathcal{V}(s(k+1)) = \max_{a(k)} \left[ \mathcal{R}(s(k+1)|s(k), a(k)) + \gamma \sum_{s(k)} \mathcal{T}(s(k+1)|s(k), a(k)) \times \mathcal{V}(s(k)) \right], \quad (2.27)$$

---

**Algorithm 1:** Value iteration

---

*Choose an initial optimal value and random policy function;*

**while**  $\varepsilon < \text{prescribed error bound}$  **do**

**foreach state do**

        Calculate the value of states (lanes) when taking each possible action;

        Use maximal operator to update the optimal value function estimate until convergence;

        Execute an optimal action as optimal policy;

---

Optimal policy  $\varphi^*$  is the set of maximizing actions, i.e.,  $a(1), a(2), \dots, a(n)$  where  $n$  is the final time of solution such that

$$\varphi^*(s(k)) = \arg \max_{a(k)} \left[ \mathcal{R}(s(k+1)|s(k), a(k)) + \gamma \sum_{s(k)} \mathcal{T}(s(k+1)|s(k), a(k)) \times \mathcal{V}(s(k)) \right], \quad (2.28)$$

Then the following equality holds

$$\mathcal{V}(s(k+1)|\varphi^*(s(k))) \geq \mathcal{V}(s(k+1)|\varphi(s(k))). \quad (2.29)$$

Then the optimal state-value function under the optimal policy is

$$\mathcal{V}_\varphi^*(s(k+1)) = \max_{a(k)} \left[ \mathcal{R}(s(k+1)|s(k), a(k)) + \gamma \sum_{s(k)} \mathcal{T}(s(k+1)|s(k), a(k)) \times \mathcal{V}_\varphi^*(s(k)) \right]. \quad (2.30)$$

Predicted based solution over a moving time horizon  $N$

$$\mathcal{V}(s(k+1)) = \max_{a(k)} \sum_{k=1}^N \left[ \mathcal{R}(s(k+1)|s(k), a(k)) + \gamma \sum_{s(k)} \mathcal{T}(s(k+1)|s(k), a(k)) \times \mathcal{V}(s(k)) \right], \quad (2.31)$$

Optimal policy  $\varphi^*$  is the set of maximizing actions, i.e.,  $a(1), a(2), \dots, a(n)$  where  $n$  is the final time of solution such that

$$\varphi^*(s(k)) = \arg \max_{a(k)} \sum_{k=1}^N \left[ \mathcal{R}(s(k+1)|s(k), a(k)) + \gamma \sum_{s(k)} \mathcal{T}(s(k+1)|s(k), a(k)) \times \mathcal{V}(s(k)) \right], \quad (2.32)$$

Then the following equality holds

$$\mathcal{V}(s(k+1)|\varphi^*(s(k))) \geq \mathcal{V}(s(k+1)|\varphi(s(k))). \quad (2.33)$$

Then the optimal state-value function under the optimal policy is

$$\mathcal{V}_\varphi^*(s(k+1)) = \max_{a(k)} \sum_{k=1}^N \left[ \mathcal{R}(s(k+1)|s(k), a(k)) + \gamma \sum_{s(k)} \mathcal{T}(s(k+1)|s(k), a(k)) \times \mathcal{V}_\varphi^*(s(k)) \right]. \quad (2.34)$$

## 2.4 Markov Game

Markov games ( $\mathcal{MG}$ ) are a generalized solution of Markov decision processes and repeated games. The big difference is the fact that several agents decide on actions over a given environment. Thus the solution outcomes are different depending on the other agents actions [108]. This is exactly what game theory approach is dedicated to solve from different agent's point of view. A comprehensive treatment is given in [109]. In autonomous driving, the main goal of including game in the MDP solution is to consider the drivers interactions in the traffic model. It is well-known that there are numerous scenarios of drivers actions while driving but game-theoretic approach can handle these scenarios by mathematically modeling possible characterization of interactions so that the autonomous vehicles can capture the agents reactions in decision making stage. The Figure 2.20 represents a 2 players or agents Markov game. The agents initial states are denoted  $s_0^1$  for the agent 1 and  $s_0^2$  the agent 2 and they have different actions over the states of the

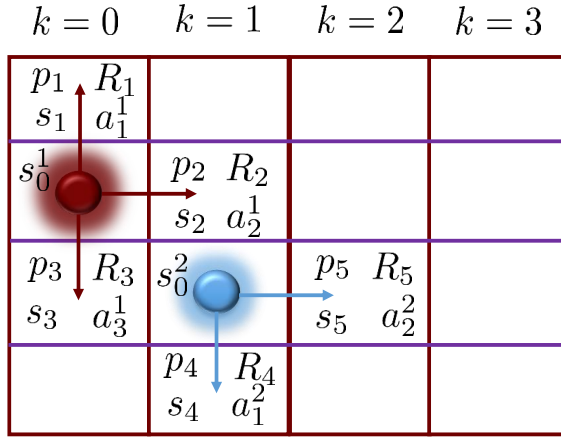


Figure 2.20: A Markov game with multiple agents

system. The formal definition then follows;

A multi-agent Markov game ( $\mathcal{MG}$ ) is represented by the tuple  $\langle \mathcal{P}, \mathcal{S}, \mathcal{A}, \mathcal{T}, \mathcal{R}, \gamma \rangle$

- $\mathcal{P} = 1, 2, \dots, p$  is the set of agents
- $\mathcal{S}$  is the set of all possible states of  $s(k)$  at time  $k$
- $\mathcal{A}^p(k)$  with  $p \in \mathcal{P}$  is the set of all possible action space  $a^p(k)$  available to agent  $p$  at time  $k$
- $\mathcal{T}$  is the  $\mathcal{S} \times \mathcal{A}^p \times \mathcal{S} \rightarrow [0, 1]$  is the transition function where  $\mathcal{T}(s(k+1)|a^p(k), s(k))$  gives the probability of ending in state  $s(k + 1)$ , if the agent  $p$  performs the action  $a^p(k)$  in state  $s(k)$  at time  $k$
- $\mathcal{R}^p$  is the  $\mathcal{S} \times \mathcal{A}^p \times \mathcal{S} \rightarrow \mathbb{R}$  is the reward function where  $\mathcal{R}^p(s(k+1)|s(k), a^p(k))$  gives the reward for the agent  $p$  in state  $s(k + 1)$  by executing the action  $a^p(k)$  in state  $s(k)$
- $\gamma$  is the discount factor,  $0 < \gamma < 1$

Now we can consider a world where multiple agents interact and outcome of the solution depends on individual strategies of the agents. As seen from the definition, one of the most important features of  $(\mathcal{MG})$  is that rewards and transition functions depend on actions of all players unlike in MDP case where it only depends on one agent actions. Some important things to remember

- Value of a state depends on individual actions
- Transitions to a state depends on individual actions
- Players might have different actions
- Game does not change the system states
- Strategies of the players are denoted as the overall behavior of a Markov game

We seek to find an equilibria at each state of the state-space. An individual strategy at the equilibrium is called the best response strategy to achieve the maximum reward for a given game and found with Nash equilibrium solution.

#### 2.4.1 Nash Equilibrium for Bimatrix Games [110]

Consider a 2-player non-zero-sum (or general sum) game with payoff matrices  $M^1$  and  $M^2$ ; A pair of  $M^1$  and  $M^2$  forms a bimatrix game with  $M^1$  and  $M^2$  are the same size. The payoff  $R^p$  for player  $p$  is the corresponding entry of the matrix  $M^p$ . The rows of  $M^p$  correspond to the player 1 with  $a^1 \in \mathcal{A}^1$  and the columns are the player 2 with  $a^2 \in \mathcal{A}^2$ . Then a pure strategy Nash equilibrium is for this bimatrix game  $\mathcal{MG}$  is

$$\begin{aligned}\mathcal{R}^1(a^{1*}, a^{2*}) &\geq \mathcal{R}^1(a^1, a^{2*}), \forall a^1 \in \mathcal{A}^1, \\ \mathcal{R}^2(a^{1*}, a^{2*}) &\geq \mathcal{R}^2(a^{1*}, a^2), \forall a^2 \in \mathcal{A}^2.\end{aligned}$$

Every general-sum discounted stochastic game has at least one equilibrium point in stationary strategies [109] Theorem 4.6.4 on page 219.

		From TV's perspective	
A bimatrix game		Player 2 (TV)	
		$a_{acc}^{TV}$	$a_{dec}^{TV}$
Player 1 (SV)	$a_{acc}^{SV}$	$\mathcal{R}(a_{acc}^{SV}, a_{acc}^{TV}) = 2R$	$\mathcal{R}(a_{acc}^{SV}, a_{dec}^{TV}) = 3R$
	$a_{dec}^{SV}$	$\mathcal{R}(a_{dec}^{SV}, a_{acc}^{TV}) = R$	$\mathcal{R}(a_{dec}^{SV}, a_{dec}^{TV}) = 2R$

Figure 2.21: Example of equilibrium

#### 2.4.2 Markov Game for Gap Selection

We now set-up a game for multiple agents in a traffic environment shown in Figure 2.22. The main underlying idea of the game theoretic modeling is that all the potential behaviors of the vehicles can be considered in the design. Benefiting from the large number of possible behavior, we can achieve the best performance in obstacle avoidance while lane changing. The Figure 2.22 shows the *TVs* and *SV* and their traveling directions. Assuming that all the vehicles are equipped with Lidar radar sensors so that the information of the traffic is available to the vehicles<sup>2</sup>. *SV* considers as number interactions as possible with the surrounding vehicles up to the number of available gaps. The Figure 2.22 shows one game pairing but the total of six games is played for six gaps.

- Longitudinal distance between vehicles, i.e.,  $\Psi_i$
- Time to reach to that gap, i.e.,  $\tau_i$
- Remaining longitudinal space to the lead vehicle, i.e.,  $\pi$

---

<sup>2</sup>This is an important assumption for cooperative case and the same assumption might not be valid for non-cooperative case

where  $i = 1, 2, \dots, n_{gap}$  in the set up.

Both cooperative and non-cooperative games are established and solved. Reward equa-

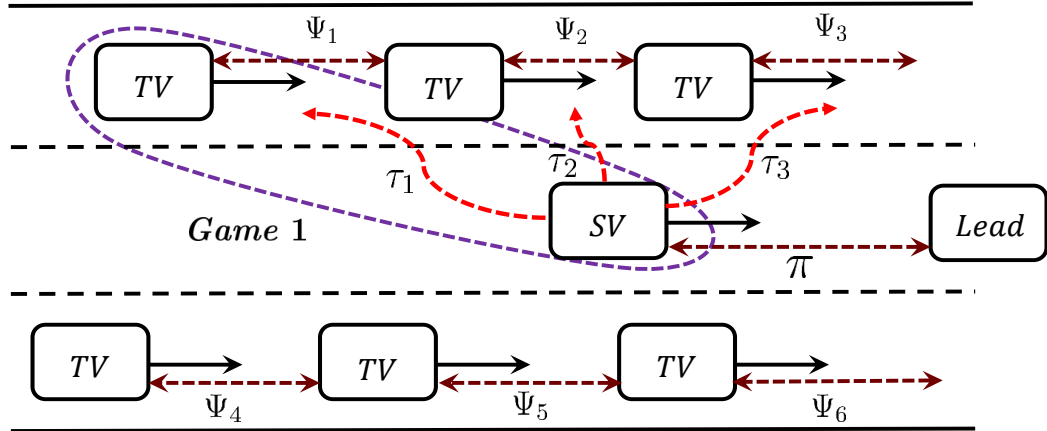


Figure 2.22: General non-zero-sum Markov game set-up with multiple agents

tion 2.35 is defined same as equation 2.12, except the value depends of the actions of a  $TV$  and  $SV$ .

$$\mathcal{R}(s(k+1), a^{SV}(k), a^{TV}(k), s(k)) = \varrho_1 \frac{\Psi_i(k)}{\tau_i(k)} + \varrho_2 \pi(k). \quad (2.35)$$

$$\mathcal{T}(s(k+1), a^{SV}(k), a^{TV}(k), s(k)) = 1 - \mathcal{L}_i \quad (2.36)$$

where  $\varrho_1$  and  $\varrho_2$  are the user defined weight terms. Individual payoff functions or so-called objectives for  $SV$  and  $TVs$  are defined below In equation 2.37, the first payoff defined for  $SV$ , i.e.,  $\mathcal{U}$  is a game theoretic notation used in analysis for a game solution. I will stick by the the reward notation  $\mathcal{R}$  since a set of repeated games is solved in Markov grid-world. The terms are given in previous section. The second payoff is for  $TV$  when it a cooperative game. In this case, the  $TV$  determines its strategy to allow the  $SV$  to achieve

the lane change process faster by opening a gap and/or minimizing the travel time for the gap that is ahead of it.

$$\begin{aligned}\mathcal{U}^{SV}(s(k+1), a^{SV}(k), s(k)) &= \varrho_1 \frac{\Psi_i(k)}{\tau_i(k)} + \varrho_2 \pi(k), \\ \mathcal{U}^{TV}(s(k+1), a^{TV}(k), s(k)) &= \varrho_1 \frac{\Psi_i(k)}{\tau_i(k)}, \\ \mathcal{U}^{TV}(s(k+1), a^{TV}(k), s(k)) &= \varrho_1 \Psi_i(k),\end{aligned}\tag{2.37}$$

The last payoff in equation 2.37 is to consider the case where *TV* is not cooperating and it minimized the gap ahead. The objective for *SV* is to maximize the worst case strategy of *TVs* for any available gap in its surrounding. This is indeed the most common case when the drivers are not gentle for another, which is basically one of the factors of traffic accidents on roads.

The optimal maximizing policy is the pure strategy of the Nash equilibrium of agent  $p$ , i.e.,  $\varphi^{p*}(k) \geq \varphi^p(k)$  at the state value function  $\mathcal{V}$ .

*Definition:* A Nash equilibrium of *SV* and a *TV* in a Markov game  $\mathcal{MG}$  is the optimal strategy  $(\varphi^{SV*}(k), \varphi^{TV*}(k))$  such that

$$\begin{aligned}\mathcal{V}^{SV}(s(k+1)|\varphi^{SV*}(k), \varphi^{TV*}(k)) &\geq \mathcal{V}^{SV}(s(k+1)|\varphi^{SV}(k), \varphi^{TV*}(k)), \forall \varphi^{SV}, \\ \mathcal{V}^{TV}(s(k+1)|\varphi^{SV*}(k), \varphi^{TV*}(k)) &\geq \mathcal{V}^{TV}(s(k+1)|\varphi^{SV*}(k), \varphi^{TV}(k)), \forall \varphi^{TV}.\end{aligned}$$

When the payoffs and strategies are defined for the players, the next step is to search for the optimal strategy. A strategy in the proposed game definition consists of lane change targets and longitudinal acceleration profiles for *SV* and only the longitudinal acceleration profiles for *TVs*. The cooperative general non-zero-sum Markov game solution maximizes the payoffs from each player's viewpoint, meaning that the optimal actions are the best pairs at each state of the system such that no player can achieve a better payoff. Payoff matrices are formed for each target gaps with respect to the discrete longitudinal accelerations  $u_x = [u_{xmin}, u_{xmax}]$ . It should be noted that the solution is calculated at each time

instant in the state-space of the system. If high precision required in the solution, a denser grid of acceleration can be used to build payoff matrices. In the matrix game shown for

		Player 2 (TV)	
		$a_{acc}^{TV}$	$a_{dec}^{TV}$
Player 1 (SV)	$a_{acc}^{SV}$	$\mathcal{R}(a_{acc}^{SV}, a_{acc}^{TV})$	$\mathcal{R}(a_{acc}^{SV}, a_{dec}^{TV})$
	$a_{dec}^{SV}$	$\mathcal{R}(a_{dec}^{SV}, a_{acc}^{TV})$	$\mathcal{R}(a_{acc}^{SV}, a_{dec}^{TV})$

Figure 2.23: Markov game matrix

$SV$  and  $TV$  in Figure 2.23, objective is to find a set of equilibrium points given the players determined their actions. In lane change  $\mathcal{MG}$  set-up, the interest is to seek for sequential equilibrium points in a grid-world with the objective of cumulative expected maximizing reward values.

Next we the following algorithm for cooperative Markov game is

$$(a^{SV*}(k), a^{TV*}(k)) = \arg \max_{a^{SV}(k), a^{TV}(k)} \sum_{k=1}^N \left[ \mathcal{R}^p(s(k+1)|s(k), a^{SV}(k), a^{TV}(k)) + \gamma \sum_{s(k)} \mathcal{T}(s(k+1)|s(k), a^{SV}(k), a^{TV}(k)) \times \mathcal{V}^p(s(k)) \right], \quad (2.38)$$

**where**

$$(a^{SV*}(k), a^{TV*}(k)) = (u_x^{SV*}(k), lc^{SV*}(k), u_x^{TV*}(k)) \quad \text{and} \quad (2.39)$$

$$(a^{SV}(k), a^{TV}(k)) = (u_x^{SV}(k), lc^{SV}(k), u_x^{TV}(k)),$$

**with**

$$\mathcal{V}^p(s(k+1)|u_x^{SV*}(k), lc^{SV*}(k), u_x^{TV*}(k)) \geq \mathcal{V}^p(s(k+1)|u_x^{SV*}(k), lc^{SV}(k), u_x^{TV}(k)),$$

$$\forall lc^{SV}(k), u_x^{TV},$$

(2.40)

$$\mathcal{V}^p(s(k+1)|u_x^{SV*}(k), lc^{SV*}(k), u_x^{TV*}(k)) \geq \mathcal{V}^p(s(k+1)|u_x^{SV}(k), lc^{SV*}(k), u_x^{TV}(k)),$$

$$\forall u_x^{SV}(k), u_x^{TV},$$

(2.41)

$$\mathcal{V}^p(s(k+1)|u_x^{SV*}(k), lc^{SV*}(k), u_x^{TV*}(k)) \geq \mathcal{V}^p(s(k+1)|u_x^{SV}(k), lc^{SV}(k), u_x^{TV*}(k)),$$

$$\forall u_x^{SV}(k), lc^{SV}(k),$$

(2.42)

**subject to**

$$\begin{pmatrix} x^p(k+1) \\ v_x^p(k+1) \end{pmatrix} = \begin{pmatrix} 1 & \Delta(k) \\ 0 & 1 \end{pmatrix} \begin{pmatrix} x^p(k) \\ v_x^p(k) \end{pmatrix} + \begin{pmatrix} 0 \\ \Delta(k) \end{pmatrix} u_x^p(k), \quad (2.43)$$

$$u_{x_{min}}^p \leq u_x^p(k) \leq u_{x_{max}}^p, \quad (2.44)$$

$$\operatorname{sgn}(\Delta u(k+1)^p) = \operatorname{sgn}(\Delta u(k)^p), \quad (2.45)$$

$$v_{x_{min}}^p \leq v_x^p(k) \leq v_{x_{max}}^p, \quad (2.46)$$

$$\tau_i^p(k) \leq N, \quad i = 1, 2, \dots, n_{gap}, \quad (2.47)$$

$$\min(\mathcal{G}_i^p(k)) \leq \Psi_i^p(k), \quad i = 1, 2, \dots, n_{gap}, \quad (2.48)$$

$$\pi^p(k) \geq \min(\pi^p(k)). \quad (2.49)$$

Objective function value is defined in terms of mutual actions of the players in equation 2.38. Solution of this game maximizes the rewards both players viewpoints from the all states over the prediction horizon  $N$ . Equation 2.39 shows the corresponding optimal policy or strategy pairs of the players. Maximizing Nash equilibrium solution pairs are the best-strategy pairs among all other candidates in equation 2.40, 2.41, 2.42. Vehicles kinematic models are shown in 2.43. Longitudinal acceleration bounds for players are given in equation 2.44 and sign change constraints in equation 2.45, which guarantees the direction of control input does not change in the optimal strategy. Equation 2.46 is for bounding the speed of the players and the condition  $\tau_i(k) \leq N$  restricts the solution for the player  $p$  of adjustment stage is inside the horizon  $N$  in equation 2.47. Minimum gap condition ahead of a player  $p$  is also checked and the safe remaining gap before lane changing are also included in the design by the equations 2.48 and 2.49, respectively. If there is no gap and/or no candidate solution exist in the solution, there exists a solution of staying in current lane by reducing the speed. Since most of the cases drivers are not willing to give away to vehicles that seek to lane changing. Considering this scenario, the

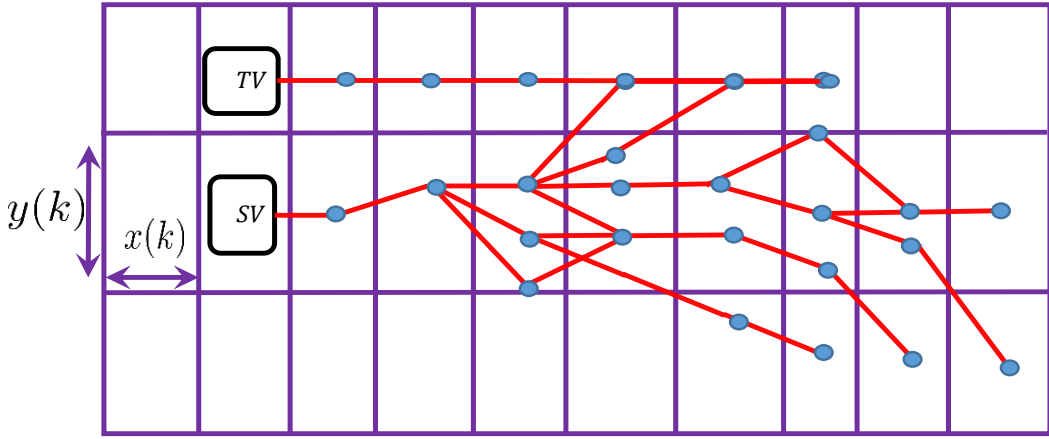


Figure 2.24: Solution of game with candidate generation by prediction

following algorithm is for non-cooperative Markov game solution

$$(a^{SV*}(k), a^{TV*}(k)) = \arg \max_{a^{SV}(k)} \left[ \min_{a^{TV}(k)} \sum_{k=1}^N \left[ \mathcal{R}^p(s(k+1)|s(k), a^{SV}(k), a^{TV}(k)) + \gamma \sum_{s(k)} \mathcal{T}(s(k+1)|s(k), a^{SV}(k), a^{TV}(k)) \times \mathcal{V}^p(s(k)) \right] \right], \quad (2.50)$$

**where**

$$\begin{aligned} (a^{SV*}(k), a^{TV*}(k)) &= (u_x^{SV*}(k), lc^{SV*}(k), u_x^{TV*}(k)) \quad \text{and} \\ (a^{SV}(k), a^{TV}(k)) &= (u_x^{SV}(k), lc^{SV}(k), u_x^{TV}(k)), \end{aligned} \quad (2.51)$$

**with**

$$\begin{aligned} \mathcal{V}^p(s(k+1)|u_x^{SV*}(k), lc^{SV*}(k), u_x^{TV*}(k)) &\leq \mathcal{V}^p(s(k+1)|u_x^{SV*}(k), lc^{SV}(k), u_x^{TV}(k)), \\ \forall lc^{SV}(k), u_x^{TV}, \end{aligned} \quad (2.52)$$

$$\begin{aligned} \mathcal{V}^p(s(k+1)|u_x^{SV*}(k), lc^{SV*}(k), u_x^{TV*}(k)) &\leq \mathcal{V}^p(s(k+1)|u_x^{SV}(k), lc^{SV*}(k), u_x^{TV}(k)), \\ \forall u_x^{SV}(k), u_x^{TV}, \end{aligned} \tag{2.53}$$

$$\begin{aligned} \mathcal{V}^p(s(k+1)|u_x^{SV*}(k), lc^{SV*}(k), u_x^{TV*}(k)) &\geq \mathcal{V}^p(s(k+1)|u_x^{SV}(k), lc^{SV}(k), u_x^{TV*}(k)), \\ \forall u_x^{SV}(k), lc^{SV}(k), \end{aligned} \tag{2.54}$$

**subject to**

$$\begin{pmatrix} x^p(k+1) \\ v_x^p(k+1) \end{pmatrix} = \begin{pmatrix} 1 & \Delta(k) \\ 0 & 1 \end{pmatrix} \begin{pmatrix} x^p(k) \\ v_x^p(k) \end{pmatrix} + \begin{pmatrix} 0 \\ \Delta(k) \end{pmatrix} u_x^p(k), \tag{2.55}$$

$$u_{x_{min}}^p \leq u_x^p(k) \leq u_{x_{max}}^p, \tag{2.56}$$

$$sgn(\Delta u(k+1)^p) = sgn(\Delta u(k)^p), \tag{2.57}$$

$$v_{x_{min}}^p \leq v_x^p(k) \leq v_{x_{max}}^p, \tag{2.58}$$

$$\tau_i^p(k) \leq N, \quad i = 1, 2, \dots, n_{gap}, \tag{2.59}$$

$$\min(\mathcal{G}_i^p(k)) \leq \Psi_i^p(k), \quad i = 1, 2, \dots, n_{gap}, \tag{2.60}$$

$$\pi^p(k) \geq \min(\pi^p(k)). \tag{2.61}$$

Now the objective of zero-sum Markov game for *SV* is to maximize the worst case reacting strategies of *TVs* during the selection of the gaps. The modified objective function is seen in equation 2.50 with the optimal pairs achieving this in equation 2.51. Optimal action candidates of a *TV* for a gap ahead is the lower bound among the all of action candidates that maximizes the rewards for the players in equation 2.52, 2.53. On the other hand, optimal action candidates of *SV* are still the upper bounds of the value function, given in equation 2.54. The rest of the elements are; vehicles kinematic models are shown

in 2.55. Longitudinal acceleration bounds for players are given in equation 2.56 and sign change constraints in equation 2.57, which guarantees the direction of control input does not change in the optimal strategy. Equation 2.58 is for bounding the speed of the players and the condition  $\tau_i(k) \leq N$  restricts the solution for the player  $p$  of adjustment stage is inside the horizon  $N$  in equation 2.59. Minimum gap condition ahead of a player  $p$  is also checked and the safe remaining gap before lane changing are also included in the design by the equations 2.60 and 2.61, respectively. If there is no gap and/or no candidate solution exist in the solution, there exists a solution of staying in current lane by reducing the speed.

### 2.4.3 Bellman Equation for Markov Game

We will first derive the conditions for cooperative a Markov game where both agents maximize their highest possible rewards and different solution for non-cooperative Markov games is also presented in the upcoming sections.

$$\mathcal{V}^p(s(k+1)) = \max_{a^1(k), a^2(k)} \left[ \mathcal{R}^p(s(k+1)|s(k), a^1(k), a^2(k)) + \gamma \sum_{s(k)} \mathcal{T}(s(k+1)|s(k), a^1(k), a^2(k)) \times \mathcal{V}^p(s(k)) \right], \quad (2.62)$$

Optimal policy/strategy  $\varphi^*$  is the set of maximizing actions, i.e.,  $a^1(1), a^2(1), a^1(2), a^2(2), \dots, a^1(n), a^2(n)$  for the player  $p$  where  $n$  is the final time of solution such that

$$\varphi^{p*}(s(k)) = \arg \max_{a^1(k), a^2(k)} \left[ \mathcal{R}^p(s(k+1)|s(k), a^1(k), a^2(k)) + \gamma \sum_{s(k)} \mathcal{T}(s(k+1)|s(k), a^1(k), a^2(k)) \times \mathcal{V}^p(s(k)) \right], \quad (2.63)$$

The equilibrium value is the optimal value such that each of the players will never achieve a better payoff value. In this sense, the strategy profile is called a Markov-perfect equilib-

rium because it holds the Markov property, i.e., the next state value only depends on the current one and there exist a Nash equilibrium at each state of the system.

Then the following equality holds

$$\mathcal{V}^1(s(k+1)|\varphi^{1*}(k), \varphi^{2*}(k)) \geq \mathcal{V}^1(s(k+1)|\varphi^1(k), \varphi^2(k)), \forall \varphi^1,$$

$\mathcal{V}^2(s(k+1)|\varphi^{1*}(k), \varphi^{2*}(k)) \geq \mathcal{V}^1(s(k+1)|\varphi^{1*}(k), \varphi^2(k)), \forall \varphi^2$ . Optimal state-value function under the optimal policy is given for player  $p$

$$\begin{aligned} \mathcal{V}_{\varphi^p}^{p*}(s(k+1)) = \max_{a^1(k), a^2(k)} & \left[ \mathcal{R}^p(s(k+1)|s(k), a^1(k), a^2(k)) + \right. \\ & \left. \gamma \sum_{s(k)} \mathcal{T}(s(k+1)|s(k), a^1(k), a^2(k)) \times \mathcal{V}_{\varphi^p}^{p*}(s(k)) \right]. \end{aligned} \quad (2.64)$$

As stated in the previous sections, we construct an imaginary grid world of the system running by prediction over the horizon length  $N$ . The best strategy pairs are search among all the possible ones and once found, the solution is implemented. Therefore the modified Bellman equations in predicted time solution are

$$\begin{aligned} \mathcal{V}^p(s(k+1)) = \max_{a^1(k), a^2(k)} & \sum_{k=1}^N \left[ \mathcal{R}^p(s(k+1)|s(k), a^1(k), a^2(k)) + \right. \\ & \left. \gamma \sum_{s(k)} \mathcal{T}(s(k+1)|s(k), a^1(k), a^2(k)) \times \mathcal{V}^p(s(k)) \right], \end{aligned} \quad (2.65)$$

Markov-perfect equilibrium with the property of existence of a Nash equilibrium at each state as well being Markov is shown for player  $p$

$$\begin{aligned} \varphi^{p*}(s(k)) = \arg \max_{a^1(k), a^2(k)} & \sum_{k=1}^N \left[ \mathcal{R}^p(s(k+1)|s(k), a^1(k), a^2(k)) + \right. \\ & \left. \gamma \sum_{s(k)} \mathcal{T}(s(k+1)|s(k), a^1(k), a^2(k)) \times \mathcal{V}^p(s(k)) \right], \end{aligned} \quad (2.66)$$

Optimal state-value function under this optimal policy is given for player  $p$

$$\begin{aligned} \mathcal{V}_{\varphi^p}^*(s(k+1)) = & \max_{a^1(k), a^2(k)} \sum_{k=1}^N \left[ \mathcal{R}^p(s(k+1)|s(k), a^1(k), a^2(k)) + \right. \\ & \left. \gamma \sum_{s(k)} \mathcal{T}(s(k+1)|s(k), a^1(k), a^2(k)) \times \mathcal{V}_{\varphi^p}^*(s(k)) \right]. \end{aligned} \quad (2.67)$$

Let us write the same equations for non-cooperative case by defining the Bellman back-up equation as follows

$$\begin{aligned} \mathcal{V}^p(s(k+1)) = & \max_{a^1(k)} \min_{a^2(k)} \left[ \mathcal{R}^p(s(k+1)|s(k), a^1(k), a^2(k)) + \right. \\ & \left. \gamma \sum_{s(k)} \mathcal{T}(s(k+1)|s(k), a^1(k), a^2(k)) \times \mathcal{V}^p(s(k)) \right], \end{aligned} \quad (2.68)$$

Optimal policy/strategy  $\varphi^*$  is the set of maximizing actions of the worst case opponent responses, i.e.,  $a^1(1), a^2(1), a^1(2), a^2(2), \dots, a^1(n), a^2(n)$  for the player  $p$  where  $n$  is the final time of solution such that

$$\begin{aligned} \varphi^{p*}(s(k)) = & \arg \max_{a^1(k)} \left[ \min_{a^2(k)} \left[ \mathcal{R}^p(s(k+1)|s(k), a^1(k), a^2(k)) + \right. \right. \\ & \left. \left. \gamma \sum_{s(k)} \mathcal{T}(s(k+1)|s(k), a^1(k), a^2(k)) \times \mathcal{V}^p(s(k)) \right] \right], \end{aligned} \quad (2.69)$$

The agent 1 tries to maximizes its rewards with respect to the worst case response of the agent 2. The strategy profile is called a Markov-perfect equilibrium because it holds the Markov property, i.e., the next state value only depends on the current one and there exist a Nash equilibrium at each state of the system.

Then the following equality holds

$$\begin{aligned} \mathcal{V}^1(s(k+1)|\varphi^{1*}(k), \varphi^{2*}(k)) & \geq \mathcal{V}^1(s(k+1)|\varphi^1(k), \varphi^{2*}(k)), \forall \varphi^1, \\ \mathcal{V}^2(s(k+1)|\varphi^{1*}(k), \varphi^{2*}(k)) & \leq \mathcal{V}^1(s(k+1)|\varphi^{1*}(k), \varphi^2(k)), \forall \varphi^2. \end{aligned}$$

Optimal state-value function under the optimal policy is given for player  $p$

$$\begin{aligned} \mathcal{V}_{\varphi^p}^*(s(k+1)) = & \max_{a^1(k)} \min_{a^2(k)} \left[ \mathcal{R}^p(s(k+1)|s(k), a^1(k), a^2(k)) + \right. \\ & \left. \gamma \sum_{s(k)} \mathcal{T}(s(k+1)|s(k), a^1(k), a^2(k)) \times \mathcal{V}_{\varphi^p}^*(s(k)) \right]. \end{aligned} \quad (2.70)$$

Therefore the modified Bellman equations in predicted time solution are

$$\begin{aligned} \mathcal{V}^p(s(k+1)) = & \max_{a^1(k)} \min_{a^2(k)} \sum_{k=1}^N \left[ \mathcal{R}^p(s(k+1)|s(k), a^1(k), a^2(k)) + \right. \\ & \left. \gamma \sum_{s(k)} \mathcal{T}(s(k+1)|s(k), a^1(k), a^2(k)) \times \mathcal{V}^p(s(k)) \right], \end{aligned} \quad (2.71)$$

Markov-perfect equilibrium with the property of existence of a Nash equilibrium at each state as well being Markov is shown for player  $p$

$$\begin{aligned} \varphi^{p*}(s(k)) = & \arg \max_{a^1(k)} \left[ \min_{a^2(k)} \sum_{k=1}^N \left[ \mathcal{R}^p(s(k+1)|s(k), a^1(k), a^2(k)) + \right. \right. \\ & \left. \left. \gamma \sum_{s(k)} \mathcal{T}(s(k+1)|s(k), a^1(k), a^2(k)) \times \mathcal{V}^p(s(k)) \right] \right], \end{aligned} \quad (2.72)$$

Optimal state-value function under this optimal policy is given for player  $p$

$$\begin{aligned} \mathcal{V}_{\varphi^p}^*(s(k+1)) = & \max_{a^1(k)} \min_{a^2(k)} \sum_{k=1}^N \left[ \mathcal{R}^p(s(k+1)|s(k), a^1(k), a^2(k)) + \right. \\ & \left. \gamma \sum_{s(k)} \mathcal{T}(s(k+1)|s(k), a^1(k), a^2(k)) \times \mathcal{V}_{\varphi^p}^*(s(k)) \right]. \end{aligned} \quad (2.73)$$

## 2.5 Optimal Control Problem

Given a system dynamics, let:

- $t$  be the time,
- $\xi$  be the state vector,
- $u$  be the control vector,
- $t_f$  be the time horizon,
- $\mathcal{J}$  be the objective function to be minimized,
- $f$  be the differential equation of the dynamics,
- $g$  be the equality constraint function,
- $h$  be the inequality constraint function,

The problem of optimal control can compactly be written as

$$\min_{\xi(\cdot), u(\cdot), t_f} \int_0^{t_f} \mathcal{J}(\xi(t), u(t)) dt \quad (2.74a)$$

*subject to*

$$\dot{\xi}(t) = f(\xi(t), u(t)) \quad (2.74b)$$

$$g(\xi(t), u(t)) = 0 \quad (2.74c)$$

$$h(\xi(t), u(t)) \geq 0 \quad (2.74d)$$

Optimal control techniques solve the above optimization problem iteratively starting with an initial value of  $\xi$  and  $u$ . Objective of the optimization is to minimize the cost function  $\mathcal{J}$  in equation (2.74a) while satisfying the system dynamics equations along with equality and inequality constraints in equations (2.74b), (2.74c), and (2.74d), respectively. The generated maneuver is expressed in terms of vehicle longitudinal and lateral dynamical quantities, i.e., position, velocity and acceleration on  $x - y$  plane.

### 2.5.1 Model Predictive Control

The MPC control strategy is defined as a method that minimizes a cost function, subject to the some types of constraints over a prediction horizon  $N$ . A sequence of control signals are calculated, from  $u(k)$  to  $u(k + N_c)$  where  $N_c$  is the control horizon, by minimizing the cost function. Only the control signal at the time instant  $k$  is applied to the process. At the next time step,  $k$  moves ahead in time, the procedure is performed again to drive the state  $\xi(k)$  to zero. There are 3 main steps summarized in predictive control strategy; the first to predict the plant behavior, the second is to solve the optimization problem, and the last one is to apply the control input to the process. This iterative process is performed at each sampling time interval on a moving horizon i.e., receding horizon problem. The algorithm is summarized below.

1. Predict the system states for  $N$  steps ahead  $\xi(k + n|k)$ , where  $n = 1, 2, \dots, N + 1$  as a function of future control sequence  $u(k + n|k)$ , where  $n = 1, 2, \dots, N$ ,
2. Calculate the future control sequence with respect to the optimization solution in (),
3. Apply only the control signal at the current time step  $k$ ,
4. Repeat the process at the next sampling period ,  $t_s$ .

The discrete optimal control problem is expressed

$$\min_{\xi(k+N+1|k), u(k+N|k)} \mathcal{J}(\xi(k+N+1|k), u(k+N|k)) \quad (2.75a)$$

*subject to*

$$\xi(k+n+1) = f(\xi(k+n), u(k+n)) \quad (2.75b)$$

$$g(\xi(k), u(k)) = 0 \quad (2.75c)$$

$$h(\xi(k), u(k)) \geq 0 \quad (2.75d)$$

where

$$\begin{aligned} \mathcal{J}(\xi(k+N+1|k), u(k+N|k)) = & \xi(k+N+1)^T Q_f \xi(k+N+1) + \\ & \sum_{n=1}^N \xi(k+n)^T Q \xi(k+n) + u(k+n)^T R u(k+n) \end{aligned}$$

where  $N$  is the prediction horizon,  $Q$  is the cost to go weight for  $n$  number of the states,  $Q \in \mathbb{R}^{n \times n}$ ,  $R$  is the weight for  $m$  number of the inputs  $R \in \mathbb{R}^{m \times m}$ , and  $Q_f$  is the terminal weight applied to the final states at the end of prediction horizon.

## 2.6 Trajectory Generation

We consider a quadratic optimization problem where the objective is maintaining the centerline of the selected lane i.e., ( $y - y_{ref} = 0$ ), traveling at a desired speed,  $v_x$ , avoiding collisions with objects in drive lane, keeping the vehicle in road limits. A simplified vehicle's point mass vehicle model is utilized to generate a path for a controller wherein

the computed path is a reference target to be followed.

$$\begin{pmatrix} \dot{x}(t) \\ \dot{v}_x(t) \\ \dot{y}(t) \\ \dot{v}_y(t) \end{pmatrix} = \begin{pmatrix} 0 & 1 & 0 & 0 \\ 0 & 0 & 0 & 0 \\ 0 & 0 & 0 & 1 \\ 0 & 0 & 0 & 0 \end{pmatrix} \begin{pmatrix} x(t) \\ v_x(t) \\ y(t) \\ v_y(t) \end{pmatrix} + \begin{pmatrix} 0 & 0 \\ 1 & 0 \\ 0 & 0 \\ 0 & 1 \end{pmatrix} \begin{pmatrix} u_x(t) \\ u_y(t) \end{pmatrix} \quad (2.76)$$

where the state vector  $\xi(t) = [x(t) \ v_x(t) \ y(t) \ v_y(t)]^T$  denotes the longitudinal position, the lateral position, the longitudinal velocity, and the lateral velocity, respectively. The control input  $u(t) = [u_x(t) \ u_y(t)]^T$  denotes the acceleration values in  $x$  and  $y$  directions. These values are our *optimal points* obtained from the optimization solution.

The discretized format of dynamics in the  $QP$  is expressed in a road aligned coordinate frame as:

$$x(k+1) = x(k) + v_x(k)t_s, \quad \forall k = 0, \dots, T, \quad (2.77a)$$

$$v_x(k+1) = v_x(k) + u_x(k)t_s, \quad \forall k = 0, \dots, T, \quad (2.77b)$$

$$y(k+1) = y(k) + v_y(k)t_s, \quad \forall k = 0, \dots, T, \quad (2.77c)$$

$$v_y(k) = v_y(k) + u_y(k)t_s, \quad \forall k = 0, \dots, T, \quad (2.77d)$$

where  $t_s$  is the sampling time. The state equations can compactly be written as

$$\xi(k+1) = f(\xi(k), u(k)), \quad \forall k = 0, \dots, T, \quad (2.78)$$

where  $\xi(k) = [x(k) \ y(k) \ v_x(k) \ v_y(k)]^T$  is the vector of optimization variables and  $u(k) = [u_x(k) \ u_y(k)]^T$  is the control input vector. The control inputs are the state feedback control gains obtained at every time instant of the optimization solution.

$$\begin{pmatrix} x(k+1) \\ v_x(k+1) \\ y(k+1) \\ v_y(k+1) \end{pmatrix} = \begin{pmatrix} 1 & t_s & 0 & 0 \\ 0 & 1 & 0 & 0 \\ 0 & 0 & 1 & t_s \\ 0 & 0 & 0 & 1 \end{pmatrix} \begin{pmatrix} x(k) \\ v_x(k) \\ y(k) \\ v_y(k) \end{pmatrix} + \begin{pmatrix} 0 & 0 \\ 1 & 0 \\ 0 & 0 \\ 0 & 1 \end{pmatrix} \begin{pmatrix} u_x(k) \\ u_y(k) \end{pmatrix} \quad (2.79)$$

Objective is maintaining the centerline of the selected lane i.e., ( $y - y_{ref} = 0$ ), traveling at a desired speed,  $v_x$ , avoiding collisions with the lead car in drive lane, keeping the vehicle in road limits. Let's write the problem statement with multi-objective terms as follows.

$$\mathcal{J}(x(k), y(k), v_x(k), v_y(k), u_x(k), u_y(k)) = \sum_{n=0}^{N-1} = R_{u_x} u_x(k)^2 + R_{u_y} u_y(k)^2 + Q_{v_x} (v_x(k) - v_{ref})^2 + Q_y (y(k) - y_{ref})^2 + Q_{v_y} v_y(k)^2 \quad (2.80)$$

The cost function is given in a matrix format with the defined units of each element.

$$\mathcal{J} = \begin{pmatrix} \mathcal{J}_1 \\ \mathcal{J}_2 \\ \mathcal{J}_3 \\ \mathcal{J}_4 \\ \mathcal{J}_5 \end{pmatrix} = \begin{pmatrix} \text{Longitudinal acceleration } (m/s^2) \\ \text{Lateral acceleration } (m/s^2) \\ \text{Reference longitudinal speed } (m/s) \\ \text{Reference distance to lane } (m) \\ \text{Lateral speed } (m/s) \end{pmatrix}$$

where  $\mathcal{J}_1 = u_x(k)^2$ ,  $\mathcal{J}_2 = u_y(k)^2$ ,  $\mathcal{J}_3 = (v_x(k) - v_{ref})^2$ ,  $\mathcal{J}_4 = [(y(k) - y_{ref})]^2$ ,  $\mathcal{J}_5 = v_y(k)^2$ . We then put all the pieces of the optimization problem as follows

$$\underset{\xi, u}{\text{minimize}} \quad \mathcal{J}$$

s.t

system dynamics

$$\dot{x} = v_x$$

$$\dot{y} = v_y$$

$$\dot{v}_x = u_x$$

$$\dot{v}_y = u_y$$

input constraints

$$u_{x_{min}} \leq u_x \leq u_{x_{max}}$$

$$u_{y_{min}} \leq u_y \leq u_{y_{max}}$$

state constraints

$$v_{x_{min}} \leq v_x \leq v_{x_{max}}$$

$$v_{y_{min}} \leq v_y \leq v_{y_{max}}$$

## 2.7 dSPACE Simulation Results

In the Figure 2.25, the symbol  $\$$  denotes the *SV*,  $\$$  is the *TV* vehicles, which are controlled by the car following model,  $\$$  is the human driven vehicle via pedals and steering connections to the simulation platform, and  $\$$  shows the lead vehicle. For the simulation model, each car is assigned a coordinate system and has certain length and width in a three lane highway set-up. All cars travel in the middle of lanes unless a lane changing is taking place. For simplicity, we assume the center of gravity of each car is exactly at the middle. Recall that the relative distance values from each *TVs*, i.e.,  $d_{ij}$  are the bumper to bumper values relative to the *SV*.  $l_f$  and  $l_r$  are defined as the distances

Table 2.3: Design Parameters Used in Optimization

Symbol	Value	Unit	Description
$t_s$	0.1	sec	<i>Sampling time</i>
$v_x$	[0, 22]	m/s	<i>Longitudinal speed</i>
$v_y$	[-5,5]	m/s	<i>Lateral speed</i>
$u_x$	[-3,3]	$m/s^2$	<i>Longitudinal acceleration</i>
$u_y$	[-1,1]	m	<i>Lateral acceleration</i>
$y_{ref}$	4	m	<i>Reference target width</i>
$t_d$	0.2	sec	<i>Desired headway time</i>
$R_{u_x}$	10	N/A	<i>Weight on longitudinal acceleration</i>
$R_{u_y}$	10	N/A	<i>Weight on lateral acceleration</i>
$Q_{v_x}$	40	N/A	<i>Weight on reference longitudinal speed</i>
$Q_{v_y}$	10	N/A	<i>Weight on lateral speed</i>
$Q_y$	20	N/A	<i>Weight on reference distance to lane</i>

for the center of gravity for all cars.  $W_c$  is the total width of the vehicles. Note that the predefined relative distance values are used as indicators to determine when the safety system modules are initiated. Such indicators include  $d_{dec}$  that is the distance of triggering an emergency situation. The lane width is set to 3.3 m. *SV* only travels in one direction i.e., backwards traveling is not considered and can be initially positioned on different lanes. The other traffic participants travel with constant speeds. The flow of *TVs* is maintained by an heuristic car following model.

The simulations are performed on a computer equipped with an Intel *Xeon E5 2.6 GHz* CPU. A virtual world of traffic is visually demonstrated in dSPACE software that is run on a Simulink® model where all the algorithms are packed. We test multiple scenarios where the threat of the *TVs* is the key element forming the transition matrices, subsequently determines the behavior of the *SV*. The first scenario, presented in Figure 2.26, the *SV* starts with an initial speed profile and encounters an obstruction with a lead car in its drive lane and starts searching a possible gap. This process is performed at each discrete time

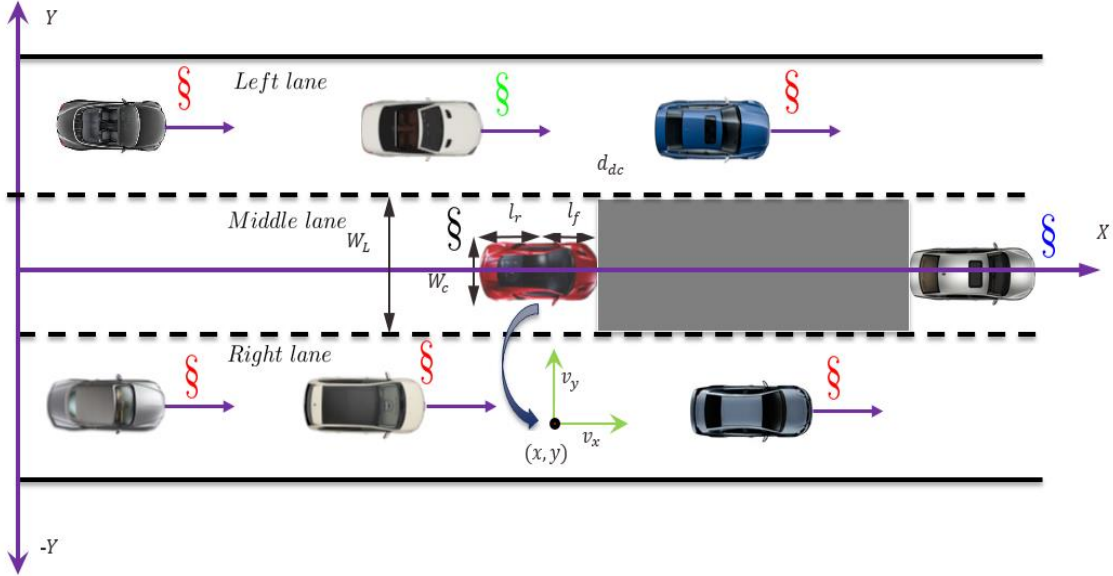


Figure 2.25: A cartesian coordinate system is assigned to all the vehicles. The quantities such as length and width of cars are same for all vehicles, which is only depicted on *SV*.

steps of the simulation where if the *SV* does not find an exit to avoid collisions, there is always a possible solution of staying and decelerating in order not to hit the lead car. A minimum safe distance of gaps is set to a variable  $\min(\mathcal{G}_{ij})$  i.e., this is called minimum required distance for decision making. This is calculated by multiplication of average time to lane change and maximum relative speed difference between *SV* and the *TVs*, i.e.,  $\min(\mathcal{G}_{ij}) = \Psi + v_{ij}t_{lc}$  as defined above. The lead car decelerates to stop. This is due to a hard braking of the lead car thus initiates an decision making and path planning.

From the *SV*'s reward function in established games, there are there important parameters in decision making, i.e.,  $\Psi$  is the being gap length,  $\tau$ , is being the time to reach to the selected gap, and  $\pi$ , remaining gap from the lead vehicle. One can observe the weights,  $\varrho_1$  and  $\varrho_2$ . The selection of which gap to enter is completely controlled by tuning of these weight values. For example, If one desires more weight on the longitudinal safe spacing,

Table 2.4: Initial conditions of vehicles for scenario1

Vehicle #	Dynamical properties			
	Long. position	Long. velocity	Lateral position	Lateral velocity
<i>SV</i>	45	22	0	0
<i>TV1</i>	60	23	3.3	0
<i>HV</i>	50	22	3.3	0
<i>TV2</i>	15	23	3.3	0
<i>TV3</i>	86	20	-3.3	0
<i>TV5</i>	57	20	-3.3	0
<i>TV6</i>	20	20	-3.3	0
<i>Lead</i>	250	0	0	0

Table 2.5: Initial conditions of vehicles of scenario 2

Vehicle #	Dynamical properties			
	Long. position	Long. velocity	Lateral position	Lateral velocity
<i>SV</i>	45	22	0	0
<i>TV1</i>	75	23	3.3	0
<i>HV</i>	50	22	3.3	0
<i>TV2</i>	0	23	3.3	0
<i>TV3</i>	66	20	-3.3	0
<i>TV5</i>	37	20	-3.3	0
<i>TV6</i>	0	20	-3.3	0
<i>Lead</i>	250	0	0	0

the *SV* is then determines its future strategy with respect to maintaining a longer longitudinal space. Or if the goal is to merge in to a gap as *SV* approaches to the lead vehicle in the lane,  $\varrho_2$  can be tuned to do so. It is well interpreted that the proposed framework exhibits a freedom such that the designers can obtain several autonomous driving modes. It is well shown that the design can easily extended to more lanes highway driving. Table 2.5 shows initial conditions of vehicles.

In scenario Figure 2.26, human driven vehicle is demonstrated with blue color and

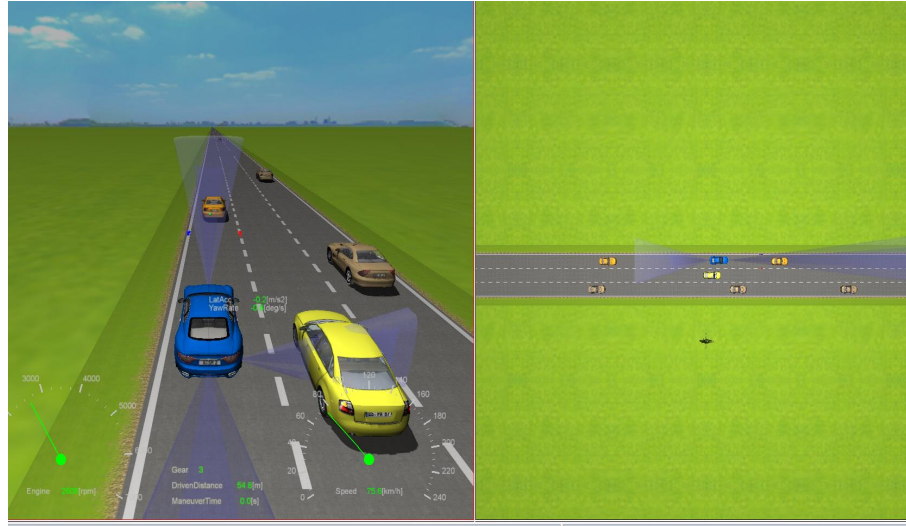


Figure 2.26: This graph is intended to show the visual set-up, with two different camera orientations of the simulated traffic. First, the *SV* starts with an initial speed of  $22 \text{ m/s}$  and it encounters an obstruction in its drive lane and searches for a gap.

the *SV* is the yellow car. *SV* turns on the turning signal for the gap behind *HV* and ahead of the *TV2*. After solving the Nash equilibrium game with the formula 2.50-2.61. This presents a non-cooperative situation where *TV2* seeks to cut-off the merging by accelerating. This is the objective for *SV*, which maximizes the worst case actions of *TV* from its perspective.

Next, the Figure 2.28 represents a different set-up where *SV* turns on the turning signal to the right gap in front of *TV4*. *TV4* acts courtesy by opening larger gap after lane changing has been initiated. From this strategy both *TV* and *SV* benefits due to the maximization of individual rewards solved by the formula 2.38- 2.49. It is important to point out the solution depends on several factors, i.e., variables of traffic. For example, the reaction delay of *TV* is expressed as the uncertainty on the actual positions of *TV*, which *SV* makes lane changing decisions with respect to. Moreover, in terms of reward function, *SV* has to check and calculate the available gap lengths, time to reach to the

gaps, and the remaining longitudinal spacing from the lead vehicle when lane changing is performed. It is easy to see these variables are all traffic dependent that actually fulfills the design requirements of human-like decision making.



Figure 2.27: *SV* turns on the turning signal and adjusts its speed in order to merge the gap ahead of *TV2*. Even though *TV2*'s objective is to prevent *SV* from lane changing, *SV* seeks to maximize the lower bound of *TV2*'s action

## 2.8 Conclusion

I presented a decision making strategy for autonomous driving in this chapter. I first model the traffic vehicles threat to mimic the driving habits of drivers by fuzzy logic. Then the first decision maker was proposed, which is based on Markov decision processes. The discretized grid-world of the 3-lane highway road was also presented. Here, the subject vehicle is the only agent and the reactions of other vehicles are not considered explicitly in the design stage. Then the game theoretic model was proposed. Taking advantage of game theory modeling of traffic vehicle interactions, Markov game was proposed. Markov game



Figure 2.28: This is a cooperative case where *SV* turns on the turning signal to the right gap in of *TV4* and *TV* yields to *SV* for lane changing.



Figure 2.29: As *SV* merges, *TV4* decelerate to open a larger gap to merge in, consequently, eases the lane change process.

holds the Markov property and Nash equilibrium ideas so that the solution points were called Markov-perfect equilibrium. I introduced both cooperative and non-cooperative games with high fidelity simulation. I performed a set of scenarios where the most common highway driving conditions are tested in case of an emergency lane change due to an unexpected stops of a car in drive lane. In addition, the algorithms are packed in a simulation where the vehicle models represent a real driving environment. It was observed that the Markov game scheme has several advantages in traffic modeling such as considering drivers' different driving strategies. This makes our method suitable to implement in a real car.

### 3. VEHICLE LATERAL DYNAMICS AND CONTROL

In this chapter, we are first going to develop a vehicle model for steering control<sup>1</sup>. Steering control is important to move an actual vehicle from one lane to another. We then discuss how to design a controller for the derived dynamical equations, more specifically an  $\mathcal{H}_\infty$  control design. The performance of the proposed scheme is compared with the so-called human-driver model (HDM) based control, which has been broadly discussed in the literature. The simulation study shows the performance of the proposed controller in terms of trajectory tracking of the reference path, disturbance rejection of the wind load, and effective control input. Since the emergency lane changes involve severe driving maneuvers at high speed, the consideration of vehicle lateral stability generated by yaw moment is a must to create an overly stable control system structure for an emergency lane changing intelligent system<sup>2</sup>. To this end, we introduce better modeling of nonlinearity of the vehicle. We formulate a synthesis methodology by taking into account the nonlinearities for increased tracking performance of a desired path by both controlling the active steering and yaw moment of the vehicle. Thus we focus on designing a AFS/DYC as lower level controller that performs a lane change task with enhanced handling performance in the presence of varying front and rear cornering stiffnesses. We obtain the nonlinear tire forces with Pacejka model [111], and convert the nonlinear tire stiffnesses to parameter space to design a linear parameter varying controller (LPV) for combined AFS and DYC to perform a commanded lane change task. Simulations are carried out to show the improved stability and performances over the entire operation range.

Further, I propose a Takagi-Sugeno modeling of vehicle lateral dynamics. Takagi-

---

<sup>1</sup>© 2016 ASME. Reprinted, with permission, from Serdar Coskun and Reza Langari, Development of an Emergency Lane Change System in Highway Driving, October 2016.

<sup>2</sup>© 2017 IEEE. Reprinted, with permission, from Serdar Coskun and Reza Langari, Enhanced vehicle handling performance for an emergency lane changing controller in highway driving, June 2017.

Sugeno (T-S) proposed a method of designing and analysis of nonlinear systems by presenting a set of local linear systems. The structure of the local linear models has the same size state vectors for each element. The local dynamics in different regions is presented with the same size state-space equations and fuzzy blending of the sub-linear models forms the overall nonlinear dynamics. Thus, the main advantages of the (T-S) fuzzy modeling is that the controller is designed in a particular operation zone, and fuzzy interpolation mechanism is employed to take into account the contribution of the each sub-model with a set of weighting functions.

### 3.1 Linear Bicycle Model

In order to define the dynamic equations of the vehicle lateral model, we utilize three coordinates  $x$ ,  $y$  and  $\psi$  in the global coordinate systems with  $\psi$  as the angle between the longitudinal direction of the vehicle and coordinate  $x$  axis. Newton's second law under body fixed coordinates gives the following relation Another table is placed here to show the effect of having tables in multiple sections. The list of tables should still double space between table titles, while single spacing long table titles.

$$m(\dot{v}_y + v_x \dot{\psi}) = 2F_{yf} + 2F_{yr}, \quad (3.1)$$

where  $v_y$  and  $v_x$  are the lateral and longitudinal velocities of the vehicle respectively.  $\dot{\psi}$  is the yaw rate. The forces  $F_{yf}$  and  $F_{yr}$  are the front and rear lateral directional forces, which are generated by the cornering stiffness( $C_f$  and  $C_r$ ) and relevant slip side angles ( $\alpha_f$  and  $\alpha_r$ ) as follows.

$$F_{yf} = C_f \alpha_f, \quad (3.2)$$

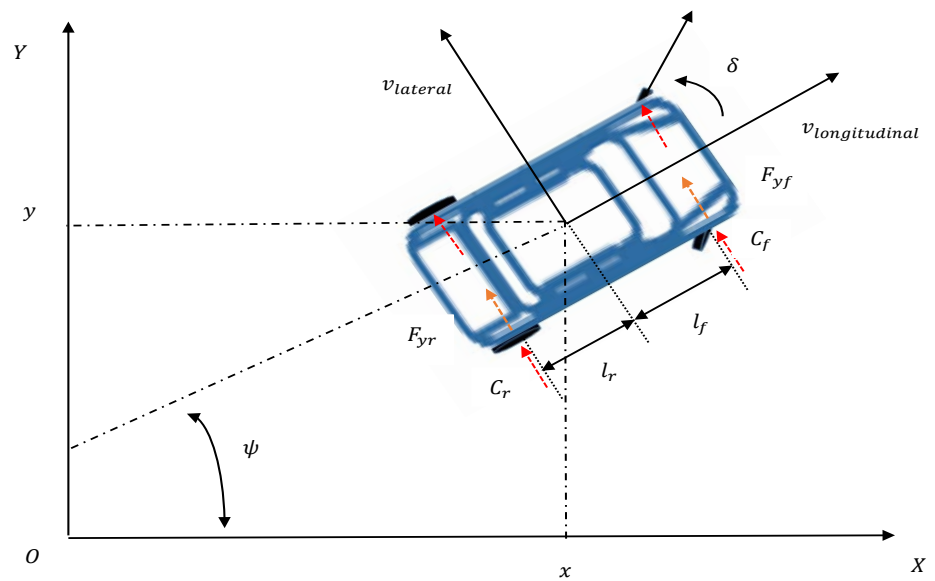


Figure 3.1: Schematic view of vehicle lateral dynamics <sup>3</sup>© 2016 ASME. Reprinted, with permission, from Serdar Coskun and Reza Langari, Development of an Emergency Lane Change System in Highway Driving, October 2016.

$$F_{yr} = C_r \alpha_r, \quad (3.3)$$

where the slip angles are defined by

$$\alpha_f = \delta - \frac{v_y + l_f \dot{\psi}}{v_x}, \quad (3.4)$$

$$\alpha_r = -\frac{v_y - l_r \dot{\psi}}{v_x}, \quad (3.5)$$

where  $\delta$  is the steering angle to be controlled,  $l_f$  and  $l_r$  are the front and rear distances from the mass center of the vehicle to the front and rear lateral forces. Note that the two left and right lateral forces on rear wheel are assumed to be same. It should also be noted that right and left steering angles are assumed to be equal. In general this is not the case because the radius of the travel path for each wheel is different.

The yaw motion is defined by the equation

$$J \ddot{\psi} = 2l_f F_{yf} - 2l_r F_{yr}, \quad (3.6)$$

Substituting (3.2) and (3.4) into (3.1) and (3.6) for the motion of center of gravity in lateral direction  $y$  and the yaw rate we have

$$\dot{v}_y = -2 \frac{C_f + C_r}{mv_x} v_y - \left[ 2 \frac{l_f C_f - l_r C_r}{mv_x} + v_x \right] \dot{\psi} + \frac{2C_f}{m} \delta + \frac{Y_w}{m}, \quad (3.7)$$

$$\ddot{\psi} = -2 \frac{l_f C_f + l_r C_r}{J v_x} v_y - \left[ 2 \frac{l_f^2 C_f - l_r^2 C_r}{J v_x} \right] \dot{\psi} + \frac{2L_f C_f}{J} \delta + \frac{J_w Y_w}{J}. \quad (3.8)$$

where  $Y_w$  is the lateral wind gust disturbance load and  $J_w$  is the distance from the vehicle mass center introduced for a more realistic design environment. Finally, we put

the dynamic equation of motions into the state space form by defining the state variables as lateral position ( $y$ ), lateral velocity ( $v_y$ ), yaw angle ( $\psi$ ) and yaw velocity is ( $\dot{\psi}$ ) i.e.,  $x=[y \ v_y \ \psi \ \dot{\psi}]^T$ . The longitudinal velocity  $v_x$  is constant during the lane change maneuver for the control design.

$$\dot{x} = \begin{bmatrix} 0 & 1 & 0 & 0 \\ 0 & -2\frac{C_f+C_r}{mv_x} & 0 & -2\frac{l_f C_f - l_r C_r}{mv_x} - v_x \\ 0 & 0 & 0 & 1 \\ 0 & -2\frac{l_f C_f + l_r C_r}{Jv_x} & 0 & -2\frac{l_f^2 C_f - l_r^2 C_r}{Jv_x} \end{bmatrix} x + \begin{bmatrix} 0 \\ \frac{1}{m} \\ 0 \\ \frac{J_w}{J} \end{bmatrix} Y_w + \begin{bmatrix} 0 \\ \frac{2C_f}{m} \\ 0 \\ \frac{2l_f C_f}{J} \end{bmatrix} \delta, \quad (3.9)$$

Since the objective is the tracking control of a reference trajectory, it is more appropriate to write the system equations in error minimizing form with a state variable  $e_1$  denoting the lateral distance error from the center line of the lane and  $e_2$  as the orientation error of the vehicle [112]. The state vector  $x=[e_1 \ \dot{e}_1 \ e_2 \ \dot{e}_2]^T$  is defined as in [112], and the equations are

$$\dot{x} = \begin{bmatrix} 0 & 1 & 0 & 0 \\ 0 & -2\frac{C_f+C_r}{mv_x} & 2\frac{C_f+C_r}{m} & -2\frac{l_f C_f - l_r C_r}{mv_x} - v_x \\ 0 & 0 & 0 & 1 \\ 0 & -2\frac{l_f C_f + l_r C_r}{Jv_x} & 2\frac{l_f C_f + l_r C_r}{J} & -2\frac{l_f^2 C_f - l_r^2 C_r}{Jv_x} \end{bmatrix} x + \begin{bmatrix} 0 \\ \frac{1}{m} \\ 0 \\ \frac{J_w}{J} \end{bmatrix} Y_w + \begin{bmatrix} 0 \\ \frac{2C_f}{m} \\ 0 \\ \frac{2l_f C_f}{J} \end{bmatrix} \delta. \quad (3.10)$$

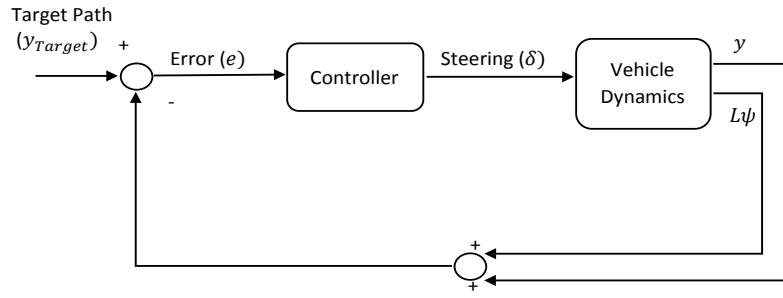


Figure 3.2: Control structure of a lane change maneuvering <sup>4</sup>© 2016 ASME. Reprinted, with permission, from Serdar Coskun and Reza Langari, Development of an Emergency Lane Change System in Highway Driving, October 2016.

### 3.1.1 $\mathcal{H}_\infty$ Steering Control Design

There are two control design strategies for lateral dynamics of the vehicle. First is via using sensors installed on the road center, and the other is via a looking ahead system using vehicle sensors. The latter approach is utilized in this paper. The idea is the controller measures the current lateral displacement and the yaw angle and estimates the deviation of the vehicle's lateral displacement relative to the target path. This relation is defined [73]

$$e = y_{Target} - y - L\psi, \quad (3.11)$$

where  $y_{Target}$  is the target path of interest,  $y$  is the lateral position of the vehicle, and  $L(m)$  is the look ahead distance. The look ahead distance plays an important role in stability of the vehicle motion. The value of the look ahead distance is proportional to the vehicle speed.

### 3.1.1.1 Performance weight selection

The weighting functions play an important role for control design. Generally, there is no explicit way of choosing the weight selections that can lead to an optimal solution for each design. For improved performance, high order weighing functions are more desirable. However, the higher order dynamics increase the controller order and the control loop tend to be more sensitive against perturbations. Therefore, constant weights are selected as opposed to the work [113]. Carefully tuning the weights is an essential step and requires an experience. We choose  $W_u=0.2$  and  $W_{\psi,y}=0.9$ . A generic LFT structure of the control design is given below.

The  $\mathcal{H}_\infty$  control design seeks a controller that provides closed-loop stability and satisfies a prescribed level of performance index for reference tracking and disturbance rejection. To start the design steps, we first define the plant matrices. In order to form the input-output pairs, the generalized plant model is derived by linear fractional transformation. To aim this, the state vector of the plant is  $x=[e_1 \ e_1 \ e_2 \ e_2]^T$  and the output is chosen as  $y=[y_e \ \psi_e]^T$ . Then the plant matrices are

$$A_p = \begin{bmatrix} 0 & 1 & 0 & 0 \\ 0 & -2\frac{C_f+C_r}{mv_x} & 2\frac{C_f+C_r}{m} & -2\frac{l_f C_f - l_r C_r}{mv_x} - v_x \\ 0 & 0 & 0 & 1 \\ 0 & -2\frac{l_f C_f + l_r C_r}{Jv_x} & 2\frac{l_f C_f + l_r C_r}{J} & -2\frac{l_f^2 C_f - l_r^2 C_r}{Jv_x} \end{bmatrix}, B_p = \begin{bmatrix} 0 \\ \frac{1}{m} \\ 0 \\ \frac{J_w}{J} \end{bmatrix}, \quad (3.12)$$

$$C_p = \begin{bmatrix} 1 & 0 & 0 & 0 \\ 0 & 0 & 1 & 0 \end{bmatrix}.$$

We deal with a single input/multi output linear time invariant (LTI) system. Consider

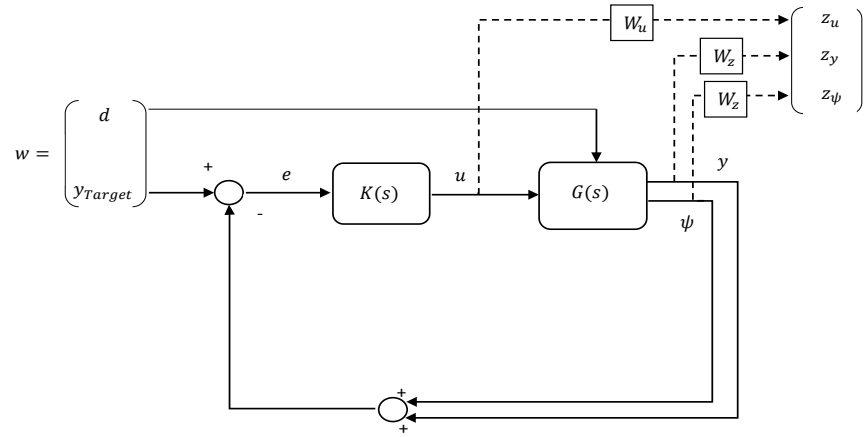


Figure 3.3: Weighting control structure<sup>5</sup> © 2016 ASME. Reprinted, with permission, from Serdar Coskun and Reza Langari, Development of an Emergency Lane Change System in Highway Driving, October 2016.

the following state-space representation of the generalized plant model

$$\begin{aligned} \dot{x} &= Ax + B_1 w + B_2 u \\ z &= C_1 x + D_{11} w + D_{12} u \\ y &= C_2 x + D_{21} w + D_{22} u \end{aligned} \tag{3.13}$$

where  $x \in \mathbb{R}^n$  is the state vector,  $w \in \mathbb{R}^{n_w}$  is the disturbance vector,  $u \in \mathbb{R}^{n_u}$  is the control input vector,  $z \in \mathbb{R}^{n_z}$  is the vector of output signals,  $y \in \mathbb{R}^{n_y}$  is the vector of measured variables. The closed-loop transfer functions are defined from  $w$  to  $z$  with a dynamical output-feedback control law  $u = Ky$ . The goal is to compute a dynamic output-feedback controller in the form of

$$\begin{aligned}\dot{x}_c &= A_c x_c + B_c y \\ u &= C_c x_c + D_c y\end{aligned}\tag{3.14}$$

The  $\mathcal{H}_\infty$  controller minimizes the energy to energy gain ( $\gamma$ ) of the system from the disturbance vector  $d$  to controlled outputs  $z$ . The control objectives  $z_u, z_y, z_\psi$  representing the steering control input  $\delta$ , the lateral offset  $y$ , and the yaw angle error  $\psi$ . The disturbance vector is  $w = [y_{Target} \ d]$ . The generalized plant is then presented in a state-space form

$$\begin{aligned}\dot{x} &= \left[ A_p \right]_{n \times n} x + \left[ \begin{matrix} 0 & 0 \end{matrix} \right]_{n \times n_w} w + \left[ B_p \right]_{n \times n_u} u \\ z &= \left[ \begin{matrix} 0 \\ K_z C_p \end{matrix} \right]_{n_z \times n} x + \left[ \begin{matrix} 0 & 0 \\ 0 & K_z \end{matrix} \right]_{n_z \times n_w} w + \left[ \begin{matrix} K_u \\ 0 \end{matrix} \right]_{n_z \times n_u} u \\ y &= \left[ -C_p \right]_{n_y \times n} x + \left[ I \quad -I \right]_{n_y \times n_w} w + \left[ 0 \right]_{n_y \times n_y} u\end{aligned}\tag{3.15}$$

We provide the  $\mathcal{H}_\infty$  output- feedback control design formulation in terms of a linear matrix inequality (LMI) solution with the following theorem.

**Theorem :** Given the open loop LFT system governed by (3.13), suppose there exists two symmetric matrices  $\mathbf{X}, \mathbf{Y}$  and four matrices  $\hat{\mathbf{A}}, \hat{\mathbf{B}}, \hat{\mathbf{C}}, \hat{\mathbf{D}}$ . The following LMI gives the controller matrices.

$$\begin{bmatrix} \mathbf{X} + \hat{\mathbf{B}} + C_2 + (\star) & \star & \star & \star \\ \hat{\mathbf{A}}^T + A + B_2 \hat{\mathbf{D}} C_2 & A \mathbf{Y} + B_2 \hat{\mathbf{C}} + (\star) & \star & \star \\ (\mathbf{X} + \hat{\mathbf{B}} D_{21})^T & (B_1 + B_2 \hat{\mathbf{D}} D_{21})^T & -\gamma I_{n_w} & \star \\ (C_1 + D_{12} \hat{\mathbf{D}} C_2) & C_1 \mathbf{Y} + D_{12} \hat{\mathbf{C}} & D_{11} + \hat{\mathbf{D}} D_{12} & \star \end{bmatrix} < 0,\tag{3.16}$$

$$\begin{bmatrix} \mathbf{X} & I \\ I & \mathbf{Y} \end{bmatrix} > 0. \quad (3.17)$$

Then, there exist a controller of the form (3.14) such that

1. The closed loop system is stable
2. The induced  $\mathcal{H}_\infty$  norm of the operator  $w \rightarrow z$  is bounded by  $\gamma > 0$  (i.e.,  $\|T_{zw}\|_{i,2} < \gamma$ .

Once matrices  $\mathbf{X}$ ,  $\mathbf{Y}$ ,  $\hat{\mathbf{A}}$ ,  $\hat{\mathbf{B}}$ ,  $\hat{\mathbf{C}}$ , and  $\hat{\mathbf{D}}$  matrices are obtained, the controller matrices are computed in the following steps:

1) Solve for  $\mathbf{N}$ ,  $\mathbf{M}$ , and the factorization problem

$$I - \mathbf{XY} = NM^T \quad (3.18)$$

2) Compute  $A_c$ ,  $B_c$ ,  $C_c$ , and  $D_c$  with

$$\begin{aligned} A_c &= N^{-1}(N\dot{M}^T + \hat{\mathbf{A}} - \mathbf{X}(A - B_2\hat{\mathbf{D}}C_2)Y - \hat{\mathbf{B}}C_2Y - XB_2\hat{\mathbf{C}})M^{-T}, \\ B_c &= N^{-1}(\hat{\mathbf{B}} - \mathbf{X}B_2\hat{\mathbf{B}}), \\ C_c &= (\hat{\mathbf{C}} - \hat{\mathbf{D}}C_2Y)M^{-T}, \\ D_c &= \hat{\mathbf{D}}. \end{aligned} \quad (3.19)$$

**Proof:** Please refer to [114].

Our focus here is to design a full order dynamic controller i.e., the size of  $A_c$  is equal to  $A$  for a given plant. Note that the new variables  $\hat{\mathbf{A}}$ ,  $\hat{\mathbf{B}}$ ,  $\hat{\mathbf{C}}$ ,  $\hat{\mathbf{D}}$  have dimensions  $n \times n$ ,  $n \times n_u$ ,  $n_y \times n$ , and  $n_y \times n_y$  respectively. If we have square matrices  $\mathbf{M}$  and  $\mathbf{N}$ , we can invert them

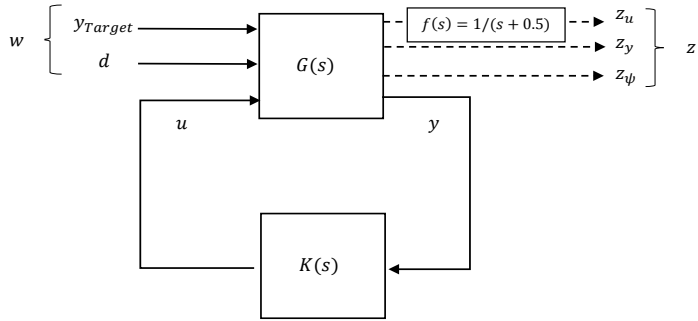


Figure 3.4: Input shaping filter <sup>6</sup>© 2016 ASME. Reprinted, with permission, from Serdar Coskun and Reza Langari, Development of an Emergency Lane Change System in Highway Driving, October 2016.

and compute the controller matrices. Note that above method requires the optimization of the control matrices along with  $\mathbf{X}$ ,  $\mathbf{Y}$ . This technique requires only one matrix inversion as seen above and can be easily implemented to the given plant.

A dynamic input shaping filter function is employed for shaping the regulated steering control input. The purpose of the filter in our control design is that enforcing integral action on the output  $\delta$ . Note that the Figure 3.4 actually presents the implementation of the closed control design that consists of both controller and plant dynamics.

### 3.1.1.2 Human driver model control for lane change maneuver

The effectiveness of the designed  $\mathcal{H}_\infty$  controller is compared with the Human Driver Model (HDM) based controller. The idea behind the HDM control is to consider a human operator exhibits adaptation to regulate the steering angle to the current vehicle target deviation. The human operator has the ability of previewing the look-ahead distance and responding to the observed error information. Several studies have been conducted about designing a HDM based controller for both longitudinal [115] and lateral [116] control aspects. Interested readers may refer to [75] for a comprehensive treatment on the subject.

Note that we study the (HDM) from a control point of view. The discussion includes providing a transfer function that relates the output error i.e., changing car trajectory to the input i.e., steering action. A various transfer functions have been proposed by the researchers for different conditions. One of the commonly used is suggested by Ragazzini [117], a human operator model that suits to a manual tracking task is given by

$$H(s) = \frac{h}{1 + \tau_D s} e^{-\tau_L s} \quad (3.20)$$

The term  $e^{-\tau_L s}$  expresses the delay for the human operator to make an action under a given input, and the lag is denoted by  $\tau_L$ . A proportional action from the output signal to the input signal is expressed by a constant term  $h$ .  $\tau_D$  denotes the derivative of control action to the input signal. These constants exhibit the distinct characteristics of the human driver controller that can be adjusted to a given condition. The assumption of the small time delay leads to a simplified linear transfer function of HDM,

$$H(s) = \frac{h}{1 + \tau_L s} \quad (3.21)$$

The optimal values of  $h = 0.02$  and  $\tau_L = 0.2$  are selected same as [75] in for the simulation purposes.

### 3.1.2 Simulation Results

Simulations were performed to validate the closed-loop performance in terms of lateral position, reference tracking and wind load disturbance rejection. LMI Control Toolbox gives a feasible solution to a minimization problem with a performance level  $\gamma$  of 0.98. This ensures that the maximum attenuation of the disturbance vectors over the regulation outputs is less than  $\gamma$  i.e.,  $\|T_{zw}\|_{i,2} < \gamma$ . For the sake of comparison,  $\mathcal{H}_\infty$  controller is compared with the Human Driver Model controller. The reference tracking, yaw angle,

and steering angle (control input) plots are produced for both cases. The dry road condition is considered and the vehicle velocity is set to  $100 \text{ km/h}$ . The lane change command is given at 5 secs of the simulation. For a conservative design, the width of the lane is considered as 3 meters for highway driving. The disturbance of the wind load is applied in two intervals from  $t = 3 \text{ secs}$  to  $t = 15 \text{ s}$  with the magnitude of  $1600 \text{ N}$  and from  $t = 20 \text{ secs}$  to  $t = 30 \text{ secs}$  with the magnitude of  $3000 \text{ N}$  considering a realistic driving environment at the highway speed of  $100 \text{ km/h}$  during the lane change maneuver. The disturbance profile is given in Figure 3.5. For simplicity, a more detailed approach of considering the uncertainties, especially on the cornering stiffnesses, is omitted in the design. However, the controller still provides a satisfactory performance around 20 % to the altered values of the cornering stiffnesses. The negative effect of these uncertainties has been well studied in the literature.

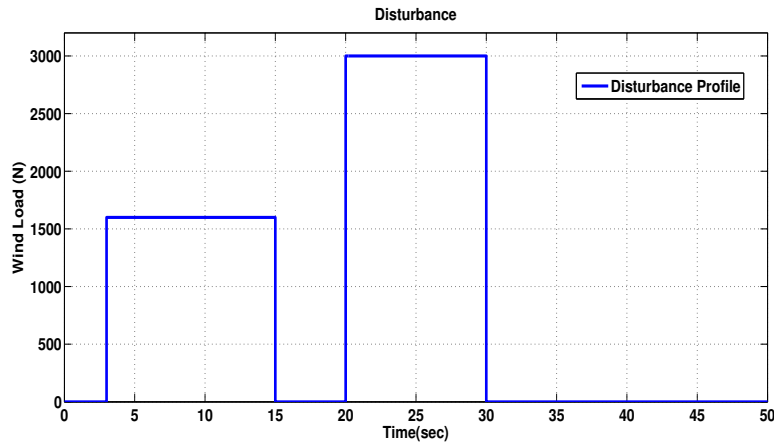


Figure 3.5: Disturbance profile <sup>7</sup>© 2016 ASME. Reprinted, with permission, from Serdar Coskun and Reza Langari, Development of an Emergency Lane Change System in Highway Driving, October 2016.

The steering angle presents the control input to the vehicle during the lane change ma-

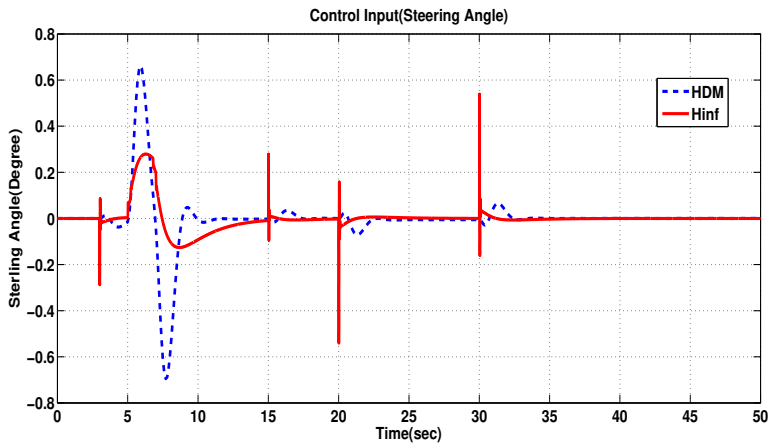


Figure 3.6: Control inputs <sup>8</sup>© 2016 ASME. Reprinted, with permission, from Serdar Coskun and Reza Langari, Development of an Emergency Lane Change System in Highway Driving, October 2016.

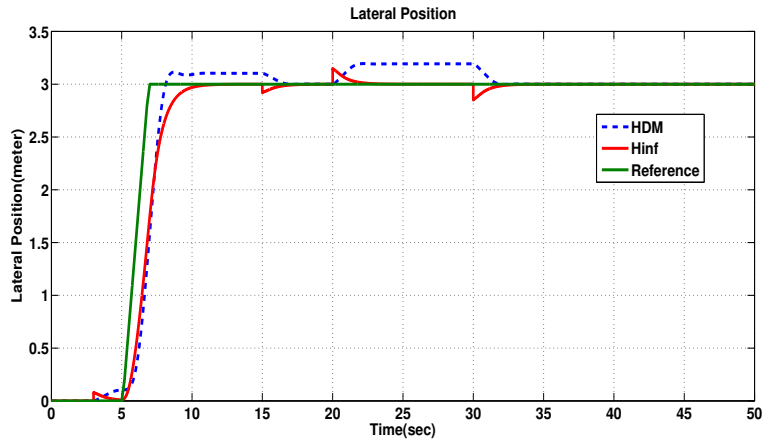


Figure 3.7: Reference tracking <sup>9</sup>© 2016 ASME. Reprinted, with permission, from Serdar Coskun and Reza Langari, Development of an Emergency Lane Change System in Highway Driving, October 2016.

neuver. As seen in Figure 3.6, the amplitude of generated control input during a given lane manuevering is smaller  $\mathcal{H}_\infty$  design than that of HDM. The applied wind load disturbance

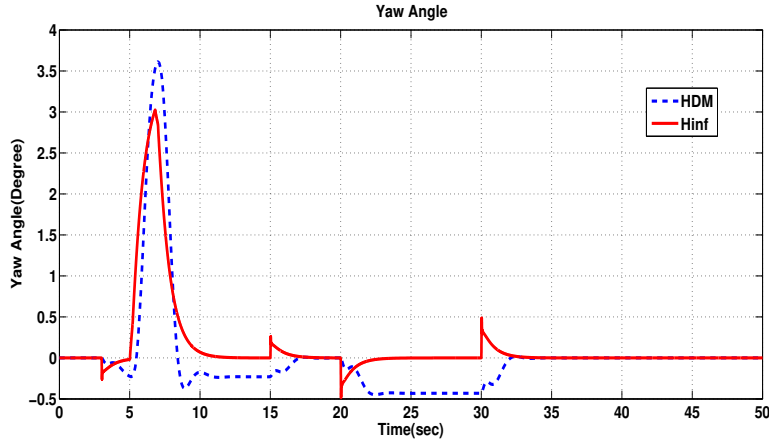


Figure 3.8: Yaw angles <sup>10</sup>© 2016 ASME. Reprinted, with permission, from Serdar Coskun and Reza Langari, Development of an Emergency Lane Change System in Highway Driving, October 2016.

Table 3.1: Vehicle parameters <sup>11</sup>© 2016 ASME. Reprinted, with permission, from Serdar Coskun and Reza Langari, Development of an Emergency Lane Change System in Highway Driving, October 2016.

$l_f(\text{meter})$	1.1
$l_r(\text{meter})$	1.6
$m(\text{kg})$	1500
$J(\text{kgm}^2)$	2500
$C_f(\text{N/rad})$	55000
$C_r(\text{N/rad})$	55000
$W_v(\text{meter})$	1.847
$W_R(\text{meter})$	3

is successfully rejected at 3 secs with a smaller amplitude  $\mathcal{H}_\infty$  design with no offset from the reference path in Figure 3.7. However, the wind load disturbance causes an offset in the vehicle's lateral position towards the wind-passing direction in HDM case. This might lead to a high risk of accidents in highway driving. The comparison result shows that the overall reference tracking of  $\mathcal{H}_\infty$  control exhibits an improved performance. The shape

of the reference lane trajectory is essential for obtaining a good tracking. A sharper signal leads to a fast control actuation (steering angle). Thus, the tracking performance is highly deteriorated. Simulations are sensitive with respect to the selection of constant weighting functions, and a careful tuning procedure is vital. Penalizing the control effort and minimizing the effect of disturbance on reference output might outperform the design on yaw angle. As observed in Figure 3.8, the  $\mathcal{H}_\infty$  controller maintains a good improvement on the yaw angle output. Our control design provides between 20 % - 30% improved overshoot, and elimination of the offset value from the target path with an overall improved tracking behavior.

### 3.2 Nonlinear Vehicle Model

In this section, I present the result of my publication in [118]<sup>12</sup>. The following notation will be used throughout the paper to denote the variables related to the wheels :  $i = (f, r)$  denote the front and rear axles and  $j = (l, r)$  denote the left and right sides of the vehicle. The variable  $(.)_{f,l}$  denotes the front left wheel of the vehicle. The nonlinear vehicle model presented in this section is adopted and modified from [91, 50, 119] for simulation purpose. The model is described with the lateral (cornering), the longitudinal, the yaw and the center of gravity slip side dynamics of the vehicle, and represented with the following nonlinear differential equations:

---

<sup>12</sup>© 2017 IEEE. Reprinted, with permission, from Serdar Coskun and Reza Langari, Enhanced vehicle handling performance for an emergency lane changing controller in highway driving, June 2017.

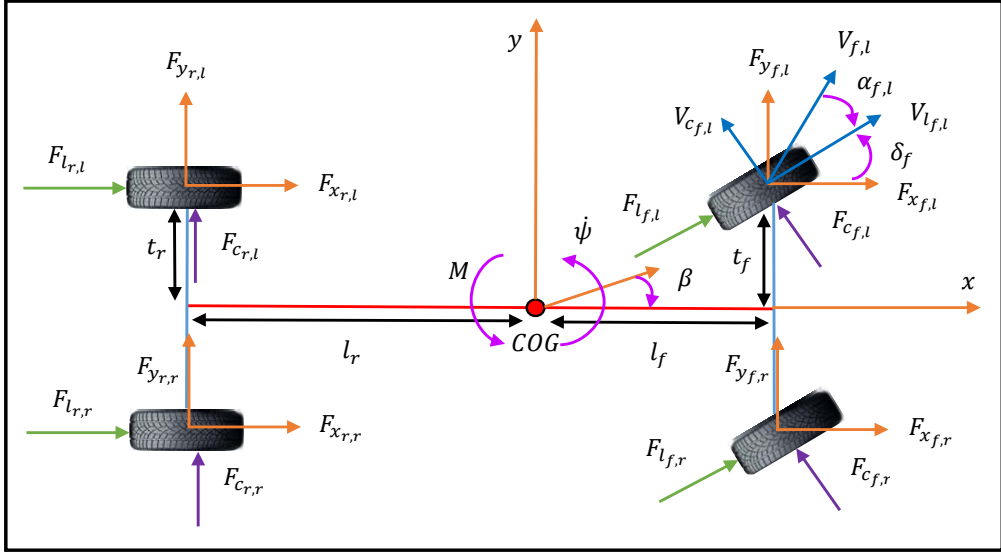


Figure 3.9: Vehicle dynamical model <sup>13</sup> © 2017 IEEE. Reprinted, with permission, from Serdar Coskun and Reza Langari, Enhanced vehicle handling performance for an emergency lane changing controller in highway driving, June 2017.

$$\begin{aligned}
m\dot{V}_x &= mV_y\dot{\psi} + (F_{l_{f,l}} + F_{l_{f,r}})\cos(\delta_f) + (F_{c_{f,l}} + F_{c_{f,r}})\sin(\delta_f) + F_{l_{r,l}} + F_{l_{r,r}}, \\
m\dot{V}_y &= -mV_x\dot{\psi} + (F_{l_{f,l}} + F_{l_{f,r}})\sin(\delta_f) + (F_{c_{f,l}} + F_{c_{f,r}})\cos(\delta_f) + F_{c_{r,l}} + F_{c_{r,r}} + Y_w, \\
J\ddot{\psi} &= [(F_{l_{f,l}} + F_{l_{f,r}})\sin(\delta_f) + (F_{c_{f,l}} + F_{c_{f,r}})\cos(\delta_f)]l_f - (F_{c_{f,l}} + F_{c_{f,r}})l_r \\
&\quad + [(F_{c_{f,l}} - F_{c_{f,r}})\sin(\delta_f) + (-F_{l_{f,l}} + F_{l_{f,r}})\cos(\delta_f)]t_f \\
&\quad + (-F_{l_{r,l}} + F_{l_{r,r}})t_r + J_wY_w + M, \\
mV_x\dot{\beta}_{cog} &= (F_{c_{f,l}} + F_{c_{f,r}}) + (F_{c_{r,l}} + F_{c_{r,r}}) - mV_x\dot{\psi}.
\end{aligned} \tag{3.22}$$

where  $F_{l_{f,l}}$ ,  $F_{l_{f,r}}$ ,  $F_{l_{r,l}}$  and  $F_{l_{r,r}}$  are the longitudinal front and rear tire forces.  $F_{c_{f,l}}$ ,  $F_{c_{f,r}}$ ,  $F_{c_{r,l}}$  and  $F_{c_{r,r}}$  are the lateral front and rear tire forces. Tire forces are highly nonlinear and

depend on the following quantities

$$\begin{aligned} F_{l_{i,j}} &= f_l(\alpha_{i,j}, s_{i,j}, \mu_{i,j}, F_{z_{i,j}}) \\ F_{c_{i,j}} &= f_l(\alpha_{i,j}, s_{i,j}, \mu_{i,j}, F_{z_{i,j}}) \end{aligned} \quad (3.23)$$

where  $\alpha_{i,j}$  are the tire slip angles,  $s_{i,j}$  are the tire slip ratios,  $\mu_{i,j}$  are the road friction coefficients and  $F_{z_{i,j}}$  are the vertical tire loads. The relevant details of the slip ratio, slip angle, and the normal tire forces are omitted for space consideration. Interested readers can find more information in [91, 119]. The notation  $Y_w$  denotes the wind load and  $J_w$  is the wind load acting distance from vehicle's mass center. The nonlinear longitudinal and cornering tire forces are described by a Pacejka model [111]. The Pacejka model, describes the relation between tire-road interaction forces, is demonstrated in the following section.

### 3.2.1 Simplified Model

A simplified nonlinear model is given by assuming

- low steering angles :  $\cos(\delta_f) \cong 1$
- low slip side angles :  $\beta < 7$  deg
- same forces on each side of front and rear axle :  $F_{l_{f,l}} = F_{l_{f,r}}$  or  $F_{c_{f,l}} = F_{c_{f,r}}$
- front and rear axle lengths are the same :  $t_f = t_r = t$

$$\begin{aligned} m\dot{V}_x &= mV_y\dot{\psi} + (F_{l_{f,*}}) + (F_{l_{r,*}}), \\ m\dot{V}_y &= -mV_x\dot{\psi} + (F_{c_{f,*}}) + (F_{c_{r,*}}) + Y_w, \\ J\ddot{\psi} &= (F_{c_{f,*}})l_f - (F_{c_{r,*}})l_r + (-F_{l_{*,l}} + F_{l_{*,r}})t + J_wY_w + M, \\ mV_x\dot{\beta}_{cog} &= (F_{c_{f,*}} + F_{c_{r,*}}) - mV_x\dot{\psi}. \end{aligned} \quad (3.24)$$

where the term  $F_{l_{*,l}}$  denotes the sum of longitudinal forces acting on left side of the vehicle, and the forces on the right side is denoted  $F_{l_{*,r}}$ . Note that the longitudinal velocity is kept

constant during a lane change in this work. Thus, the first differential equation is omitted in the design.

### 3.2.2 Tire Model

Tire forces are crucial in vehicle dynamics and control because they determine the handling characteristics of the vehicle. These forces significantly affect the cornering, longitudinal, yaw and the slip side dynamics of the vehicle. The behavior of tire forces is nonlinear, it has a large variation depending on the road condition. Equation 3.24 shows that the forces are coupled and the slip angle  $\alpha$ , slip ratio  $s$ , tire-road friction coefficient  $\mu$ , and the tire normal force  $F_z$  that play an important role in handling capability of the vehicle. In this work, we use the Pacejka tire model which is an empirical model and commonly used in industrial and research activities. The model calculates the cornering tire forces based on slip angle, and the longitudinal forces based on percent longitudinal slip ratio. The cornering forces plot as a function of slip angle with a varying road-tire friction coefficients for a front wheel is shown in Figure 3.10. While looking at the simple force characteristics of the tire is quite useful in understanding effects of the varying quantities, we also plot the cornering stiffness versus slip angle curve with different friction coefficients shown in Figure 3.11. This is an important analysis plot which we later use to obtain the cornering stiffness parameters and rates of change to capture the tire-road nonlinearity for control design purposes. Then the bicycle model with cornering stiffnesses is shown

in equation 3.25.

$$\begin{bmatrix} \dot{V}_y \\ \ddot{\psi} \\ \dot{\beta} \end{bmatrix} = \begin{bmatrix} -2\frac{C_f+C_r}{mv_x} & -2\frac{C_f l_f - C_r l_r}{mv_x} - V_x & 0 \\ -2\frac{C_f l_f - C_r l_r}{J} & -2\frac{C_f l_f^2 - C_r l_r^2}{JV_x} & 0 \\ 0 & 2\frac{C_r l_r - C_f l_f}{mV_x^2} - 1 & -2\frac{C_f + C_r}{mV_x} \end{bmatrix} \begin{bmatrix} V_y \\ \dot{\psi} \\ \beta \end{bmatrix} + \begin{bmatrix} \frac{2C_f}{m} \\ \frac{2C_f l_f}{J} \\ \frac{2C_f}{mV_x} \end{bmatrix} \delta + \begin{bmatrix} 0 & 0 \\ \frac{2C_f l_f}{J} & \frac{1}{J} \\ \frac{2C_f}{mV_x} & 0 \end{bmatrix} \begin{bmatrix} \delta^* \\ M \end{bmatrix} + \begin{bmatrix} \frac{1}{m} \\ \frac{J_w}{J} \\ 0 \end{bmatrix} Y_w. \quad (3.25)$$

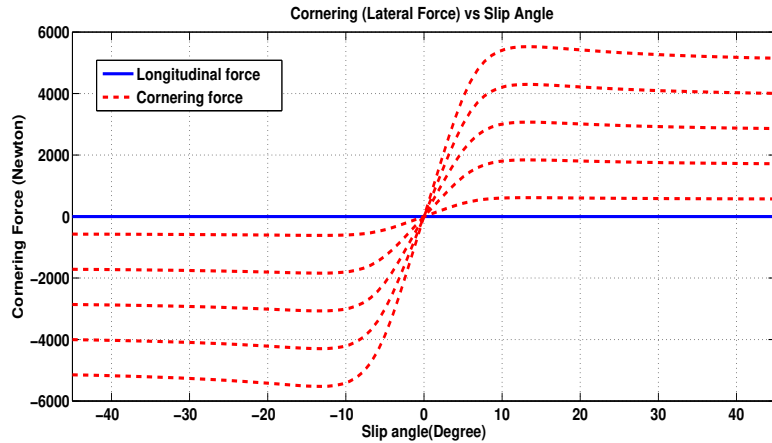


Figure 3.10: Cornering force for  $\mu=[0.1, 0.3, 0.5, 0.7, 0.9]$ <sup>14</sup> © 2017 IEEE. Reprinted, with permission, from Serdar Coskun and Reza Langari, Enhanced vehicle handling performance for an emergency lane changing controller in highway driving, June 2017.

### 3.2.3 Control Design Procedure

We start the control design steps by employing a reference model (equation 3.25) to output the desired reference values for the controller. The vehicle then follows the desired

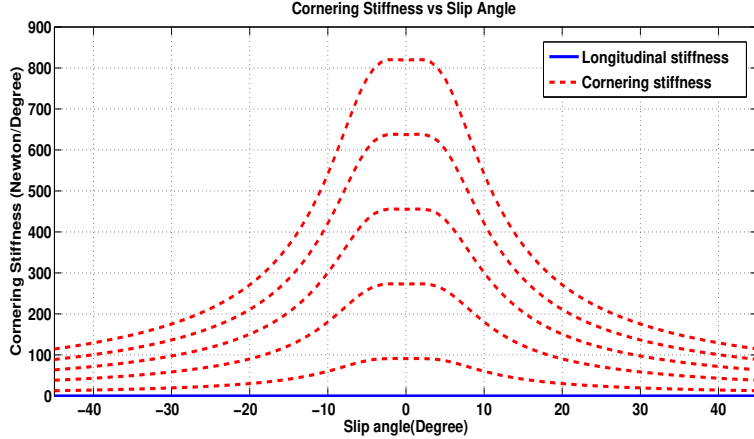


Figure 3.11: Cornering stiffness for  $\mu=[0.1, 0.3, 0.5, 0.7, 0.9]$ <sup>15</sup> © 2017 IEEE. Reprinted, with permission, from Serdar Coskun and Reza Langari, Enhanced vehicle handling performance for an emergency lane changing controller in highway driving, June 2017.

dynamics by a feedback signal of the yaw rate. The vehicle center of gravity slip side angle  $\beta_{cog}$  is not directly measured, but can be estimated by an observer. In the controller synthesis, the slip side angle is not directly controlled. However, the yaw rate controller bounds the slip side angle limit within an acceptable region to prevent the loss of maneuverability. The reference model is here to used a bicycle model with constant parameters, its output generates the desired yaw rate  $\dot{\psi}_d$ , vehicle slip side angle  $\beta_{cog}$ , and the lane change trajectory. The equation (3.25) is employed to obtain the desired outputs by assuming constant cornering stiffnesses values<sup>16</sup>. Consequently, the outputs are function of the commanded steering angle  $\delta_d$  (see [120]), the wind load (disturbance), and the vehicle longitudinal speed  $V_x$ . Note that the wind load that is modeled in equation (3.22) and (3.25) is only used to output the reference signals that are fed to the nonlinear plant model. Therefore, the outputs of the nonlinear model become function of the disturbance load. We use the nonlinear vehicle model is used in synthesis steps of the controller. Notice that

---

<sup>16</sup>We assume a dry road profile where  $\mu = 1$  that gives the number of 60000 N/rad for both  $C_f$  and  $C_r$ .

we use the third and forth equation in equation (3.32) to follow the reference yaw rate for control design. We convert the nonlinearities in cornering stiffnesses into parameter space (via Figures 3.10-3.11) and design the LPV/ $\mathcal{H}_\infty$  controller for simulation demonstration. The varying cornering stiffnesses and their rates of change are fed to the controller as the scheduling parameters. The nonlinear vehicle inputs are the commanded steering  $\delta_d$ , is the steering that achieves a successful lane change maneuver, the yaw moment  $M$ , and the corrective steering  $\delta^*$  that are coming out of the controller. The main objective in the proposed controller design is to minimize the error between the desired yaw rate  $\dot{\psi}_d$  and the actual yaw rate output  $\dot{\psi}$  i.e.,  $e_{\dot{\psi}} = \dot{\psi}_d - \dot{\psi} \cong 0$ . The proposed control system is shown in Fig 3.12.

### 3.2.3.1 Performance weight selection

The weighting functions play an important role for control design. Generally, there is no explicit way of choosing the weight selections that can lead to an optimal solution for each design. For improved performance, high order weighing functions are more desirable. However, the higher order dynamics increase the controller order and the control loop tend to be more sensitive against perturbations. Therefore, constant weights are selected as opposed to the work [91]. Carefully tuning the weights is an essential step and requires an experience. We choose the input/output weights in Figure 3.13 as  $W_{\delta^*,M}=0.3$  and  $W_{\dot{\psi},\beta}=20$ . This assures a good yaw moment output as well as good reference tracking of yaw rate and vehicle slip angle.

### 3.2.3.2 LPV/ $\mathcal{H}_\infty$ controller design

The  $\mathcal{H}_\infty$  control design finds a controller that provides both closed-loop stability and a satisfied level of performance index for reference tracking and disturbance rejection. To start the design process, we first define the plant matrices. In order to form the input-output pairs, the generalized plant model is derived by linear fractional transformation

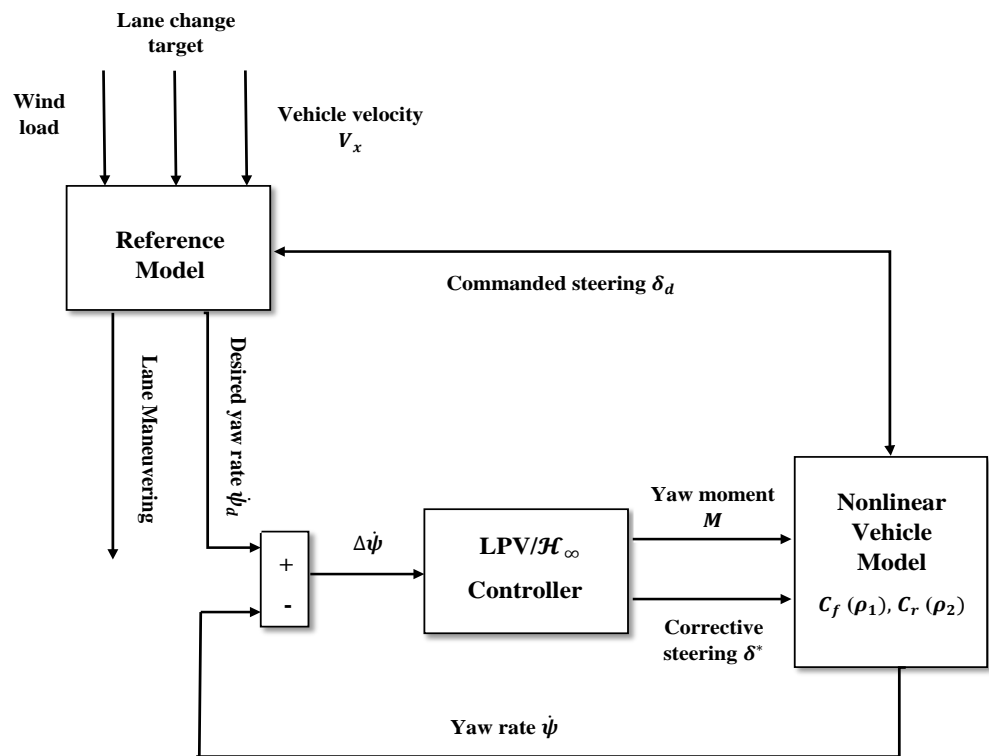


Figure 3.12: The control system structure <sup>17</sup> © 2017 IEEE. Reprinted, with permission, from Serdar Coskun and Reza Langari, Enhanced vehicle handling performance for an emergency lane changing controller in highway driving, June 2017.

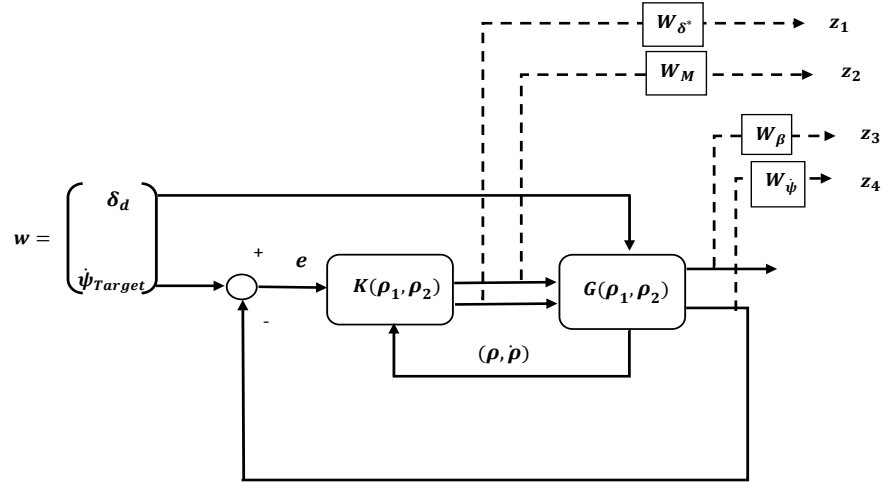


Figure 3.13: Weighting control structure <sup>18</sup> © 2017 IEEE. Reprinted, with permission, from Serdar Coskun and Reza Langari, Enhanced vehicle handling performance for an emergency lane changing controller in highway driving, June 2017.

(LFT). Figure 3.13 portrays the LFT structure of the generalized plant model with a set of selected weights. We then consider the following state space presentation of an open loop LPV system

$$\begin{aligned}
 \dot{x}(t) &= A(\rho(t))x(t) + B_1(\rho(t))w(t) + B_2(\rho(t))u(t) \\
 z(t) &= C_1(\rho(t))x(t) + D_{11}(\rho(t))w(t) + D_{12}(\rho(t))u(t) \\
 y(t) &= C_2(\rho(t))x(t) + D_{21}(\rho(t))w(t) + D_{22}(\rho(t))u(t)
 \end{aligned} \tag{3.26}$$

$$\left\{
 \begin{array}{ll}
 w(t) = [\dot{\psi}_d(t)] & \text{External disturbance vector} \\
 u(t) = [M(t) \quad \delta^*(t)] & \text{Control input vector} \\
 z(t) = [z_1(t) \quad z_2(t) \quad z_3(t) \quad z_4(t)] & \text{Regulated output vector} \\
 y(t) = e_\psi(t) & \text{Measurement vector}
 \end{array}
 \right.$$

where  $x \in \mathbb{R}^n$  is the state vector,  $w \in \mathbb{R}^{n_w}$  is the disturbance vector,  $u \in \mathbb{R}^{n_u}$  is the control input vector,  $z \in \mathbb{R}^{n_z}$  is the vector of output signals,  $y \in \mathbb{R}^{n_y}$  is the vector of measured variables. The varying parameter vector  $\rho(t)$  that is defined as  $\rho(t) = [C_f(t), C_r(t)]^T$  lies in a compact set with bounded parameters and the rates of variation, *i.e.*,  $\rho \in \mathcal{F}_{\mathcal{P}}^v$  with

$$\mathcal{F}_{\mathcal{P}}^v \equiv \{\rho(t) \in \mathcal{P}, |\dot{\rho}_i(t)| \leq v_i i = 1, 2, \dots, s\},$$

where  $\mathcal{P}$  is a compact set of  $\mathbb{R}^s$ .

The dimensions are given for the generalized plant model  $A \in \mathbb{R}^{n \times n}$ ,  $B_1 \in \mathbb{R}^{n \times n_w}$ ,  $B_2 \in \mathbb{R}^{n \times n_u}$ ,  $C_1 \in \mathbb{R}^{n_z \times n}$ ,  $D_{11} \in \mathbb{R}^{n_z \times n_w}$ ,  $D_{12} \in \mathbb{R}^{n_z \times n_u}$ ,  $C_2 \in \mathbb{R}^{n_y \times n}$ ,  $D_{12} \in \mathbb{R}^{n_y \times n_w}$ ,  $D_{22} \in \mathbb{R}^{n_y \times n_y}$ . Then the LPV/ $\mathcal{H}_{\infty}$  output- feedback control design formulation is given with the following linear matrix inequality (LMI) solution. **Theorem 1:** Given the open loop LFT system governed by (3.26), suppose there exists parameter dependent two symmetric Lyapunov matrices  $\mathbf{X}(\rho)$ ,  $\mathbf{Y}(\rho)$  and four auxiliary controller matrices matrices  $\hat{\mathbf{A}}(\rho)$ ,  $\hat{\mathbf{B}}(\rho)$ ,  $\hat{\mathbf{C}}(\rho)$ ,  $\hat{\mathbf{D}}(\rho)$ . The following LMI gives the controller matrices.

$$\begin{bmatrix} \dot{\mathbf{X}}(\rho) + \mathbf{X}(\rho)A(\rho) + \hat{\mathbf{B}}(\rho) + C_2(\rho) + (\star) & \star \\ \hat{\mathbf{A}}^T(\rho) + A(\rho) + B_2(\rho)\hat{\mathbf{D}}(\rho)C_2(\rho) & -\dot{\mathbf{Y}}(\rho) + A(\rho)\mathbf{Y}(\rho) + B_2(\rho)\hat{\mathbf{C}}(\rho) + (\star) \\ (\mathbf{X}(\rho) + \hat{\mathbf{B}}(\rho)D_{21}(\rho))^T & (B_1(\rho) + B_2(\rho)\hat{\mathbf{D}}(\rho)D_{21}(\rho))^T \\ (C_1(\rho) + D_{12}(\rho)\hat{\mathbf{D}}(\rho)C_2(\rho)) & C_1(\rho)\mathbf{Y}(\rho) + D_{12}(\rho)\hat{\mathbf{C}}(\rho) \\ \star & \star \\ \star & \star \\ -\gamma I_{n_w} & \star \\ D_{11}(\rho) + \hat{\mathbf{D}}(\rho)D_{12}(\rho) & -\gamma I_{n_z} \end{bmatrix} \quad (3.27)$$

$$\begin{bmatrix} \mathbf{X}(\rho) & I \\ I & \mathbf{Y}(\rho) \end{bmatrix} > 0 \quad (3.28)$$


---

Then, there exist a dynamic controller such that

1. The closed loop system is parameter-dependent quadratic (PDQ) stable over  $\mathcal{F}_{\mathcal{P}}^v$ .
2. The induced  $\mathcal{L}_2$  norm of the operator  $w \rightarrow z$  is bounded by  $\gamma > 0$  (i.e.,  $\|T_{zw}\|_{i,2} < \gamma$ ).

Once the parameter dependent  $\mathbf{X}(\rho)$ ,  $\mathbf{Y}(\rho)$ ,  $\hat{\mathbf{A}}(\rho)$ ,  $\hat{\mathbf{B}}(\rho)$ ,  $\hat{\mathbf{C}}(\rho)$ , and  $\hat{\mathbf{D}}(\rho)$  are obtained, the controller matrices are computed in the following steps:

1) Solve for  $N$ ,  $M$ , and the factorization problem

$$I - \mathbf{XY} = NM^T \quad (3.29)$$

2) Compute  $A_c$ ,  $B_c$ ,  $C_c$ , and  $D_c$  with

$$\begin{aligned} A_c &= N^{-1}(N\dot{M}^T + \hat{\mathbf{A}} - \mathbf{X}(A - B_2\hat{\mathbf{D}}C_2)Y - \hat{\mathbf{B}}C_2Y - XB_2\hat{\mathbf{C}})M^{-T}, \\ B_c &= N^{-1}(\hat{\mathbf{B}} - \mathbf{X}B_2\hat{\mathbf{B}}), \\ C_c &= (\hat{\mathbf{C}} - \hat{\mathbf{D}}C_2Y)M^{-T}, \\ D_c &= \hat{\mathbf{D}} \end{aligned} \quad (3.30)$$

All the matrices above are parameter dependent and the varying parameter notation is omitted.

**Proof:** Please refer to [121].

Note that the above LMIs are parameterized. We choose some basis functions for the LMI variables  $\mathbf{X}$  and  $\mathbf{Y}$ . These matrix functions can be selected as constants. However, this choice leads to a poor performance of the closed loop system due to disregarding the parameter dependency in solution steps. Therefore, we use a set of second order set matrix functions as follows

$$X = X_0 + \rho X_1 + \frac{\rho^2}{2} X_2$$

$$Y = Y_0 + \rho Y_1 + \frac{\rho^2}{2} Y_2$$

where  $\rho$  is the cornering stiffness change front and rear tires. Note that the LMIs solution is now dependent on the scheduling parameter  $\rho$  for both matrix functions  $\mathbf{X}$  and  $\mathbf{Y}$ . This choice of the basis functions for the matrices  $\mathbf{X}$  and  $\mathbf{Y}$  presents the dependency of the scheduling parameter  $\rho$  in the LMIs solution. We have assumed  $C_f = C_r \in [30000, 60000]$ <sup>19</sup>. And the rates of change in parameter variation is assumed to be  $\dot{C}_f = \dot{C}_r \in [-20, 20]$  for computational purposes. To handle an infinite dimensional convex optimization problem, the parameter space is gridded for each  $\rho=5000$  N/rad and a set of finite dimensional LMIs is solved at these grid points.

### 3.2.4 Simulation Results

In this section, a number of simulations are performed on time-varying vehicle model. The performance of the LPV/ $\mathcal{H}_\infty$  controller is compared with the LTI/ $\mathcal{H}_\infty$  in terms of minimization of the yaw rate error  $e_{\dot{\psi}}$ , deviation of the slip side angle and yaw rate, and the generated yaw moment control input. It is noted that the corrective steering moment has a small magnitude which is only used to increase the handling performance over the entire operational envelope of the system. The commanded steering that is generated by a driver

---

<sup>19</sup>Note that we convert cornering stiffness values from N/deg in Figure 3.11 to N/rad. Assume that the dry road profile has  $\mu = 1$  that corresponds to approximately 1050 N/deg, the conversion gives the number of 60000 N/rad in our design.

or a controller initiates the lane change operation. The reference model responses are the reference tracking of the lane change trajectory, vehicle side slip angle, and the yaw rate that is to be followed by the designed LPV/ $\mathcal{H}_\infty$  controller in existence of the parameter variation in the model. Therefore, the yaw rate  $\dot{\psi}_d$  is a function of the commanded steering. Then, the goal is to define a suitable feedback control law that achieves good tracking and disturbance performance over the entire operating range. The proposed LPV/ $\mathcal{H}_\infty$  yaw controller in Figure 3.12 is a single input multi output controller, which responds to the  $e_{\dot{\psi}}$ , outputs the yaw moment and the corrective steering input. The scheduling parameters  $C_f = C_r \in [30000, 60000]$ <sup>20</sup>. This range is defined according to Figure 3.11 and the lower bound in  $\rho$  denotes a wet road profile (due to rain), whereas the upper bound of  $\rho$  presents a dry road profile. And the rates of change in parameter variation is assumed to be  $\dot{C}_f = \dot{C}_r \in [-20, 20]$  for computational purposes. The LMIs in Theorem 1 are solved by the LMI Control Toolbox in Matlab<sup>®</sup>, the performance level  $\mathcal{L}_2$  norm of the LTI design is  $\gamma = 0.4243$  while the LPV design is  $\gamma = 0.7892$ . This result ensures that the maximum attenuation of the disturbance vectors over the regulated outputs over the entire parameter range is less than  $\gamma$  i.e.,  $\|T_{zw}\|_{i,2} < \gamma$ . The closed loop simulation is performed in Simulink<sup>®</sup> software where the LPV controllers are implemented using s-Functions. The duration of the LPV/ $\mathcal{H}_\infty$  on a computer equipped with Core i7 3.2 GHz CPU is about 30 minutes. Furthermore, the LTI controller (fixed) is designed such that the variations of the road profile are kept constant. Then, the simulation is performed by assuming the cornering stiffness changes in the plant model.

It is important to state that a steering signal either from a driver or a controller<sup>26</sup> to the reference model leads to a successful lane change maneuver with an optimal yaw rate and

---

<sup>20</sup>We did not consider a snowy road profile in highway driving where the cornering stiffness values would be lower than that of the rainy road.

<sup>26</sup>Notice that the steering profile in Figure 3.16, activated at 5 seconds of the simulation, is produced as a function of lane change maneuver signal and disturbance wind load [120].

---

**Algorithm 2:** Computation of controller matrices

---

**Input:**  $A(\rho), B_1(\rho), B_2(\rho), C_1(\rho), D_{11}(\rho), D_{12}(\rho), C_2(\rho)$   
 $D_{21}(\rho), D_{22}(\rho)$   
**Output:**  $A_c(\rho), B_c(\rho), C_c(\rho), D_c(\rho)$

**for**  $\dot{\rho} \in [\dot{\rho}_{min}, \dot{\rho}_{max}]$  **do**

**for**  $\rho \in [\rho_{min}, \rho_{max}]$  **do**

Form open loop nonlinear plant matrices (equation 3.26);  
Solve the optimization problem with LMIs constraints at each grid points  
with equations (3.27) and (3.28);

**end**

**end**

Compute controller matrices with equation (3.29) and equation (3.30).

---

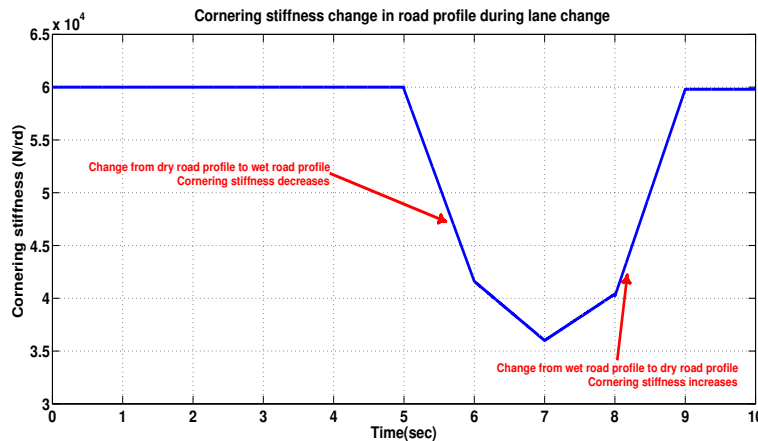


Figure 3.14: Tire cornering stiffness change in road profile<sup>21</sup> © 2017 IEEE. Reprinted, with permission, from Serdar Coskun and Reza Langari, Enhanced vehicle handling performance for an emergency lane changing controller in highway driving, June 2017.

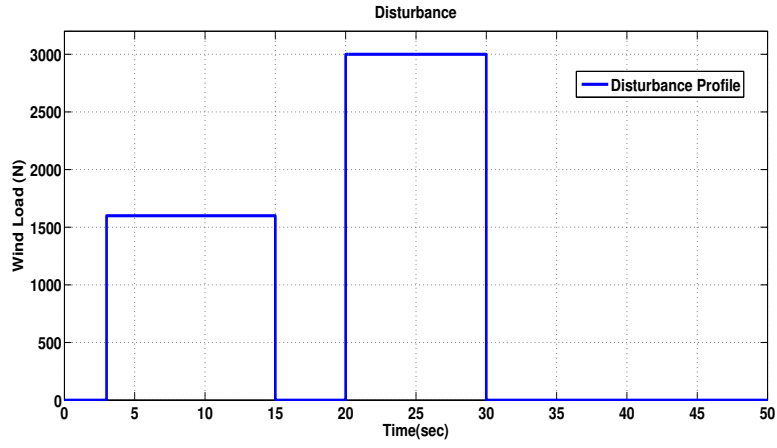


Figure 3.15: Wind disturbance <sup>22</sup> © 2017 IEEE. Reprinted, with permission, from Serdar Coskun and Reza Langari, Enhanced vehicle handling performance for an emergency lane changing controller in highway driving, June 2017.

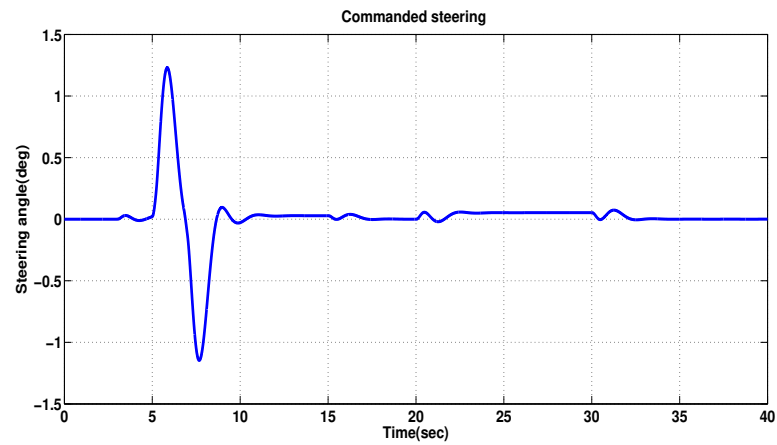


Figure 3.16: Commanded steering <sup>24</sup> © 2017 IEEE. Reprinted, with permission, from Serdar Coskun and Reza Langari, Enhanced vehicle handling performance for an emergency lane changing controller in highway driving, June 2017.

Table 3.2: Vehicle parameters <sup>23</sup> © 2017 IEEE. Reprinted, with permission, from Serdar Coskun and Reza Langari, Enhanced vehicle handling performance for an emergency lane changing controller in highway driving, June 2017.

<b>Symbol</b>	<b>Value</b>	<b>Unit</b>	<b>Description</b>
$m$	1500	kg	<i>Vehicle mass</i>
$m_z$	350	kg	<i>Vehicle rear mass</i>
$J$	2500	$kgm^2$	<i>Yaw inertia</i>
$l_f$	1.1	m	<i>Distance of front axle to COG</i>
$l_r$	1.5	m	<i>Distance of rear axle to COG</i>
$C_f$	[30000,60000]	N/rad	<i>Varying front cornering stiffness</i>
$C_r$	[30000,60000]	N/rad	<i>Varying rear cornering stiffness</i>
$t_f = t_r$	1.4	m	<i>Front and rear axle length</i>
$V_x$	100	km/h	<i>Vehicle longitudinal velocity</i>
$W_R$	3	m	<i>Width of the road</i>
$W_v$	1.847	m	<i>Wind load acting distance to COG</i>

slip performance in Figure 3.17. Notice that the wind disturbance effect is only employed in reference model so that the outputs present the effect of wind load. Then this yaw rate is a desired yaw rate to be followed by the LPV and LTI controllers that react to the nonlinear model. We consider a scenario where there is a sharp decrease and increase in cornering stiffness values (sudden change from a dry road to a wet road profile and vice versa) during a lane change in Figure 3.14. Figures 3.17, 3.18, 3.19 show the regulated output responses for both LPV and LTI cases for this scenario. It is observed that the LPV presents better tracking performance than that of the LTI controller in both Figure 3.17 and Figure 3.18. The deviations from the nominal value are satisfactory. Notice that the uncontrolled yaw rate performance is the worst in terms of reference following and disturbance rejection<sup>27</sup>. Moreover, the generated yaw moment control input in LPV design, as expected (due to the higher performance index value  $\gamma$ ), is slightly bigger than that of the LTI design in Fig

---

<sup>27</sup>The magnitude of the yaw rate almost two times bigger than that of the LPV controller case. We reach to our goal to enhance the yaw rate for the nonlinear vehicle model.

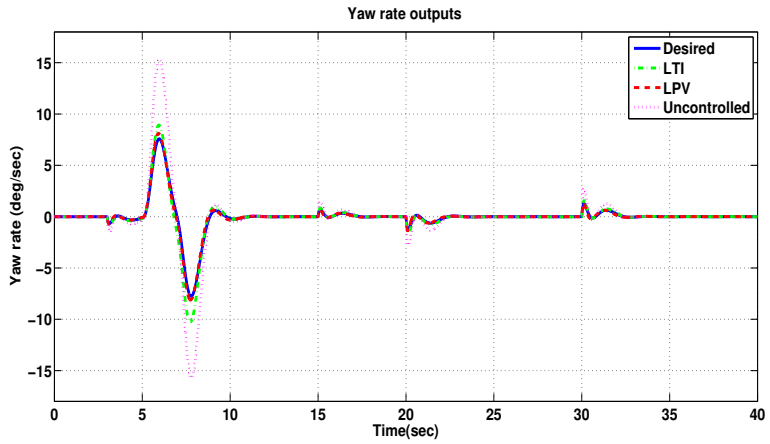


Figure 3.17: Yaw rate outputs <sup>25</sup> © 2017 IEEE. Reprinted, with permission, from Serdar Coskun and Reza Langari, Enhanced vehicle handling performance for an emergency lane changing controller in highway driving, June 2017.

3.19. Note that the exertion of the yaw moment to the brake forces by taking into account actuator dynamics is a possible future direction in our research. To better analyze the handling performance over the varying cornering stiffnesses, Figure 3.20 is plotted to show the relation between the front steering angle and the yaw rate. This result simply means that deterioration of yaw rate of the system is affected to parameter changes with respect to the steering angle. It is shown that the LPV design better follows the desired value than the LTI case. It is interpreted that if the commanded steering is applied to the nonlinear model with no control, the generated yaw rate results in poor handling with respect to the degree steering angle. This result certainly assures that a safe lane change, initiated by the steering angle with an improved rate tracking even when the road conditions are varying. We can conclude that both the LTI and LPV enhance the handling performance with respect to the parameter changes. But, the LPV design provides better results in each case.

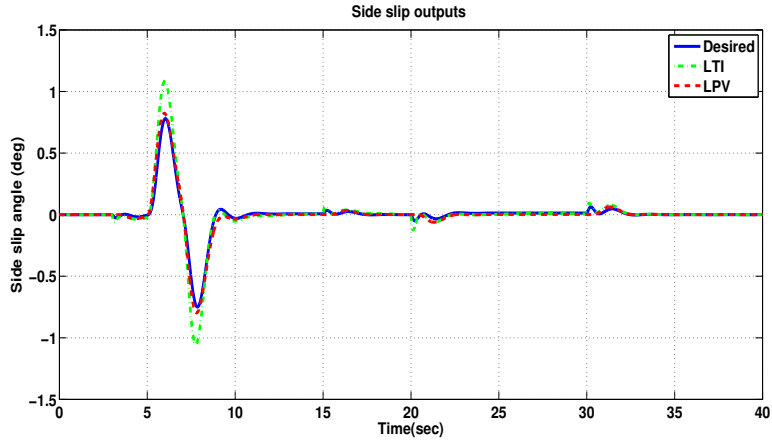


Figure 3.18: Slip side angle outputs<sup>28</sup> © 2017 IEEE. Reprinted, with permission, from Serdar Coskun and Reza Langari, Enhanced vehicle handling performance for an emergency lane changing controller in highway driving, June 2017.

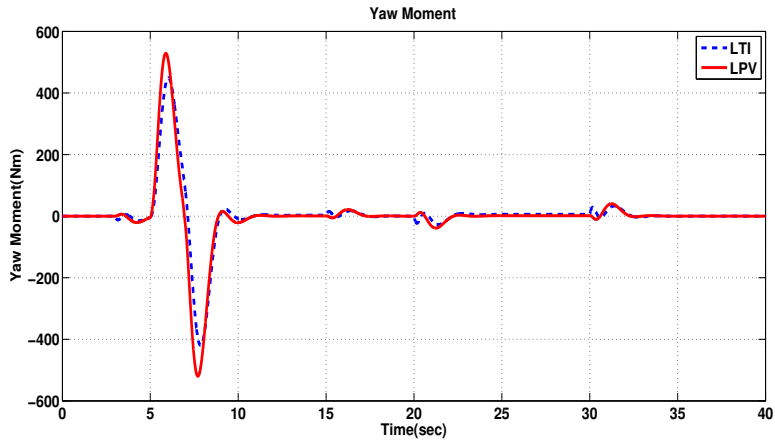


Figure 3.19: Yaw moments<sup>29</sup> © 2017 IEEE. Reprinted, with permission, from Serdar Coskun and Reza Langari, Enhanced vehicle handling performance for an emergency lane changing controller in highway driving, June 2017.

### 3.3 Takagi-Sugeno Modeling for Vehicle Lateral Dynamics

The state-space equation with uncertain cornering stiffness values is expressed as [122]

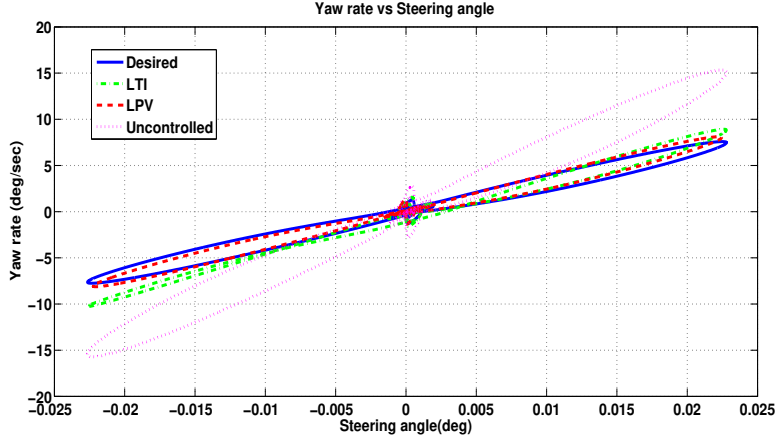


Figure 3.20: Yaw rate vs steering<sup>30</sup> © 2017 IEEE. Reprinted, with permission, from Serdar Coskun and Reza Langari, Enhanced vehicle handling performance for an emergency lane changing controller in highway driving, June 2017.

$$\dot{x}(t) = Ax(t) + B_1 w(t) + B_2 u(t) \quad (3.31)$$

where  $x \in \mathbb{R}^n$  is the state vector,  $x(t) = (\beta \ \dot{\psi})^T$ ,  $w \in \mathbb{R}^{n_w}$  is the disturbance vector,  $w(t) = \delta_f$ , and  $\mathbb{R}^{n_u}$  is the control input vector,  $u(t) = (\delta^* \ M)^T$  with

$$A = \begin{pmatrix} 2\frac{-C_f - C_r}{mV_x} & 2\frac{C_r l_r - C_f l_f}{mV_x^2} - 1 \\ 2\frac{C_r l_r - C_f l_f}{J} & 2\frac{-C_f l_f^2 - C_r l_r^2}{JV_x} \end{pmatrix}, B_1 = \begin{pmatrix} \frac{2C_f}{mV_x} \\ \frac{2C_f l_f}{J} \end{pmatrix},$$

$$B_2 = \begin{pmatrix} \frac{2C_f}{mV_x} & 0 \\ \frac{2C_f l_f}{J} & \frac{1}{J} \end{pmatrix}.$$

where the corrective steering input is  $\delta^*$  that is used by AFS and the total steering input is the summation of  $\delta_f$  and  $\delta^*$ .

### 3.3.1 T-S Fuzzy modeling

Consider a continuous-time T-S fuzzy system which is composed of  $r$  model rules presented as following

Model rule  $i$ : IF  $\varrho_1(t)$  is  $M_{i1}$  and ... and  $\varrho_l(t)$  is  $M_{il}$  THEN

$$\dot{x}(t) = A_i x(t) + B_{1i} w(t) + B_{2i} u(t)$$

$$i = 1, 2, \dots, r,$$

where  $r$  is the number of IF-THEN rules,  $A_i$ ,  $B_{1i}$ , and  $B_{2i}$  are real-valued constant matrices with appropriate dimensions;  $\varrho_j(t) = (1, 2, \dots, l)$  and  $M_{il} = (1, 2, \dots, r)$  are the premise variables and the membership function grades, respectively. Given a pair of  $x(t)$  and  $u(t)$  the global model outputs of the fuzzy system are written as follows:

$$\begin{aligned}\dot{x}(t) &= \frac{\sum_{i=1}^r w_i(\varrho(t)) [A_i x(t) + B_{1i} w(t) + B_{2i} u(t)]}{\sum_{i=1}^r w_i(\varrho(t))}, \\ &= \sum_{i=1}^r h_i(\varrho(t)) [A_i x(t) + B_{1i} w(t) + B_{2i} u(t)],\end{aligned}\tag{3.32}$$

The truth value for the  $i$ -th rule is defined as

$$w_i(\varrho(t)) = \prod_{j=1}^l M_{ij}(\varrho(t)).$$

where  $M_{ij}(\varrho(t))$  is the grade of membership with  $w_i(\varrho(t)) \geq 0$ ,  $i = 1, 2, \dots, r$  and  $\sum_{i=1}^r w_i(\varrho(t)) > 0$ . Then the fuzzy weighting function for the  $i$ -th rule is defined as

$$h_i(\varrho(t)) = \frac{w_i(\varrho(t))}{\sum_i^r w_i(\varrho(t))}.$$

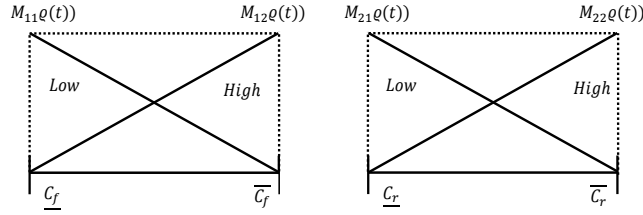


Figure 3.21: Triangular membership functions

Moreover, the fuzzy weighting functions  $h_i(\varrho(t))$  satisfy

$$\sum_{i=1}^r h_i(\varrho(t)) = 1, \quad h_i(\varrho(t)) \geq 0.$$

Note that the membership functions and the defuzzification method are continuous.

It is assumed that vehicle operates at constant vertical load  $F_{z_{i,j}}$ , with bounded slip angle  $\alpha_{i,j}$ , ratio  $s_{i,j}$ , and road friction  $\mu_{i,j}$ . Then cornering stiffnesses  $C_f$  and  $C_r$  are expressed as bounded uncertain values due to the change in tire-road friction coefficient  $\mu$  on the road surface profile. Then the nonlinear bounded uncertainty is given as

$$\begin{aligned} \min \Delta C_f &= \underline{C}_f, & \max \Delta C_f &= \overline{C}_f, \\ \min \Delta C_r &= \underline{C}_r, & \max \Delta C_r &= \overline{C}_r. \end{aligned} \tag{3.33}$$

Then the grade of membership functions, i.e.,  $M_{il}$  and premise variables, i.e.,  $\varrho_j(t)$  for cornering stiffnesses are

$$\begin{aligned} \Delta C_f &= M_{11}(\varrho_1(t)) \underline{C}_f + M_{12}(\varrho_1(t)) \overline{C}_f \\ \Delta C_r &= M_{21}(\varrho_2(t)) \underline{C}_r + M_{22}(\varrho_2(t)) \overline{C}_r, \end{aligned} \tag{3.34}$$

Recall that  $M_{11}(\varrho_1(t)) \geq 0$ ,  $M_{12}(\varrho_1(t)) \geq 0$ ,  $M_{21}(\varrho_2(t)) \geq 0$ ,  $M_{22}(\varrho_2(t)) \geq 0$  and

$$M_{11}(\varrho_1(t)) + M_{12}(\varrho_1(t)) = 1, \quad M_{21}(\varrho_2(t)) + M_{22}(\varrho_2(t)) = 1.$$

The proposed T-S model exactly presents the nonlinear vehicle dynamics, which is  $C_f \in [\underline{C}_f, \overline{C}_f] \times C_r \in [\underline{C}_r, \overline{C}_r]$ , in the defined range. The T-S fuzzy model consists of 4 sub-models with corresponding fuzzy rules. To make the process more clear, the sub-models are defined as follows;

Model rule 1: IF  $\varrho_1(t)$  is low and  $\varrho_2(t)$  is low, THEN

$$\dot{x}(t) = A_1x(t) + B_{11}w(t) + B_{21}u(t)$$

where  $A_1 = A(\underline{C}_f, \underline{C}_r)$ ,  $B_{11} = B_1(\underline{C}_f, \underline{C}_r)$ , and  $B_{21} = B_2(\underline{C}_f, \underline{C}_r)$  in equation (3.31),

Model rule 2: IF  $\varrho_1(t)$  is low and  $\varrho_2(t)$  is high, THEN

$$\dot{x}(t) = A_2x(t) + B_{12}w(t) + B_{22}u(t)$$

where  $A_2 = A(\underline{C}_f, \overline{C}_r)$ ,  $B_1 = B_1(\underline{C}_f, \overline{C}_r)$ , and  $B_{21} = B_2(\underline{C}_f, \overline{C}_r)$  in equation (3.31),

Model rule 3: IF  $\varrho_1(t)$  is high and  $\varrho_2(t)$  is low, THEN

$$\dot{x}(t) = A_3x(t) + B_{13}w(t) + B_{23}u(t)$$

where  $A_2 = A(\overline{C_f}, \underline{C_r})$ ,  $B_{13} = B_1(\overline{C_f}, \underline{C_r})$ , and  $B_{23} = B_2(\overline{C_f}, \underline{C_r})$  in equation (3.31),

Model rule 4: IF  $\varrho_1(t)$  is high and  $\varrho_2(t)$  is high, THEN

$$\dot{x}(t) = A_4x(t) + B_{14}w(t) + B_{24}u(t)$$

where  $A_4 = A(\overline{C_f}, \overline{C_r})$ ,  $B_{14} = B_1(\overline{C_f}, \overline{C_r})$ , and  $B_{24} = B_2(\overline{C_f}, \overline{C_r})$  in equation (3.31).

Table 3.3: Fuzzy Rule Table

Rule	Premise variables	
1	Low	Low
2	Low	High
3	High	Low
4	High	High

Fuzzy blended nonlinear vehicle lateral dynamics equation is written same as in (3.32)

$$\dot{x}(t) = \sum_{i=1}^r h_i(\varrho(t)) [A_i x(t) + B_{1i} w(t) + B_{2i} u(t)]. \quad (3.35)$$

Notice that the dependence of  $\varrho(t)$  and  $M_{ij}$  in (3.34) is nonlinear. Therefore the state-space presented by (3.35) is a nonlinear equation.

### 3.3.2 Controller Design

In order to facilitate the general steps in control design procedure, it is found important to describe the control objectives and design specifications. In our previous work [118], the set points are generated by a reference model and fed to the controller to be tracked. In this work, we adopt the following yaw rate and slip side angle reference set values for the controller [88].

$$\dot{\psi}_{ref} = \frac{V_x}{(l_f + l_r)(1 + k_{us}V_x^2)}\delta_f, \quad \beta_{ref} = 0.$$

where  $k_{us}$  is the stability coefficient. The slip side angle is related with vehicle stability and the yaw rate determines vehicle handling performance. To maintain the system stability, the slip side angle is driven to zero and the yaw rate reference is followed as much as possible. Since the tire model is nonlinear and the cornering stiffness is a function of commanded steering, vehicle yaw rate, vehicle slip, and tire slip side angles, the fuzzy  $\mathcal{H}_\infty$  control law ensures to compensate the nonlinear variations of tire model parameters with the objective of tracking the set point references. In our work, the states of the system, reference targets, and the cornering stiffness values are made available to the controller. Then the designed controller is a state-feedback tracking controller.

Parallel distributed compensation (PDC) utilizes a set of control gains for each sub-model. The main idea is to determine the state-feedback gain for the associated sub-model of the system. The resulting control law is

$$u(t) = h_i(\varrho(t)) F_i x(t). \quad (3.36)$$

Notice that the equation (3.36) is a nonlinear control action. Substituting the (3.36) into

(3.35) gives the following closed-loop equation.

$$\dot{x}_{cl}(t) = \sum_{i=1}^r \sum_{j=1}^r h_i(\varrho(t)) h_j(\varrho(t)) [(A_i + B_{2i}F_j))x(t) + B_{1i}w(t)]. \quad (3.37)$$

**Remark 1:** The closed to equation given by (3.37) can also be written as

$$\begin{aligned} \dot{x}_{cl}(t) = & \sum_{i=1}^r h_i(\varrho(t)) h_i(\varrho(t)) [(A_i + B_{2i}F_i))x(t) + B_{1i}w(t)] \\ & + 2 \sum_{i < j}^r h_i(\varrho(t)) h_j(\varrho(t)) \left[ \frac{(A_i + B_{2i}F_j) + (A_j + B_{2j}F_i)}{2} x(t) \right. \\ & \left. + B_{1j}w(t) \right]. \end{aligned} \quad (3.38)$$

Next we show the sufficient condition to construct a fuzzy  $\mathcal{H}_\infty$  state-feedback controller with the bounded real lemma condition for the closed-loop system (3.38).

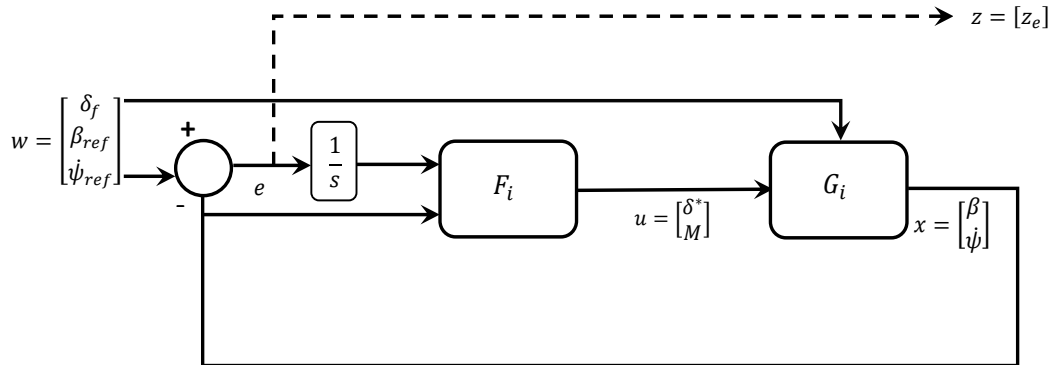


Figure 3.22: State-feedback tracking controller

### 3.3.3 Fuzzy $\mathcal{H}_\infty$ Controller Synthesis

The fuzzy  $\mathcal{H}_\infty$  state-feedback controller stabilize the vehicle closed-loop system with an induced performance index to reject the disturbances and to track the reference targets. The control design procedure starts with pairing the input-output pairs to attenuate the maximum input energy over the energy of regulated outputs transfer matrix of the system with an energy-to-energy performance index  $\gamma$ , i.e.,

$$\|T_{wz}\|_\infty = \sup_{w \in \mathcal{L}_2, w \neq 0} \frac{\|z\|_{\mathcal{L}_2}}{\|w\|_{\mathcal{L}_2}} \leq \gamma. \quad (3.39)$$

This norm searches the worst case energy magnitude of the output signals over the input signal energy. Therefore, this work defines the controller norm as the energy-to-energy norm of the system. Other approaches define the performance norm as the energy-to-peak norm [88], [89] to examine the effect of the energy of the input signals over the peak value of the output signals. Next, the generalized plant model is derived by linear fractional transformation (LFT) with the input-output pairs. Consider the following state space presentation of an open loop fuzzy system for  $i$  th model rule

$$\begin{aligned} \dot{x}(t) &= A_i x(t) + B_{1i} w(t) + B_{2i} u(t) \\ z(t) &= C_{1i} x(t) \end{aligned} \quad (3.40)$$

where  $x \in \mathbb{R}^n$  is the state vector,  $w \in \mathbb{R}^{n_w}$  is the disturbance vector,  $u \in \mathbb{R}^{n_u}$  is the control input vector,  $z \in \mathbb{R}^{n_z}$  is the vector of output signals.

$$\left\{ \begin{array}{ll} w(t) = [\delta_f(t) \quad \beta_{ref}(t) \quad \dot{\psi}_{ref}(t)] & \text{Exogenous dist. vector} \\ u(t) = [\delta^*(t) \quad M(t)] & \text{Control input vector} \\ z(t) = [z_1(t) \quad z_2(t)] & \text{Regulated output vector} \end{array} \right.$$

Note that  $\delta_f(t)$  is the commanded steering,  $\dot{\psi}_{ref}(t)$  and  $\beta_{ref}(t)$  are targets to be followed,  $M(t)$  denotes the direct yaw moment (DYC),  $\delta^*(t)$  is the corrective steering (AFS) (the total steering exerted to the vehicle is the sum of  $\delta_f(t)$  and  $\delta^*(t)$ , i.e.,  $(\delta(t) = \delta_f(t) + \delta^*(t))$ ) and  $z_1(t)$ ,  $z_2(t)$  are presenting the regulated tracking outputs. The dimensions are given for the generalized plant model as  $A \in \mathbb{R}^{n \times n}$ ,  $B_1 \in \mathbb{R}^{n \times n_w}$ ,  $B_2 \in \mathbb{R}^{n \times n_u}$ ,  $C_1 \in \mathbb{R}^{n_z \times n}$ . The feedback gains are computed with the following linear matrix inequalities (LMIs) solution.

**Remark 2:** An integrator to eliminate the steady-state error is augmented to the control design by defining a new state vector in Figure 3.22, i.e., the number of states is increased to  $n = 4$ . The designed fuzzy state-feedback controller therefore does not only stabilize the closed-loop system but also tracks the reference targets with the integral action. Thus the final control law consists of augmented control gains that correspond to the stabilization and reference tracking of the system.

**Theorem 1:** Given the open loop LFT system governed by 3.40, suppose there exists a symmetric Lyapunov matrix  $X \in \mathbb{R}^{n \times n}$  and four auxiliary feedback-controller matrices for each  $i$  rule of the model  $\Upsilon_i \in \mathbb{R}^{n_u \times n}$  such that

$$\begin{pmatrix} A_i X + X A_i^T + B_{2i} \Upsilon_i + \Upsilon_i^T B_{2i}^T & B_{1i} & X C_1^T \\ B_{1i}^T & -\gamma I & 0 \\ X C_1^T & 0 & -\gamma \end{pmatrix} < 0 \quad (3.41)$$

for  $i = j = 1, 2, 3, \dots, r$ ,

$$\begin{pmatrix}
\frac{A_i X + X A_i^T + B_{2i} \Upsilon_j + \Upsilon_j^T B_{2i}^T}{2} + \frac{A_j X + X A_j^T + B_{2j} \Upsilon_i + \Upsilon_i^T B_{2j}^T}{2} & B_{1j} & X C_1^T \\
B_{1j}^T & -\gamma I & 0 \\
X C_1^T & 0 & -\gamma
\end{pmatrix} < 0 \quad (3.42)$$

for  $i < j$ .

Given a feasible solution  $(X, \Upsilon_i)$  to the above LMIs, the state feedback gain is computed as

$$F_i = \Upsilon_i X^{-1}. \quad (3.43)$$

Notice that the time notation is omitted. Derivation of bounded real lemma inequalities can be found in [123]. Followed by the Lyapunov stability and performance conditions, there will be 16 matrix inequalities to be satisfied by the positive definite symmetric matrix  $X$  and four auxiliary state-feedback controller matrices  $\Upsilon_i$  by the solution of the LMIs (3.41) and (3.42).

### 3.3.4 Simulation Results

In order to verify the performance of the proposed controller, we demonstrate the reference tracking results. The fuzzy  $\mathcal{H}_\infty$  is evaluated in terms of minimization of the yaw rate error i.e.,  $e_\psi$  for vehicle handling characteristics and  $e_\beta$  for vehicle stability characteristics along with the generated yaw moment. We initiate the AFS/DYC controller by exerting the exogenous steering signal into the system. The steering signal is expected to perform an emergency lane changing in highway driving. For this purpose, the magnitude of the steering signal is kept high. Notice in Figure 3.23 that the first steering action is activated at 2 seconds and finished at 6 seconds. The second steering action is performed at 8 sec-

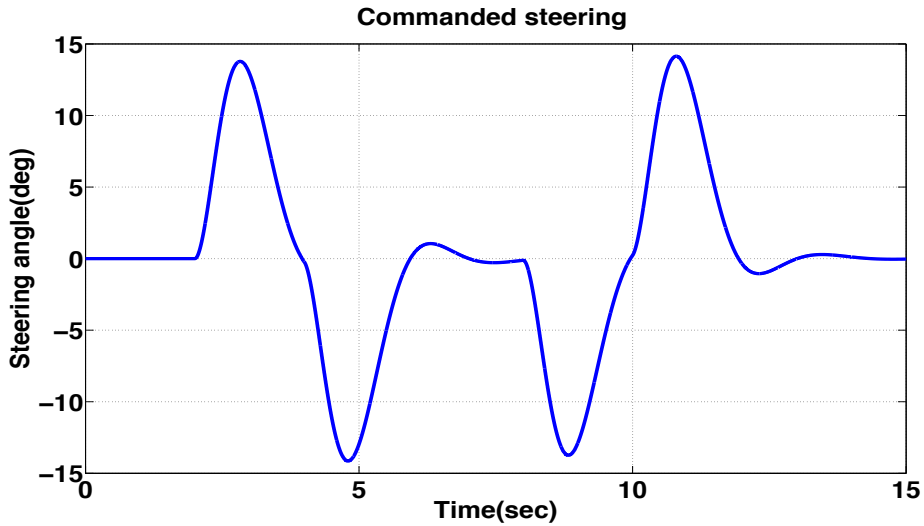


Figure 3.23: Commanded steering for double lane changing

onds. This scenario is for a double lane changing. The goal is to define a suitable feedback control law that ensures the stability of vehicle with an enhanced handling feature. The proposed fuzzy  $\mathcal{H}_\infty$  controller is a multi input multi output, which reacts to the deviation of the yaw rate and slip angle by producing yaw moment and corrective steering. Note that the corrective steering input has a small magnitude, which provides an additional tire forces to obtain the required yaw moment. It is assumed that tire slip side angle is bounded such that the tire road coefficient  $\mu$  plays an important role for the variations of cornering stiffnesses (see Figure 3.11). To this end,  $\Delta C_f$  and  $\Delta C_r$  change in an interval  $[30000, 60000] \text{ N/rad}$ , i.e.,  $\underline{C}_f = \underline{C}_r = 30000 \text{ N/rad}$  and  $\overline{C}_f = \overline{C}_r = 60000 \text{ N/rad}$ . Lower stiffnesses value implies a wet road profile, higher value means a dry road<sup>31</sup>. The LMIs (3.41), (3.42) in Theorem 1 are solved by the LMI Control Toolbox in Matlab<sup>®</sup>, by setting the performance level  $\mathcal{L}_2 \gamma = 30$ . Since the commanded steering signal magnitude is very high i.e., 15 deg at 25 m/s highway speed, the set performance index successfully

---

<sup>31</sup>It is well known that cornering stiffness also depends on slip side angle change (see in Fig ??). Since we keep it bounded, we assume the change in road surface actually changes the cornering stiffness value.

dissipates the energy of regulated outputs over the given energy of the inputs, i.e.,  $\gamma$  sub-optimal design guarantees that the energy of the outputs is upper bounded by  $\gamma\|w\|_{\mathcal{L}_2}$  in (3.39). The closed loop simulation is performed in Simulink® software where the fuzzy controllers are implemented on a computer equipped with Intel *Xeon E5 2.6 GHz* CPU.

Table 3.4: Vehicle parameters

Symbol	Value	Unit	Description
$m$	1500	$kg$	<i>Vehicle mass</i>
$J$	2500	$kgm^2$	<i>Yaw inertia</i>
$l_f$	1.1	$m$	<i>Distance of front axle to COG</i>
$l_r$	1.5	$m$	<i>Distance of rear axle to COG</i>
$C_f$	[30000,60000]	$N/rd$	<i>Varying front cornering stiffness</i>
$C_r$	[30000,60000]	$N/rd$	<i>Varying rear cornering stiffness</i>
$t_f = t_r$	1.4	$m$	<i>Front and rear axle length</i>
$V_x$	25	$m/s$	<i>Vehicle longitudinal velocity</i>
$k_{us}$	0.005	$N/A$	<i>Stability factor</i>

Next we report the findings of the design. We compare the controller performance with non-controlled case. Figure 3.23 shows a steering signal that performs a double lane change. Recall that the main objective of the design to ensure the vehicle stability and handling during emergency maneuvers with a possible high steering magnitude shown in Figure 3.23. As the steering is performed, the slip angle increase is bounded but the tire-road coefficient  $\mu(t)$  is varied at certain extent. The yaw rate reference  $\dot{\psi}(t)$  tracking guarantees the handling performance shown in Figure 3.24. As expected, for such a steering command, the vehicle loses maneuvering ability without control. Notice the steady-state error for uncontrolled case, which is driven to zero with fuzzy control. The slip side angle  $\beta(t)$  tracking performance is also driven to zero in Figure 3.25, therefore

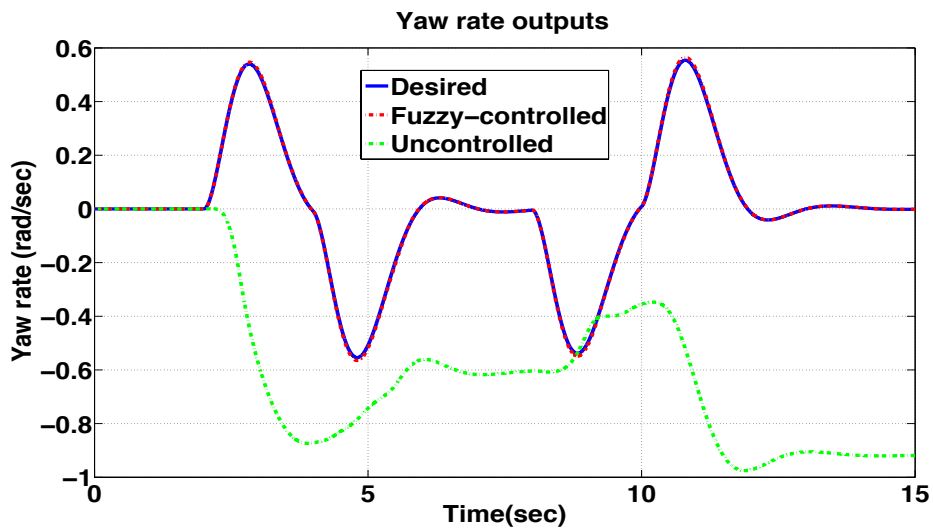


Figure 3.24: Yaw rate outputs

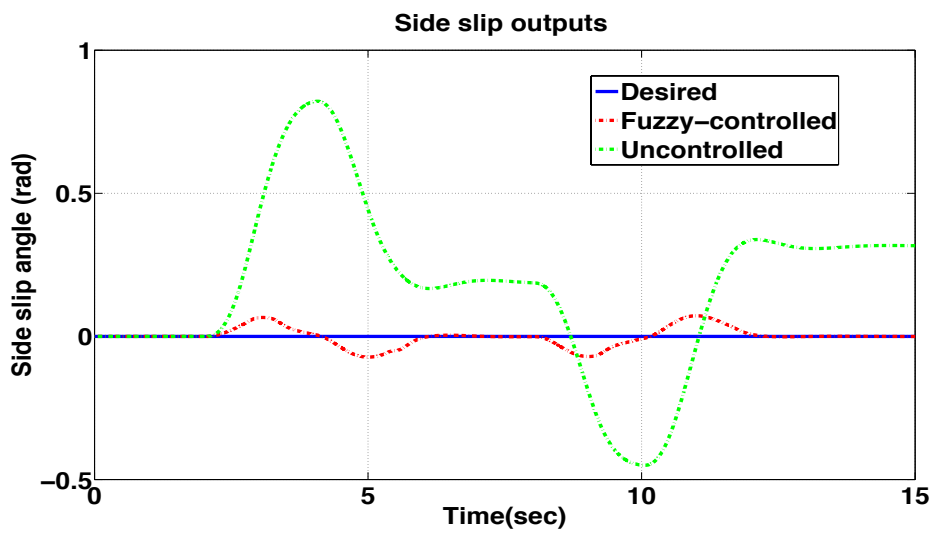


Figure 3.25: Slip angle outputs

vehicle stability is maintained. The steady-state error is seen for uncontrolled case. The Figure 3.26 shows the yaw moment in  $Nm$  for the double lane change steering excitation given in Figure 3.23. An interesting analysis result is seen in Figure 3.27. It simply means how much deterioration occurs on yaw rate with respect the steering angle change. The fuzzy control result closely follows the reference unlike the uncontrolled case where the vehicle experiences a failure on the stability and performance. We can conclude that the proposed design is promising for possible future implementation in a real car.

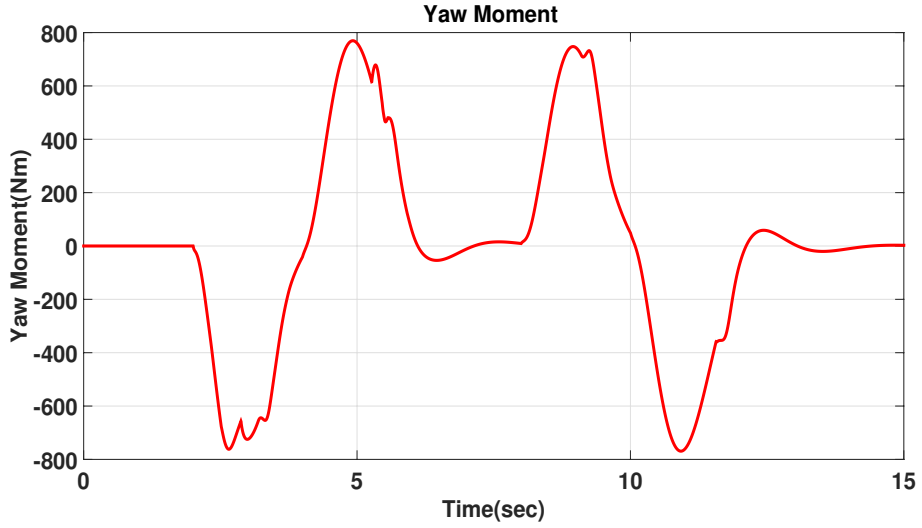


Figure 3.26: Yaw moment

### 3.4 Conclusion

A  $\mathcal{H}_\infty$  controller is first proposed to perform the actual lane change maneuver. The proposed controller performance is compared with a HDM controller, simulations are performed to demonstrate the improvements on the reference trajectory following, the yaw angle and the wind disturbance rejection. We then extend the design to a robust controller

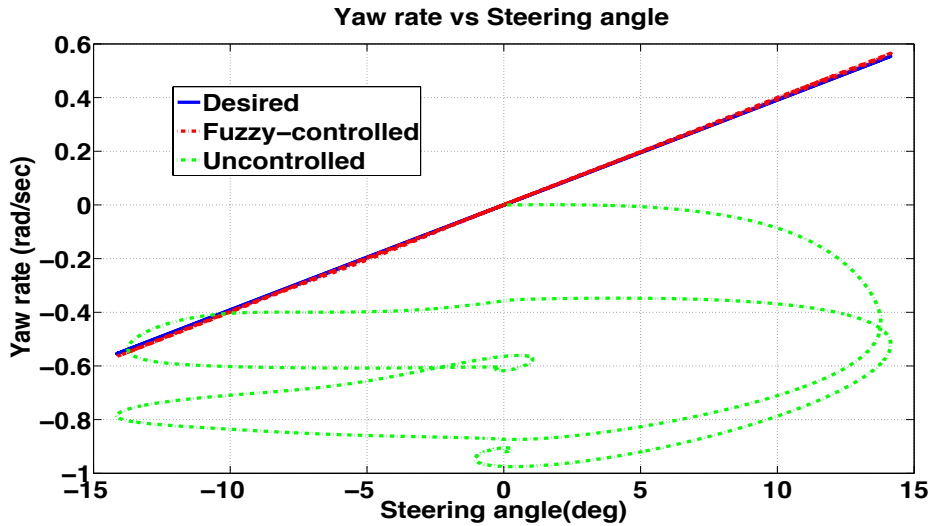


Figure 3.27: Steering-yaw rate outputs

for enhanced vehicle handling and stability features. As continuation of our work, a robust LPV/ $\mathcal{H}_\infty$  controller is design for combined active steering and direct yaw moment control in existence of parameter uncertainty in road conditions, subsequently, in cornering stiffness forces. The proposed control system provides a set of improved tracking performances to make the nonlinear vehicle model responses follow the desired values in varying road conditions. Thus, the overall emergency lane change safety system design attains an improved level of robustness.

Further, a fuzzy  $\mathcal{H}_\infty$  state-feedback suboptimal controller is designed for AFS/DYC system to improve the stability and handling performance of vehicle lateral dynamics. The main challenge of the tire nonlinear forces is modeled by Takagi-Sugeno (T-S) scheme with membership functions. Then the fuzzy blended linear controllers are computed with linear matrix inequalities based on bounded real lemma condition. It is observed from the simulations that the designed controller is capable of tracking the references with high accuracy. Future research in vehicle lateral dynamics involves the design of intelligent

distribution of yaw moment to braking forces in a real time vehicle dynamics simulator.

The future work also in vehicle design involves three tasks. For the distribution of the yaw moment to the tires, we first add an actuator dynamics for a possible real time application in a vehicle. Second, instead of using a constant velocity during a lane change, we set a varying longitudinal velocity range in LPV design framework and propose a robust control law for the vehicle lower level controller. Third, we implement the combined control structure in dSPACE real time driving simulator, which is an available software, located in the Laboratory of Control, Robotics and Automation at the Texas A&M University.

#### 4. CONCLUSION

In this study, I proposed a human-like driver model for mandatory gap selection. I first showed threat estimation of drivers with fuzzy logic. The main goal is to mimic drivers' driving habits such that useful information about surrounding vehicles can be captured. Then I established a Markov decision processes based decision strategy for intelligent gap selection. A grid-world type environment of traffic is rendered where  $SV$  is the only agent, which seeks to find a possible gap to merge in by performing lane changing. Since traffic environment is highly dynamic, the information at current time may be obsolete for making decisions in the future driving. To address this, predictions of all vehicles are computed and solution is proposed with the information in future time. The complete system scheme is named as predictive fuzzy Markov decision process because of the integration of all the elements in the design stage. Further, I considered the interactions of  $TVs$  with  $SV$ , and extended to MDPs to Markov game where a multi-agent traffic set-up is established. Cooperative and non-cooperative cases are both formulated and solved by defining novel algorithms. Different scenarios were demonstrated in a real time driver simulation where cooperative Markov game has some superiority over other methods in terms of easing the lane changing process. On the other hand, non-cooperative Markov game reflects more realistic real-time scenario in which drivers' courtesy are not included.

Moreover, some research results in vehicle dynamics and control were also presented for contributing the safety of vehicles in general. Inherited nonlinear tire forces are modeled with Pajeka tyre model where the nonlinear variations are converted to the changes in cornering stiffnesses. Then, LPV and and fuzzy  $\mathcal{H}_\infty$  controllers were designed. Both controller results ensure vehicle lateral stability and handling performance in terms of reference tracking performance. Fuzzy  $\mathcal{H}_\infty$  controller is more preferred due to its computation

speed.

In conclusion, this dissertation strives to contribute to the state-of-the-art developments in autonomous driving technologies as well as advanced vehicular control systems with well established controller formulation and solution.

## REFERENCES

- [1] “Nsc motor vehicle fatality estimates - national safety council.”
- [2] D. Fambro, R. Koppa, D. Picha, and K. Fitzpatrick, “Driver braking performance in stopping sight distance situations,” *Transportation Research Record: Journal of the Transportation Research Board*, no. 1701, pp. 9–16, 2000.
- [3] Y. Sugimoto and C. Sauer, “Effectiveness estimation method for advanced driver assistance system and its application to collision mitigation brake system,” in *Proceedings of the 19th International Technical Conference on the Enhanced Safety of Vehicles*, pp. 5–148, 2005.
- [4] F. Borrelli, A. Bemporad, M. Fodor, and D. Hrovat, “An mpc/hybrid system approach to traction control,” *IEEE Transactions on Control Systems Technology*, vol. 14, no. 3, pp. 541–552, 2006.
- [5] J. D. Lee, D. V. McGehee, T. L. Brown, and M. L. Reyes, “Collision warning timing, driver distraction, and driver response to imminent rear-end collisions in a high-fidelity driving simulator,” *Human factors*, vol. 44, no. 2, pp. 314–334, 2002.
- [6] S. Ishida and J. E. Gayko, “Development, evaluation and introduction of a lane keeping assistance system,” in *Intelligent Vehicles Symposium, 2004 IEEE*, pp. 943–944, IEEE, 2004.
- [7] J. Pohl, W. Birk, and L. Westervall, “A driver-distraction-based lane-keeping assistance system,” *Proceedings of the Institution of Mechanical Engineers, Part I: Journal of Systems and Control Engineering*, vol. 221, no. 4, pp. 541–552, 2007.
- [8] L. Li and F.-Y. Wang, *Advanced motion control and sensing for intelligent vehicles*. Springer Science & Business Media, 2007.

- [9] R. Bishop, “Intelligent vehicle applications worldwide,” *IEEE Intelligent Systems and Their Applications*, vol. 15, no. 1, pp. 78–81, 2000.
- [10] T. A. Dingus, S. G. Klauer, V. L. Neale, A. Petersen, S. E. Lee, J. Sudweeks, M. Perez, J. Hankey, D. Ramsey, S. Gupta, *et al.*, “The 100-car naturalistic driving study, phase ii-results of the 100-car field experiment,” tech. rep., 2006.
- [11] P. Hancock and R. Parasuraman, “Human factors and safety in the design of intelligent vehicle-highway systems (ivhs),” *Journal of Safety Research*, vol. 23, no. 4, pp. 181–198, 1993.
- [12] D. Parker, J. T. Reason, A. S. Manstead, and S. G. Stradling, “Driving errors, driving violations and accident involvement,” *Ergonomics*, vol. 38, no. 5, pp. 1036–1048, 1995.
- [13] D. D. Salvucci, “Modeling driver behavior in a cognitive architecture,” *Human factors*, vol. 48, no. 2, pp. 362–380, 2006.
- [14] T. Vaa, “Modelling driver behaviour on basis of emotions and feelings: intelligent transport systems and behavioural adaptations,” *Modelling driver behaviour in automotive environments*, pp. 208–232, 2007.
- [15] C. C. Macadam, “Understanding and modeling the human driver,” *Vehicle System Dynamics*, vol. 40, no. 1-3, pp. 101–134, 2003.
- [16] P. Hidas, “Modelling lane changing and merging in microscopic traffic simulation,” *Transportation Research Part C: Emerging Technologies*, vol. 10, no. 5, pp. 351–371, 2002.
- [17] M. Oaksford and N. Chater, *Bayesian rationality: The probabilistic approach to human reasoning*. Oxford University Press, 2007.

- [18] M. Plöchl and J. Edelmann, “Driver models in automobile dynamics application,” *Vehicle System Dynamics*, vol. 45, no. 7-8, pp. 699–741, 2007.
- [19] M. Kondo and A. Ajimine, “Driver’s sight point and dynamics of the driver-vehicle-system related to it,” tech. rep., SAE Technical Paper, 1968.
- [20] D. T. McRuer and E. S. Krendel, “The human operator as a servo system element,” *Journal of the Franklin Institute*, vol. 267, no. 6, pp. 511–536, 1959.
- [21] D. T. McRuer, R. W. Allen, D. H. Weir, and R. H. Klein, “New results in driver steering control models,” *Human factors*, vol. 19, no. 4, pp. 381–397, 1977.
- [22] D. T. McRuer, D. H. Weir, H. R. Jex, R. E. Magdaleno, and R. W. Allen, “Measurement of driver-vehicle multiloop response properties with a single disturbance input,” *IEEE Transactions on Systems, Man, and Cybernetics*, no. 5, pp. 490–497, 1975.
- [23] L. D. Reid, W. Graf, and A. Billing, “The validation of linear driver model,” tech. rep., University of Toronto, 1980.
- [24] D. T. McRuer, D. Graham, E. Krendel, and W. Reisener Jr, “Human pilot dynamics in compensatory systems. theory, models and experiments with controlled element and forcing function variations,” *Wright-Patterson AFB (OH): Air Force Flight Dynamics Laboratory*, 1965.
- [25] E. Donges, “A two-level model of driver steering behavior,” *Human Factors*, vol. 20, no. 6, pp. 691–707, 1978.
- [26] M. Mitschke, “Anticipatory steering in a driver-vehicle control loop,” *VEHICLE SYSTEM DYNAMICS*, vol. 18, pp. 405–413, 1989.

- [27] R. Mayr and E. Freund, “On the design of nonlinear path control in automated vehicle guidance,” in *Intelligent Robots and Systems, 1992., Proceedings of the 1992 IEEE/RSJ International Conference on*, vol. 1, pp. 613–620, IEEE, 1992.
- [28] T. Hessburg and M. Tomizuka, “Fuzzy logic control for lateral vehicle guidance,” *IEEE Control Systems*, vol. 14, no. 4, pp. 55–63, 1994.
- [29] D. James, F. Boehringer, K. Burnham, and D. Copp, “Adaptive driver model using a neural network,” *Artificial life and Robotics*, vol. 7, no. 4, pp. 170–176, 2004.
- [30] J. H. Yoo and R. Langari, “Development of a predictive collision avoidance for subjective adjacent risk estimation,” in *American Control Conference (ACC), 2015*, pp. 3334–3341, IEEE, 2015.
- [31] S. Shalev-Shwartz, N. Ben-Zrihem, A. Cohen, and A. Shashua, “Long-term planning by short-term prediction,” *arXiv preprint arXiv:1602.01580*, 2016.
- [32] C. Kim and R. Langari, “Adaptive analytic hierarchy process-based decision making to enhance vehicle autonomy,” *IEEE Transactions on Vehicular Technology*, vol. 61, no. 7, pp. 3321–3332, 2012.
- [33] H. Wang, K. Rudy, J. Li, and D. Ni, “Calculation of traffic flow breakdown probability to optimize link throughput,” *Applied Mathematical Modelling*, vol. 34, no. 11, pp. 3376–3389, 2010.
- [34] D. Sadigh, K. Driggs-Campbell, A. Puggelli, W. Li, V. Shia, R. Bajcsy, A. L. Sangiovanni-Vincentelli, S. S. Sastry, and S. A. Seshia, “Data-driven probabilistic modeling and verification of human driver behavior,” *Formal Verification and Modeling in Human-Machine Systems*, 2014.
- [35] S. Brechtel, T. Gindele, and R. Dillmann, “Probabilistic mdp-behavior planning for cars,” in *Intelligent Transportation Systems (ITSC), 2011 14th International IEEE*

*Conference on*, pp. 1537–1542, IEEE, 2011.

- [36] S. Brechtel, T. Gindele, and R. Dillmann, “Probabilistic decision-making under uncertainty for autonomous driving using continuous pomdps,” in *Intelligent Transportation Systems (ITSC), 2014 IEEE 17th International Conference on*, pp. 392–399, IEEE, 2014.
- [37] S. Ulbrich and M. Maurer, “Probabilistic online pomdp decision making for lane changes in fully automated driving,” in *Intelligent Transportation Systems-(ITSC), 2013 16th International IEEE Conference on*, pp. 2063–2067, IEEE, 2013.
- [38] J. Wei, J. M. Dolan, J. M. Snider, and B. Litkouhi, “A point-based mdp for robust single-lane autonomous driving behavior under uncertainties,” in *Robotics and Automation (ICRA), 2011 IEEE International Conference on*, pp. 2586–2592, IEEE, 2011.
- [39] E. Semsar and K. Khorasani, “Optimal control and game theoretic approaches to cooperative control of a team of multi-vehicle unmanned systems,” in *Networking, Sensing and Control, 2007 IEEE International Conference on*, pp. 628–633, IEEE, 2007.
- [40] H. Kita, “A merging–giveaway interaction model of cars in a merging section: a game theoretic analysis,” *Transportation Research Part A: Policy and Practice*, vol. 33, no. 3-4, pp. 305–312, 1999.
- [41] A. Talebpour, H. S. Mahmassani, and S. H. Hamdar, “Modeling lane-changing behavior in a connected environment: A game theory approach,” *Transportation Research Procedia*, vol. 7, pp. 420–440, 2015.
- [42] M. Wang, S. P. Hoogendoorn, W. Daamen, B. van Arem, and R. Happee, “Game theoretic approach for predictive lane-changing and car-following control,” *Trans-*

*portation Research Part C: Emerging Technologies*, vol. 58, pp. 73–92, 2015.

- [43] H. Yu, H. E. Tseng, and R. Langari, “A human-like game theory-based controller for automatic lane changing,” *Transportation Research Part C: Emerging Technologies*, vol. 88, pp. 140–158, 2018.
- [44] F. Meng, J. Su, C. Liu, and W.-H. Chen, “Dynamic decision making in lane change: Game theory with receding horizon,” in *Control (CONTROL), 2016 UKACC 11th International Conference on*, pp. 1–6, IEEE, 2016.
- [45] N. Li, D. W. Oyler, M. Zhang, Y. Yildiz, I. Kolmanovsky, and A. R. Girard, “Game theoretic modeling of driver and vehicle interactions for verification and validation of autonomous vehicle control systems,” *IEEE Transactions on control systems technology*, 2017.
- [46] D. W. Oyler, Y. Yildiz, A. R. Girard, N. I. Li, and I. V. Kolmanovsky, “A game theoretical model of traffic with multiple interacting drivers for use in autonomous vehicle development,” in *American Control Conference (ACC), 2016*, pp. 1705–1710, IEEE, 2016.
- [47] A. Eskandarian, *Handbook of intelligent vehicles*. Springer, 2014.
- [48] C. Katrakazas, M. Quddus, W.-H. Chen, and L. Deka, “Real-time motion planning methods for autonomous on-road driving: State-of-the-art and future research directions,” *Transportation Research Part C: Emerging Technologies*, vol. 60, pp. 416–442, 2015.
- [49] Y. Gao, A. Gray, J. V. Frasch, T. Lin, E. Tseng, J. K. Hedrick, and F. Borrelli, “Spatial predictive control for agile semi-autonomous ground vehicles,” in *Proceedings of the 11th International Symposium on Advanced Vehicle Control*, 2012.

- [50] A. Gray, Y. Gao, T. Lin, J. K. Hedrick, H. E. Tseng, and F. Borrelli, “Predictive control for agile semi-autonomous ground vehicles using motion primitives,” in *American Control Conference (ACC), 2012*, pp. 4239–4244, IEEE, 2012.
- [51] J. Nilsson, Y. Gao, A. Carvalho, and F. Borrelli, “Manoeuvre generation and control for automated highway driving,” *IFAC Proceedings Volumes*, vol. 47, no. 3, pp. 6301–6306, 2014.
- [52] J. Nilsson, P. Falcone, M. Ali, and J. Sjöberg, “Receding horizon maneuver generation for automated highway driving,” *Control Engineering Practice*, vol. 41, pp. 124–133, 2015.
- [53] U. Rosolia, S. De Bruyne, and A. G. Alleyne, “Autonomous vehicle control: A nonconvex approach for obstacle avoidance,” *IEEE Transactions on Control Systems Technology*, vol. 25, no. 2, pp. 469–484, 2017.
- [54] S. Hosseini, N. Murgovski, G. R. de Campos, and J. Sjöberg, “Adaptive forward collision warning algorithm for automotive applications,” in *American Control Conference (ACC), 2016*, pp. 5982–5987, IEEE, 2016.
- [55] E. H. Lim and J. K. Hedrick, “Lateral and longitudinal vehicle control coupling for automated vehicle operation,” in *American Control Conference, 1999. Proceedings of the 1999*, vol. 5, pp. 3676–3680, IEEE, 1999.
- [56] D. C. Gazis, R. Herman, and R. B. Potts, “Car-following theory of steady-state traffic flow,” *Operations research*, vol. 7, no. 4, pp. 499–505, 1959.
- [57] P. G. Gipps, “A behavioural car-following model for computer simulation,” *Transportation Research Part B: Methodological*, vol. 15, no. 2, pp. 105–111, 1981.
- [58] M. Bando, K. Hasebe, A. Nakayama, A. Shibata, and Y. Sugiyama, “Dynamical model of traffic congestion and numerical simulation,” *Physical review E*, vol. 51,

no. 2, p. 1035, 1995.

- [59] M. Bando, K. Hasebe, K. Nakanishi, and A. Nakayama, “Analysis of optimal velocity model with explicit delay,” *Physical Review E*, vol. 58, no. 5, p. 5429, 1998.
- [60] M. Treiber, A. Hennecke, and D. Helbing, “Congested traffic states in empirical observations and microscopic simulations,” *Physical review E*, vol. 62, no. 2, p. 1805, 2000.
- [61] A. Kesting, M. Treiber, and D. Helbing, “Enhanced intelligent driver model to access the impact of driving strategies on traffic capacity,” *Philosophical Transactions of the Royal Society of London A: Mathematical, Physical and Engineering Sciences*, vol. 368, no. 1928, pp. 4585–4605, 2010.
- [62] R. Rajamani, “Adaptive cruise control,” *Encyclopedia of Systems and Control*, pp. 13–19, 2015.
- [63] H. Winner and M. Schopper, “Adaptive cruise control,” in *Handbuch Fahrerassistenzsysteme*, pp. 851–891, Springer, 2015.
- [64] C. Kim and R. Langari, “Application of brain limbic system to adaptive cruise control,” *International Journal of Vehicle Autonomous Systems*, vol. 11, no. 1, pp. 22–41, 2013.
- [65] Q. Xu, K. Hedrick, R. Sengupta, and J. VanderWerf, “Effects of vehicle-vehicle/roadside-vehicle communication on adaptive cruise controlled highway systems,” in *Vehicular Technology Conference, 2002. Proceedings. VTC 2002-Fall. 2002 IEEE 56th*, vol. 2, pp. 1249–1253, IEEE, 2002.
- [66] A. Kanaris, E. B. Kosmatopoulos, and P. A. Loannou, “Strategies and spacing requirements for lane changing and merging in automated highway systems,” *IEEE transactions on vehicular technology*, vol. 50, no. 6, pp. 1568–1581, 2001.

- [67] C. Kim and R. Langari, “Development of an autonomous vehicle highway merging strategy,” *International journal of vehicle design*, vol. 60, no. 3/4, pp. 350–368, 2012.
- [68] J. H. Yoo and R. Langari, “A stackelberg game theoretic driver model for merging,” in *ASME 2013 Dynamic Systems and Control Conference*, pp. V002T30A003–V002T30A003, American Society of Mechanical Engineers, 2013.
- [69] K. Ahmed, M. Ben-Akiva, H. Koutsopoulos, and R. Mishalani, “Models of free-way lane changing and gap acceptance behavior,” *Transportation and traffic theory*, vol. 13, pp. 501–515, 1996.
- [70] J. Hedrick, M. Tomizuka, and P. Varaiya, “Control issues in automated highway systems,” *IEEE Control Systems*, vol. 14, no. 6, pp. 21–32, 1994.
- [71] G. Palmieri, M. Baric, F. Borrelli, and L. Glielmo, “A robust lateral vehicle dynamics control,” in *10th International Symposium on Advanced Vehicle Control*, 2010.
- [72] W. Chee and M. Tomizuka, “Lane change maneuver of automobiles for the intelligent vehicle and highway system (ivhs),” in *American Control Conference, 1994*, vol. 3, pp. 3586–3587, IEEE, 1994.
- [73] C. Kim and R. Langari, “Brain limbic system-based intelligent controller application to lane change manoeuvre,” *Vehicle system dynamics*, vol. 49, no. 12, pp. 1873–1894, 2011.
- [74] C. Hatipoglu, U. Ozguner, and K. A. Redmill, “Automated lane change controller design,” *IEEE transactions on intelligent transportation systems*, vol. 4, no. 1, pp. 13–22, 2003.
- [75] M. Abe, *Vehicle handling dynamics: theory and application*. Butterworth-Heinemann, 2015.

- [76] P. Gahinet, A. Nemirovskii, A. J. Laub, and M. Chilali, “The lmi control toolbox,” in *Decision and Control, 1994., Proceedings of the 33rd IEEE Conference on*, vol. 3, pp. 2038–2041, IEEE, 1994.
- [77] P. Apkarian and P. Gahinet, “A convex characterization of gain-scheduled h/sub/spl infin//controllers,” *IEEE Transactions on Automatic Control*, vol. 40, no. 5, pp. 853–864, 1995.
- [78] F. Wu and K. Dong, “Gain-scheduling control of lft systems using parameter-dependent lyapunov functions,” *Automatica*, vol. 42, no. 1, pp. 39–50, 2006.
- [79] F. Wu, X. H. Yang, A. Packard, and G. Becker, “Induced l/sub 2/-norm control for lpv system with bounded parameter variation rates,” in *American Control Conference, Proceedings of the 1995*, vol. 3, pp. 2379–2383, IEEE, 1995.
- [80] C. Poussot-Vassal, O. Sename, L. Dugard, P. Gaspar, Z. Szabo, and J. Bokor, “A new semi-active suspension control strategy through lpv technique,” *Control Engineering Practice*, vol. 16, no. 12, pp. 1519–1534, 2008.
- [81] A.-L. Do, O. Sename, and L. Dugard, “An lpv control approach for semi-active suspension control with actuator constraints,” in *American Control Conference (ACC), 2010*, pp. 4653–4658, IEEE, 2010.
- [82] M.-Q. Nguyen, J. G. da Silva, O. Sename, and L. Dugard, “Semi-active suspension control problem: Some new results using an lpv/hâLd state feedback input constrained control,” in *Decision and Control (CDC), 2015 IEEE 54th Annual Conference on*, pp. 863–868, IEEE, 2015.
- [83] M. Fleps-Dezasse and J. Brembeck, “Lpv control of full-vehicle vertical dynamics using semi-active dampers,” *IFAC-PapersOnLine*, vol. 49, no. 11, pp. 432–439, 2016.

- [84] M. Fleps-Dezasse, M. M. Ahmed, J. Brembeck, and F. Svaricek, “Experimental evaluation of linear parameter-varying semi-active suspension control,” in *Control Applications (CCA), 2016 IEEE Conference on*, pp. 77–84, IEEE, 2016.
- [85] A. Zin, O. Sename, P. Gaspar, L. Dugard, and J. Bokor, “Robust lpv– $\dot{A}$  control for active suspensions with performance adaptation in view of global chassis control,” *Vehicle System Dynamics*, vol. 46, no. 10, pp. 889–912, 2008.
- [86] I. J. Fialho and G. J. Balas, “Design of nonlinear controllers for active vehicle suspensions using parameter-varying control synthesis,” *Vehicle System Dynamics*, vol. 33, no. 5, pp. 351–370, 2000.
- [87] X. Yang, Z. Wang, and W. Peng, “Coordinated control of afs and dyc for vehicle handling and stability based on optimal guaranteed cost theory,” *Vehicle System Dynamics*, vol. 47, no. 1, pp. 57–79, 2009.
- [88] H. Zhang, X. Zhang, and J. Wang, “Robust gain-scheduling energy-to-peak control of vehicle lateral dynamics stabilisation,” *Vehicle System Dynamics*, vol. 52, no. 3, pp. 309–340, 2014.
- [89] H. Zhang and J. Wang, “Vehicle lateral dynamics control through afs/dyc and robust gain-scheduling approach,” *IEEE Transactions on Vehicular Technology*, vol. 65, no. 1, pp. 489–494, 2016.
- [90] M. Doumiati, O. Sename, L. Dugard, J.-J. Martinez-Molina, P. Gaspar, and Z. Szabo, “Integrated vehicle dynamics control via coordination of active front steering and rear braking,” *European Journal of Control*, vol. 19, no. 2, pp. 121–143, 2013.
- [91] C. Poussot-Vassal, O. Sename, L. Dugard, and S. Savaresi, “Vehicle dynamic stability improvements through gain-scheduled steering and braking control,” *Vehicle System Dynamics*, vol. 49, no. 10, pp. 1597–1621, 2011.

- [92] H. O. Wang, K. Tanaka, and M. F. Griffin, “An approach to fuzzy control of non-linear systems: Stability and design issues,” *IEEE transactions on fuzzy systems*, vol. 4, no. 1, pp. 14–23, 1996.
- [93] K. Tanaka and M. Sugeno, “Stability analysis and design of fuzzy control systems,” *Fuzzy sets and systems*, vol. 45, no. 2, pp. 135–156, 1992.
- [94] K. Mehran, “Takagi-sugeno fuzzy modeling for process control,” *Industrial Automation, Robotics and Artificial Intelligence (EEE8005)*, vol. 262, 2008.
- [95] S.-K. Hong and R. Langari, “An lmi-based hâLd fuzzy control system design with ts framework,” *Information sciences*, vol. 123, no. 3-4, pp. 163–179, 2000.
- [96] S. Aouaouda, M. Chadli, and H.-R. Karimi, “Robust static output-feedback controller design against sensor failure for vehicle dynamics,” *IET Control Theory & Applications*, vol. 8, no. 9, pp. 728–737, 2014.
- [97] D. Saifia, M. Chadli, H. Karimi, and S. Labiod, “Fuzzy control for electric power steering system with assist motor current input constraints,” *Journal of the Franklin Institute*, vol. 352, no. 2, pp. 562–576, 2015.
- [98] X. Jin, G. Yin, and J. Wang, “Robust fuzzy control for vehicle lateral dynamic stability via takagi-sugeno fuzzy approach,” in *American Control Conference (ACC), 2017*, pp. 5574–5579, IEEE, 2017.
- [99] H. Jula, E. B. Kosmatopoulos, and P. A. Ioannou, “Collision avoidance analysis for lane changing and merging,” *IEEE Transactions on vehicular technology*, vol. 49, no. 6, pp. 2295–2308, 2000.
- [100] K. Aso and T. Kindo, “Stochastic decision-making method for autonomous driving system that minimizes collision probability,” in *Proc. of the FISITA World Automotive Congress*, 2008.

- [101] S. Danielsson, L. Petersson, and A. Eidehall, “Monte carlo based threat assessment: Analysis and improvements,” in *Intelligent Vehicles Symposium, 2007 IEEE*, pp. 233–238, IEEE, 2007.
- [102] A. Broadhurst, S. Baker, and T. Kanade, “Monte carlo road safety reasoning,” in *Intelligent Vehicles Symposium, 2005. Proceedings. IEEE*, pp. 319–324, IEEE, 2005.
- [103] M. Althoff and A. Mergel, “Comparison of markov chain abstraction and monte carlo simulation for the safety assessment of autonomous cars,” *IEEE Transactions on Intelligent Transportation Systems*, vol. 12, no. 4, pp. 1237–1247, 2011.
- [104] O. Maler, “Computing reachable sets: An introduction,” *Tech. rep. French National Center of Scientific Research*, 2008.
- [105] M. Althoff, O. Stursberg, and M. Buss, “Safety assessment of driving behavior in multi-lane traffic for autonomous vehicles,” in *Intelligent Vehicles Symposium, 2009 IEEE*, pp. 893–900, IEEE, 2009.
- [106] M. Althoff, O. Stursberg, and M. Buss, “Model-based probabilistic collision detection in autonomous driving,” *IEEE Transactions on Intelligent Transportation Systems*, vol. 10, no. 2, pp. 299–310, 2009.
- [107] S. Coskun and R. Langari, “Predictive fuzzy markov decision strategy for autonomous driving in highways,” in *Conference on Control Technology and Applications (CCTA), 2018 IEEE*, IEEE, 2018.
- [108] M. L. Littman, “Markov games as a framework for multi-agent reinforcement learning,” in *Machine Learning Proceedings 1994*, pp. 157–163, Elsevier, 1994.
- [109] J. Filar and K. Vrieze, *Competitive Markov decision processes*. Springer Science & Business Media, 2012.

- [110] J. Hu, M. P. Wellman, *et al.*, “Multiagent reinforcement learning: theoretical framework and an algorithm.,” in *ICML*, vol. 98, pp. 242–250, Citeseer, 1998.
- [111] E. Bakker, L. Nyborg, and H. B. Pacejka, “Tyre modelling for use in vehicle dynamics studies,” tech. rep., SAE Technical Paper, 1987.
- [112] R. Rajamani, *Vehicle dynamics and control*. Springer Science & Business Media, 2011.
- [113] J. Y. Choi, “Robust controller for an autonomous vehicle with look-ahead and look-down information,” *Journal of mechanical science and technology*, vol. 25, no. 10, pp. 2467–2474, 2011.
- [114] C. Scherer, P. Gahinet, and M. Chilali, “Multiobjective output-feedback control via lmi optimization,” *IEEE Transactions on automatic control*, vol. 42, no. 7, pp. 896–911, 1997.
- [115] P. Fancher and Z. Bareket, “Evolving model for studying driver-vehicle system performance in longitudinal control of headway,” *Transportation Research Record: Journal of the Transportation Research Board*, no. 1631, pp. 13–19, 1998.
- [116] G. Prokop, “Modeling human vehicle driving by model predictive online optimization,” *Vehicle System Dynamics*, vol. 35, no. 1, pp. 19–53, 2001.
- [117] J. Ragazzini, “Engineering aspects of the human being as a servo-mechanism,” in *Meeting of the American Psychological Association*, 1948.
- [118] S. Coskun and R. Langari, “Enhanced vehicle handling performance for an emergency lane changing controller in highway driving,” in *Intelligent Vehicles Symposium (IV), 2017 IEEE*, pp. 334–340, IEEE, 2017.

- [119] P. Falcone, H. Eric Tseng, F. Borrelli, J. Asgari, and D. Hrovat, “Mpc-based yaw and lateral stabilisation via active front steering and braking,” *Vehicle System Dynamics*, vol. 46, no. S1, pp. 611–628, 2008.
- [120] S. Coskun and R. Langari, “Development of an emergency lane change system in highway driving,” in *ASME 2016 Dynamic Systems and Control Conference*, pp. V002T31A003–V002T31A003, American Society of Mechanical Engineers, 2016.
- [121] D. B. Fernando, d. B. Hernán, and J. M. Ricardo, “Wind turbine control systems: principles, modelling and gain scheduling design (advances in industrial control),” 2006.
- [122] S. Coskun and R. Langari, “Improved vehicle lateral dynamics with takagi-sugeno hâLd fuzzy control strategy for emergency maneuvering,” in *Conference on Control Technology and Applications (CCTA), 2018 IEEE*, IEEE, 2018.
- [123] B. D. Anderson and S. Vongpanitlerd, *Network analysis and synthesis: a modern systems theory approach*. Courier Corporation, 2013.